Spring 2015

Climate change impact assessments using the Water Erosion Prediction Project model

Joseph Trotochaud
Purdue University

Graduate School Form 30
(Revised 08/14)

PURDUE UNIVERSITY
GRADUATE SCHOOL
Thesis/Dissertation Acceptance

This is to certify that the thesis/dissertation prepared

By Joseph Trotochaud

Entitled
CLIMATE CHANGE IMPACT ASSESSMENTS USING THE WATER EROSION PREDICTION PROJECT MODEL

For the degree of Master of Science in Agricultural and Biological Engineering

Is approved by the final examining committee:

Bernard A. Engel

Dennis C. Flanagan

Jane R. Frankenberger

To the best of my knowledge and as understood by the student in the Thesis/Dissertation Agreement, Publication Delay, and Certification/Disclaimer (Graduate School Form 32), this thesis/dissertation adheres to the provisions of Purdue University's "Policy on Integrity in Research" and the use of copyrighted material.

Approved by Major Professor(s): Bernard A. Engel
Dennis C. Flanagan

Approved by: Bernard A. Engel 04/17/2015

Head of the Department Graduate Program Date

CLIMATE CHANGE IMPACT ASSESSMENTS USING THE WATER EROSION PREDICTION PROJECT MODEL

A Thesis
Submitted to the Faculty
of
Purdue University
by
Joseph Trotochaud

In Partial Fulfillment of the
Requirements for the Degree
of
Master of Science in Agricultural and Biological Engineering

May 2015
Purdue University
West Lafayette, Indiana

Dedicated to:

My parents, Jim and Robyn

My sister, Lena

My lifelong friends, Thomas, Wyatt, and Ben

And the love of my life, Cininta

ACKNOWLEDGEMENTS

I would like to thank all of those who gave me technical support throughout my studies.

Two of Dennis Flanagan's undergraduate students, Tyler Anderson and Kelly Del Ponte did prior work on the WEPP models for the Cedar Creek and Tifton catchments which saved time during calibration/validation for those sites. ARS support scientists Stan Livingston and James Frankenberger were of great assistance in helping me obtain and understand observed data from the Cedar Creek Watershed. Dr. David Bosch in Tifton provided me with very high quality observed data which made calibration/validation at the Tifton site much simpler. Dr. Mariana Dobre and Dr. Erin Brooks were invaluable for the Lake Tahoe fire assessment, both for providing modeling inputs for the Blackwood Creek watershed and for providing extensive technical support for the 626 hillslope model. Dr. William Elliot was also extremely encouraging while working on the Blackwood Creek assessment. I would also like to thank my Committee members, Drs. Dennis Flanagan, Bernard Engel, and Jane Frankenberger for the countless suggestions and guidance they provided me in completing this work.

This work was made possible by the United States Department of Agriculture Agricultural Research Service, Natural Resources Conservation Service, and Forest Service.

TABLE OF CONTENTS

Page

Page

LIST OF TABLES

LIST OF FIGURES

Figure Page

Figure Page

Figure Page

ABSTRACT

Trotochaud, Joseph. M.S.A.B.E., Purdue University, May 2015. Climate Change Impact Assessments using the Water Erosion Prediction Project Model. Major Professors: Bernard Engel and Dennis Flanagan.

This study was conducted to develop a simplified method of obtaining future climate data inputs for natural resource models and apply that method to three locations within the continental United States to assess the effect of climate change on soil erosion, runoff, and fire risk. A method was developed for quickly obtaining future climate data over a wide range of scenarios, General Circulation Models (GCMs), and timescales from the Intergovernmental Panel on Climate Change (IPCC) Fourth Assessment Report (AR4) and Fifth Assessment Report (AR5) model families using the MarkSim® DSSAT Weather Generator and a Microsoft Excel VBA Macro, the final result being a properly formatted parameter file which can be used by CLIGEN (CLImate GENerator) within the Water Erosion Prediction Project (WEPP) model. By using software which already exists on most computers and not requiring climatological or modeling knowledge to operate, the method herein for creating WEPP climate input files is fast and simple, requiring as little as 15 minutes.

At the first site, analysis of a small (6.7 acre, 2.71 ha) field site monitored as part of the USDA-ARS Conservation Effects Assessment Project in NE Indiana was conducted to determine the effect of climate change on agricultural resources. Precipitation, runoff, soil erosion, and crop growth were modeled using WEPP and the four Representative Concentration Pathway (RCP) scenarios used with the CMIP5 model family from the IPCC 5AR to determine the effectiveness of common agricultural Best Management Practices (BMPs) under predicted climate change. Although precipitation is predicted

here to increase by 2100, sediment loss and runoff will decrease due to a reduction of concrete frost conditions during late winter. However, an increase in the amount of precipitation falling in spring and earlier soybean senescence was predicted to lead to increased soil loss in early spring and fall.

At the second site, a small agricultural hillslope managed by the USDA-ARS in the Southern Coastal Plain of the United States was modeled using WEPP under current and future climates to assess the effect of predicted future climate change on soil erosion, runoff, and BMP effectiveness. Future climate data was similar to that used at the first site. Predicted climatic shift caused soil loss and runoff to be reduced in the first three months of the year, while late fall and early winter months had increases in predicted soil loss and runoff. Increased temperatures were predicted to cause winter cover crops to grow faster, unhindered by frost in winter. Soil loss increased when cotton senesced earlier under warmer temperatures. Early season water deficits and higher evapotranspiration also increased irrigation demands in the growing season. The combination of no-till, rye cover crop, and riparian buffer increased in effectiveness into the future, while all other management systems had either similar or slightly reduced effectiveness under predicted future climate.

At the third site, the Blackwood Creek watershed, a tributary of Lake Tahoe in California, was assessed for potential changes in climate and fire risk under 21st century climates projected by the IPCC AR5. While total precipitation varied by decade, the portion of precipitation falling as snow decreased by as much as 26%, and projected air temperatures increased by as much as 3.4°C by 2090. Total soil water (TSW) predictions by WEPP indicated that fire ignition in the Sierra Nevada region from 1984-2013 coincided with simulated minimum TSW. Risk categories based on simulated TSW changed under projected future climate, with an increase in the number of high risk days defined by TSWs less than 40 mm. Simulated TSW in the Blackwood Creek watershed at the time of historic fires in the region also indicated that the Keetch-Byram Drought Index (KBDI) was correlated to TSW (R^2 = 0.59) when KBDI was less than 500.

CHAPTER 1. INTRODUCTION

Stationarity, the concept that natural systems operate within fixed boundaries, has dominated the engineering and natural science disciplines since their inception. Design and/or practices based on results of empirically derived models of historical data may be flawed due to now poor (or invalid) stationarity assumptions (Milly et al., 2008). As such, the scientific and engineering communities must begin to adopt planning strategies to account for changes in natural systems, particularly climate, if we are to adequately address the problems discovered today. Large scientific and political bodies, most recognizably the Intergovernmental Panel on Climate Change (IPCC), exist which aid in guiding national and regional policies to curtail the extent of and adapt to the realities of climate change. Meanwhile, research continues to satisfy the need to understand how climate change will impact communities, industries, and ecosystems on more localized scales. Evidence based studies which examine specific relationships between climate and other natural or human systems are needed to help policymakers and communities adapt to the future.

A critical first step in conducting climate change assessments is obtaining projected future climate data. While the IPCC is the authoritative body on climate change studies, obtaining future climate projections from their databases presents several challenges for those desiring to conduct impact assessments. The General Circulation Models (GCM), atmospheric and oceanic mathematical models which are used to project future climate, have large map grid cells which generate climate over areas of hundreds of thousands of square kilometers. This complicates studies which examine a specific point on the globe, requiring the individual conducting a site assessment to scale the larger GCM output down to a specific point on the globe (Wilby et al., 2004). Chapter 2 contains more detail

on the scaling process, as well as a tool based on a Microsoft Excel Visual Basic for Applications macro which simplifies the process of obtaining and scaling GCM outputs from the IPCC Fourth (AR4) and Fifth (AR5) Assessment Reports.

Once climate projections have been obtained, natural resource models which use weather to drive fundamental equations can be used to examine the response of specific environmental variables to climate change. Each region will likely have different concerns with regards to weather, requiring engineering practices or risk metrics assessed to be specific to those regions. Three regions are examined in this body of work, two agricultural and one forestland, using the Water Erosion Prediction Project (WEPP, Flanagan and Nearing, 1995) model. WEPP is a mathematical model which combines fundamental equations of soil water, sediment erosion and transport, and plant growth to simulate hillslope and field-scale natural processes related to soil erosion. The WEPP model has been continuously developed since 1985 as a replacement to more simplistic soil erosion tools so that engineers, scientists, and government agents can be more well informed on soil and water conservation and environmental planning and assessment (Flanagan et al., 2007). The WEPP model is used throughout this body of work to assess soil water, soil erosion, best management practices, and crop growth under historical and potential future climate projected under the IPCC AR4 and AR5 model families.

In the Midwestern United States, increasing concern over agro-chemical pollution in runoff from agricultural fields has spurred governments and communities to monitor freshwater drinking sources for agricultural pollutants (Flanagan et al., 2003, 2008). Further downstream, these same pollutants have been linked to the algal blooms and eutrophication which has plagued coastal (Alexander et al., 2008) and inland lake (Michalak et al., 2013) communities. Research in that region has therefore focused heavily on identifying the sources of agricultural pollutants and assessing best management practices for mitigation of pollutant flux and runoff into receiving waters (Flanagan et al., 2008; Heathman et al., 2008; Cechova et al., 2010; Ascough et al., 2012). In Chapter 3, projected future climate is used as an input to the WEPP model to

assess various agricultural practices on a small 2.7 hectare catchment in Northeast Indiana to determine their effectiveness into the future.

In the Southeastern United States, a similar concern exists with regard to the highly erosive, sandy soils which dominate the southeastern coastal plain. Convective summer thunderstorms provide much of the rain in the region (Bosch et al., 1999) while supplemental irrigation during periods of drought is common. The use of riparian buffers and strip-tillage to limit pollutant and sediment transport to streams is widespread in the region, but despite the agroeconomic value of the cash crops grown in the fertile soils, only a few studies have examined other BMPs to compare effectiveness in sequestering agricultural pollutants (Suttles et al., 2003; Cho et al., 2010b). In Chapter 4, multiple BMPs are assessed for their effectiveness in reducing runoff and soil losses under current and future climates at an experimental plot in South Georgia.

Forested regions have very different ecologies and climates compared to agricultural lands. Additionally, forested lands are not managed to the same degree or with the same tools as agricultural lands. A growing concern in the Western United States is the occurrence of large, severe wildfires during drought periods. Earlier spring snowmelt and higher spring and summer temperatures have been linked to recent increases in wildfire severity (Westerling et al., 2006). In some watersheds of the Sierra Nevada mountains in particular, a legacy of fire fuel removal through logging has created a fire deficit and the lowest level of wildfire occurrence in thousands of years (Beaty and Taylor, 2009; Marlon et al., 2012). In Chapter 5, one such watershed is examined to assess changes in climate and fire risk using the Keetch-Byram Drought Index and soil water simulated by the WEPP model.

In Chapter 6, the conclusions from the entire body of work are summarized. This work is intended to show the utility of the climate data tool described in Chapter 2, as well as provide detailed impact assessments for various regions of agricultural and natural value.

CHAPTER 2. A SIMPLE TECHNIQUE FOR OBTAINING FUTURE CLIMATE DATA INPUTS FOR NATURAL RESOURCE MODELS

2.1 Abstract

Those conducting impact studies using natural resource models need to be able to quickly and easily obtain downscaled future climate data from multiple GCMs, future scenarios, and timescales for multiple locations. This paper describes a method of quickly obtaining future climate data over a wide range of scenarios, GCMs, and timescales from the Intergovernmental Panel on Climate Change AR4 and AR5 model families using the MarkSim® DSSAT Weather Generator and a Microsoft Excel VBA Macro, the final result being a properly formatted .par file which can be used by CLIGEN (CLImate GENerator) within the Water Erosion Prediction Project (WEPP) model. By using software which already exists on most computers and not requiring climatological or modeling knowledge to operate, the method herein for creating WEPP climate input files is much faster and simpler than commonly used statistical methods currently described in the literature. Ultimately, the method was modified to create continuous daily data for use with the Soil and Water Assessment Tool (SWAT) as well. The final product is an automated spreadsheet with a simple user interface which imports, analyzes, and generates climate input files for the WEPP and SWAT models. This paper describes the methods, development, and testing of the tool for use with CLIGEN and WEPP model simulations.

2.2 Introduction

With the reality of a changing climate comes the need for scientists, policymakers, and engineers to consider the effects of increasing weather extremes when analyzing, regulating, and designing natural resource conservation systems and strategies. Soil research needs to determine if erosion will increase under projected future climates and whether or not current conservation measures will be effective in the future. The lack of the latter, referred to as impact studies, can partially be explained by two factors: the difficulty of retrieving and downscaling future climate data, and the uncertainty associated with predicting future climates as far as 80 years into the future. With persistent advances in General Circulation Models (GCM) and ever-expanding climate databases comes a decrease in uncertainty, allowing for the gap between the detailed science of climate change and the use of future climate data in localized impact studies to close.

To obtain precipitation and temperature projections from GCMs for use in localized impact studies, the combined technique of spatial and temporal downscaling is recommended (Wilby et al., 2004). GCMs produce synoptic-scale data which must be scaled down to avoid leaving out local meteorological, topographical, and circulatory phenomena which exist at the meso- or micro-scale. Downscaling is a quantitative method which involves regressing modeled 20th century synoptic-scale atmospheric trends to observed micro-scale localized weather to determine correlations which are then applied to modeled 21st century synoptic-scale data in the same location to create micro-scale, localized weather. The Intergovernmental Panel on Climate Change (IPCC) is the most widely recognized source for GCM output (IPCC website is http://www.ipcc.ch).

Downscaling methods can be broken into several simplified categories based on the mathematical or technological methods they use. Delta-change or change-factor methods are the simplest and involve linearly scaling 21st century GCM outputs based on the absolute or relative difference between micro-scale historical observations and synoptic-scale 20th century GCM output for each variable independently (Zhang, 2004; Joh et al.,

2011; Woznicki et al., 2011). Transfer function methods operate similar to change-factor methods, in that they scale GCM output variables independently, but use non-linear relationships to scale historical data relative to synoptic-scale GCM output (Zhang et al., 2005; Sheshukov, 2011). More sophisticated statistical methods regress one or more input predictors to one or more local variables and scale synoptic-scale 21st century GCM output based on those multi-variable regression models to obtain downscaled data on a much finer scale (Mearns et al., 1999; Wilby et al., 2002). Cutting-edge computer modeling methods such as meso-scale Regional Circulatory Model coupling or artificial neural networks generate high-quality downscaled data, but require computational, financial, and human resources which are prohibitive to most institutions (Kendon et al., 2010).

The chaotic nature of the atmosphere and the uncertainty of any one model to produce realistic results necessitate the use of multiple GCMs under multiple greenhouse gas forcings to conduct a comprehensive impact assessment of climate change (Mearns et al., 2003; Wilby et al., 2004; Chiew et al., 2009, 2010). Issues arise when determining which downscaling method to use, since emulating previous impact studies which have traditionally focused on a single downscaling method, GCM, scenario, or time period limit the scope of results. Creating a spread of possible climates using multiple GCMs and emission scenarios involves an often steep learning curve, and can take substantial resources and time to downscale for even a single location. Additionally, locating raw GCM output and predictor variables has only recently become readily available through the IPCC.

Several combinations of GCMs and future time periods have been used in published research involving the Water Erosion Prediction Project (WEPP, Flanagan et al., 2007; Flanagan and Frankenberger, 2012), with little to no similarity in the techniques employed by each author. Zhang published a number of papers in which he used several different downscaling techniques for use with WEPP (Zhang et al., 2004, 2011; Zhang, 2005, 2007). Taken as a whole, these papers represent a spread of the most common

statistical and transfer function downscaling techniques. In the first three papers, Zhang used native GCM output cells from the Hadley Centre Coupled Model version 3 under various IPCC Special Reports on Emission Scenarios (SRES) and Greenhouse Gas (GGa) emission scenarios from the IPCC 3AR and 4AR for a variety of locations. He then spatially and temporally downscaled the GCM outputs to modify the precipitation and temperature parameters within a CLIGEN (CLImate GENerator, Nicks et al., 1995) input file. These three studies analyzed only a single location using climate data from a single model, possibly due to time and resource constraints. However, the most recent study (Zhang et al., 2011) used multiple GCMs and emission scenarios.

The IPCC acknowledges that impact studies have traditionally been restricted to single locations and climate scenarios, likely due to the resource requirements involved with advanced statistical methods and computer software (Wilby et al., 2004). Several barriers exist for those wishing to obtain downscaled future climate data for impact studies. Time requirements for learning and applying downscaling methods, while absent from the literature, can be daunting for those with limited statistical or programming skills. Statistical downscaling methods, for example, represent a balance between spatial resolution and resource requirements, but have steep learning curves which require extensive time to produce data for a single location. Time requirements can be compounded in regional or national collaboration projects where climate data inputs must be developed for multiple locations. Additionally, with each new iteration of the IPCC assessment report every few years, new or updated GCMs and emission scenarios are released, and regression equations or transfer functions must be updated to downscale the GCM output. For regions outside of the United States, and in developing countries in particular, is that it may be difficult to obtain observed weather data required for validating the accuracy of the chosen downscaling method to reproduce historical climate, a key requirement for assessing the usefulness of any future climate impact analysis. A rapid method of obtaining downscaled future climate data using models which are already globally validated to observed datasets would therefore greatly expand

the availability of such data to scientists and policy planners wishing to conduct future climate impact analyses.

The objective of this study was to develop a rapid and simple method for creating future climate inputs for the WEPP model. WEPP is a continuous simulation, physically-based model which uses process-based equations to predict runoff, soil erosion, water balance, and crop yield with input from four parameter files: slope topography, crop/land management, soil, and climate. Climate input to WEPP is normally simulated using the CLIGEN stochastic weather generator (Nicks et al., 1995), which requires monthly means of daily weather for various temperature and precipitation statistics stored in a parameter file. The goal of this project was to devise a method of creating CLIGEN parameter files which takes less than 15 minutes and has a minimal learning curve. The purpose of this paper is to describe the tool developed and the procedure to use it together with CLIGEN and WEPP model simulations. We also present results of example applications. The MarkSim® Decision Support System for Agrotechnology Transfer (DSSAT) Weather Generator was used to downscale climate data from various GCMs under three SRES scenarios for multiple future time periods.

2.3 Materials and Methods

MarkSim® is a weather simulator based on a third-order Markov Chain process which predicts the occurrence of a rain day (Jones and Thornton, 1993, 1997, 1999, 2000) and as a result of its continuous development over the past 20 years, is now a globally valid model. MarkSim® has been calibrated to the WorldClim dataset which incorporates historical weather data from a number of databases including the National Oceanic and Atmospheric Administration's (NOAA) National Climate Data Center (NCDC) Global Historical Climatology Network (GHCN), which uses stochastic downscaling and climate typing to downscale future climate projections for the IPCC GCM model families (Hijmans et al., 2005; Jones and Thornton, 2013). The DSSAT weather file generator was developed for use with the DSSAT crop model, but can also be used to produce rainfall, temperature, and solar radiation information for other model applications.

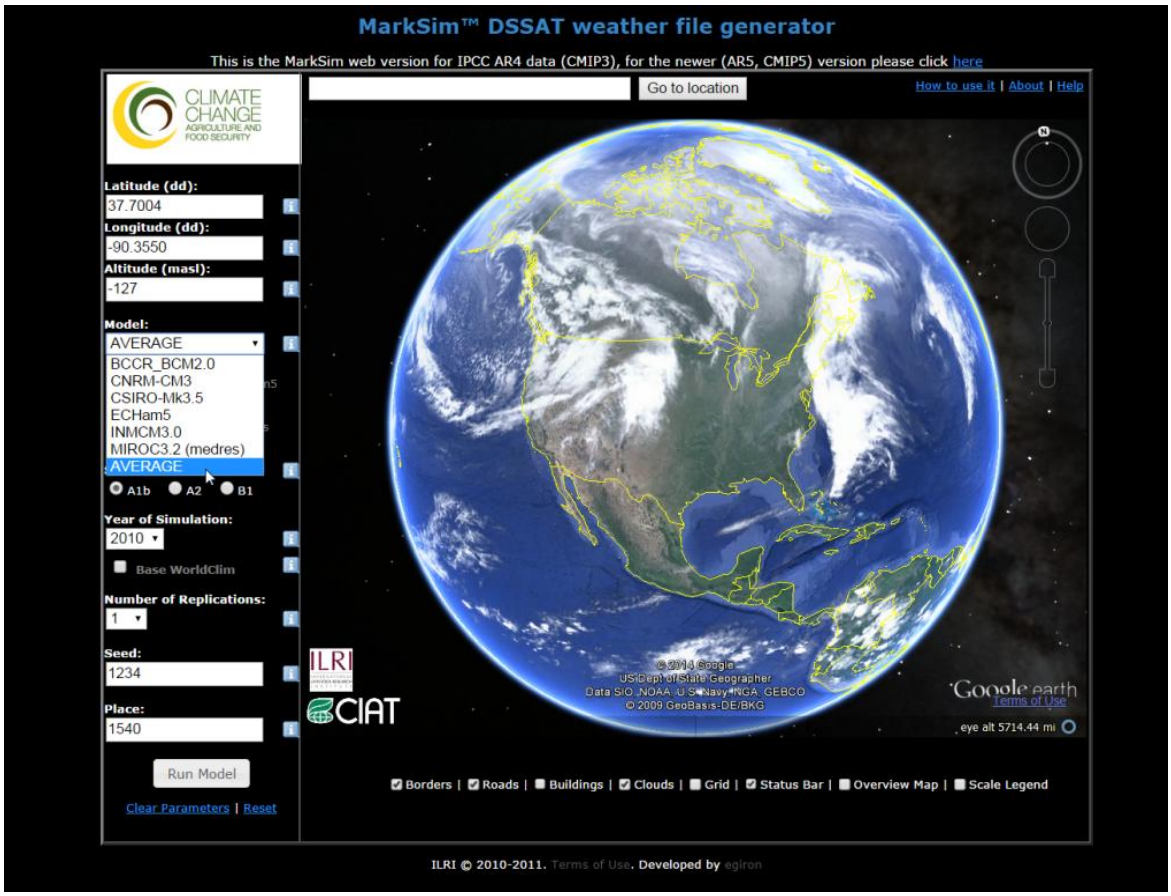

Figure 2.1: Screen captured image of the MarkSim® DSSAT Weather Generator for the IPCC 4th Assessment Report, available online at http://gismap.ciat.cgiar.org/MarkSimGCM/

In addition to the standalone DSSAT weather generator, an easy-to-use online web application (http://gismap.ciat.cgiar.org/MarkSimGCM) has also been released to retrieve MarkSim® model output (Figure 2.1) for the 4th IPCC assessment report (Pachauri and Reisinger, 2007). The web application downscales future climate data from 6 GCMs using 3 SRES scenarios from the IPCC 4AR (Pachauri and Reisinger, 2007). An ensemble average of the 6 GCMs is also available. The data generated are representative of a climate that could be expected within a 10-year time slice. The user can also specify a number of replications to produce, each containing continuous daily series for precipitation, minimum temperature, maximum temperature, and solar radiation.

The MarkSim® DSSAT weather file generator web application was used to acquire downscaled future climate data on a daily time step. A Microsoft Excel VBA macro (Figure 2.2) specifically designed as a user interface was then used to produce and write a CLIGEN parameter file based on the future climate data. CLIGEN is a stochastic weather generator which generates daily weather variables for a single location using summary statistics for precipitation, temperature, solar radiation, and wind patterns derived from historical observations (Nicks et al., 1995). Initially, 40 replicates representing 40 years of daily future weather were generated, based on the observation that existing CLIGEN .par files were typically generated from around 40 year periods of record. The replicates are downloaded from the web application as 40 individual text files formatted for use in the DSSAT model; aggregation is needed to format the data for use with CLIGEN.

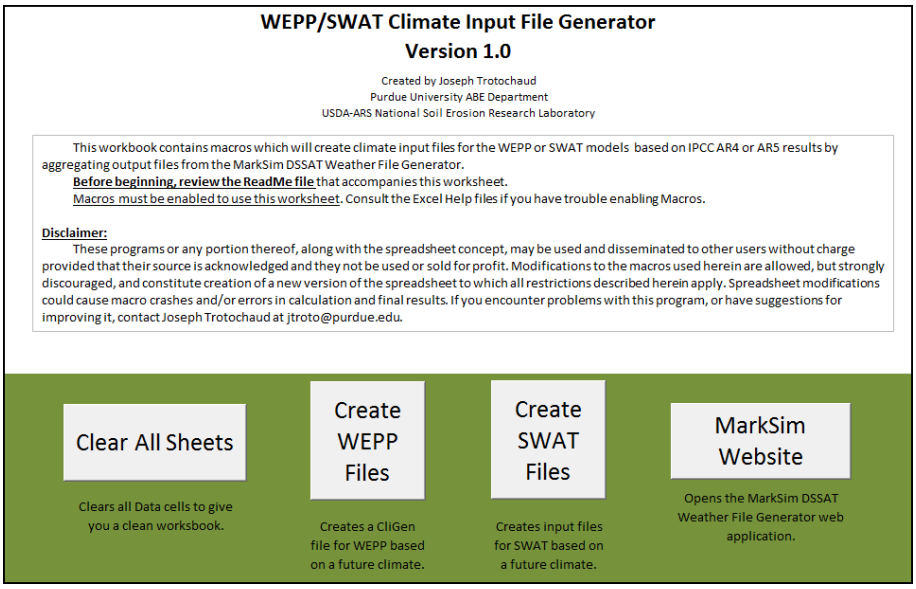

Figure 2.2: Screen captured image of the main screen of the Excel VBA Macro

The Microsoft Excel VBA macro automated importing, analyzing, aggregating, calculating the necessary statistics, and writing the CLIGEN .par file, a process which undertaken manually takes several hours. The function of this macro is similar to adding a climate station in the WEPP windows interface, with the added benefit of being able to visualize the data, compare the new data with other CLIGEN .par files, and make changes to the data before creating a new .par file. Microsoft Excel was chosen for

several reasons, the most immediate being its availability on most computers. Additionally, file reverse-compatibility and VBA persistence over multiple releases of Excel eliminates compatibility issues, as confirmed by testing on three computers with different Excel releases and Windows operating systems.

2.3.1 Calculated Values

For non-precipitation variables, the CLIGEN parameter file (.par file) requires mean and standard deviations for minimum temperature, maximum temperature, and solar radiation variables. Monthly standard deviations and means for temperature and solar radiation were determined using conventional methods in which all days of the month were aggregated. Precipitation statistics were calculated based only on those days in which precipitation occurred. Additional probability variables required by CLIGEN include the probability of a wet day following a wet day ($P_{W/W}$), probability of a wet day following a dry day ($P_{W/D}$), and a skew coefficient for the distribution of the precipitation data.

Mean daily dew point temperature for future climates ($T_{DPfuture}$) was determined using the delta change method based on the historical and future mean temperatures, as direct prediction and calculation of this variable are not possible using the MarkSim® output. The following equation was used:

$$T_{DPfuture} = (T_{future} - T_{hist}) + T_{DPhist} \qquad (2.1)$$

where T_{future} is the mean daily projected future temperature, T_{hist} is the mean daily historical temperature for the location, and T_{DPhist} is the historical mean daily dew point temperature.

2.3.2 Assumed Values

CLIGEN uses several variables which relate to storm intensity distribution curves that require sub-daily or sub-hourly future climate data to calculate. Most GCMs report climate variables on daily time steps, and most do not forecast precipitation directly but regress precipitation based on other atmospheric variables. This makes it difficult to forecast daily rainfall with any confidence, more so at the sub-daily level required for

peak intensity hyetographs. Nearing et al. (1990) found in a detailed sensitivity analysis of WEPP that the peak rainfall intensities and time to peak rainfall intensities did not play a significant role in soil loss prediction.

Table 2.1: Summary of parameter data sources for modified CLIGEN .par file inputs

Parameter description	CLIGEN variable	Line in .par file	Source		
			Historical .par file	MarkSim® output	From macro
Max 6hr and 30min precip. depth	TP5/6	3	X		
Mean precip. for a wet day	MEAN P	4		X	
Standard deviation of daily precip.	S DEV P	5			X
Skewness coeff. of daily precip.	SKEW P	6			X
Prob. of wet day after a wet day	$P_{W/W}$	7			X
Prob. of wet day after a dry day	$P_{W/D}$	8			X
Mean daily max. air temperature	TMAX AV	9		X	
Mean daily min. air temperature	TMIN AV	10		X	
Standard deviation of TMAX AV	SD TMAX	11			X
Standard deviation of TMIN AV	SD TMIN	12			X
Mean daily solar radiation	SOL.RAD	13		X	
Standard deviation of SOL.RAD	SD SOL	14			X
Mean max. 30min precip. Intensity	MX .5P	15	X		
Mean daily dew point temperature	DEW PT	16			X
Time to peak rainfall intensity	Time Pk	17	X		
Wind direction and speed values	WIND	18-82	X		

Therefore, based on the lack of downscaled sub-daily data, historical values for variables related to intensity were assumed for the future climate. The macro extracts these values

from a user-specified historical CLIGEN .par file from the WEPP database. Over half of the text in a CLIGEN .par file provides information on surface wind direction and speed (Table 2.1). Synoptic-scale wind patterns at higher altitudes are modeled within GCMs, but the turbulence associated with near-surface wind patterns is not, forcing historical near-surface wind patterns to be assumed for the future climates, also from the historical CLIGEN .par file.

2.3.3 Validation

MarkSim® downscales future data by calibrating 20th century output from the GCMs to match the WorldClim data through Markov Chain regression (Jones and Thornton, 2013). The regression equations developed are then applied to 21st century output from GCMs to create downscaled future climate data. For the United States, the WorldClim dataset primarily utilized NCDC data, so the 20th century calibration data from MarkSim® should closely match the historical CLIGEN files which were derived from National Weather Service (NWS) data. The option to download the calibrated MarkSim® 20th century climate for 1961-1990 (herein referred to as the MarkSim® baseline) exists. To determine if the MarkSim® baseline climate matched well with the historical .par file from the WEPP directory created from NWS data (herein referred to as the WEPP baseline), the macro was written to include a graphical and tabular comparison of the .par file created from the MarkSim® baseline and the WEPP baseline for all calculated variables.

Climate data were compared for twelve locations in the contiguous United States (Table 2.2). These were chosen based on their spatial separation, different climatic regimes, unique agricultural conditions, and availability of a WEPP baseline for that site. Comparisons were also performed by conducting WEPP version 2012.8 model simulations under both baseline climates as well as for three future time periods forecast by MarkSim® under the IPCC SRES A1b storyline (Pachauri and Reisinger, 2007). WEPP runs were conducted for four sites representing one good (WI), two acceptable (CO, IN), and one poor (GA) fits according to correlations between MarkSim® baselines with WEPP baselines as described in the previous paragraph. CLIGEN version 5.3 was

used with the Fourier interpolation scheme to simulate 100 years of weather. A USLE Unit Slope, 22.1 m long at 9% uniform grade, was used throughout, with soils specific to each region as determined by USDA Natural Resources Conservation Service (NRCS) soil surveys. Tilled fallow field conditions were used throughout. WEPP 100-year model simulations were run for each climate, with annual means analyzed for percent change from the WEPP baseline and MarkSim® baseline.

2.4 Results and Discussion

Validation comparisons for each of the twelve sites were conducted using Q-Q plots to indicate how well the MarkSim® baseline reproduced a particular variable compared to the WEPP baseline. The MarkSim® baseline showed a mix of good and poor fits, with temperature expectedly showing a better fit than precipitation as indicated by both Q-Q plots and R^2 values (Figure 2.3). Mean precipitation showed mixed results, with stations in the southern and southeastern United States showing the poorest, most scattered Q-Q plots. All other regions' mean precipitation correlations were better with R^2 greater than 0.47. Mean precipitation correlations were best in Wisconsin (WI) and California (CA) with $R^2>0.80$, although the MarkSim® baseline under-predicted the precipitation mean and standard deviation for the CA site. Precipitation standard deviations were also mixed, with an average R^2 of 0.43, and only five sites had $R^2\geq0.50$. Precipitation skew coefficient fits were poor for all sites and had scattered Q-Q plots, as was also evidenced by low correlation across sites. R^2 values for the twelve sites' precipitation variables are shown in Table 2.2.

Initially, low means and skew coefficients for precipitation were observed from the MarkSim® baseline. Upon removal of days in which precipitation was below 1.0 mm, the standard deviations and skew coefficients had much better fits to the observed data. Errors in the historical CLIGEN .par files were ruled out by reanalysis of historical data from the NCDC. The scattered nature of the Q-Q plots for precipitation skew could not be explained. Probability values for $P_{W/W}$ were generally poor and showed non-linear correlation for most sites. $P_{W/D}$ showed a better fit than $P_{W/W}$ as was evidenced by higher

R^2 values for all but one site. NCDC reanalysis was also conducted to create historical CLIGEN .par files which had identical periods of record to the MarkSim® Baseline (1961-1990), but showed R^2 and Q-Q plots similar to the WEPP Baseline. This ruled out differences in the periods of record as an explanation for the poor correlations.

Table 2.2: Coefficients of determination for regression comparisons of precipitation variables for MarkSim® and WEPP baseline climates

Site	Mean Precip.	S.D. of Precip.	Skew of Precip.	P(W/W)	P(W/D)
San Bernardino, CA	0.80	0.49	0.01	0.65	0.87
Boulder, CO	0.57	0.80	0.01	0.52	0.76
Clermont, FL	0.47	0.23	0.04	0.48	0.55
Tifton, GA	0.02	0.01	0.00	0.03	0.30
Waterloo, IN	0.77	0.67	0.37	0.25	0.56
Springfield, MO	0.48	0.27	0.00	0.00	0.25
Greenville, NC	0.23	0.04	0.00	0.00	0.18
Bismarck, ND	0.60	0.44	0.00	0.00	0.50
Albany, NY	0.71	0.67	0.00	0.31	0.38
Portland, OR	0.64	0.48	0.10	0.87	0.74
El Paso, TX	0.48	0.19	0.05	0.22	0.87
Merrill, WI	0.89	0.93	0.01	0.71	0.75

Q-Q plots for the four representative sites used in WEPP simulations are shown in Figure 2.3. Wisconsin (WI) showed the best overall fit, with R^2 values over 0.80 for all but the skew variable. Tifton, Georgia (GA) was the worst, with 4 out of 5 precipitation variables having $R^2<0.04$. These four sites were further analyzed to determine if changes in the number of years replicated by MarkSim® had any effect on correlation to historical data. All metrics had lower R^2 values for sample sizes less than 45. For sample size over 50, R^2 increased for precipitation mean and variance, but decreased for the probability and skew values. Therefore, while the macro allows the user to download and generate a future .par file based on 1-99 replications, a sample size of 50 is recommended.

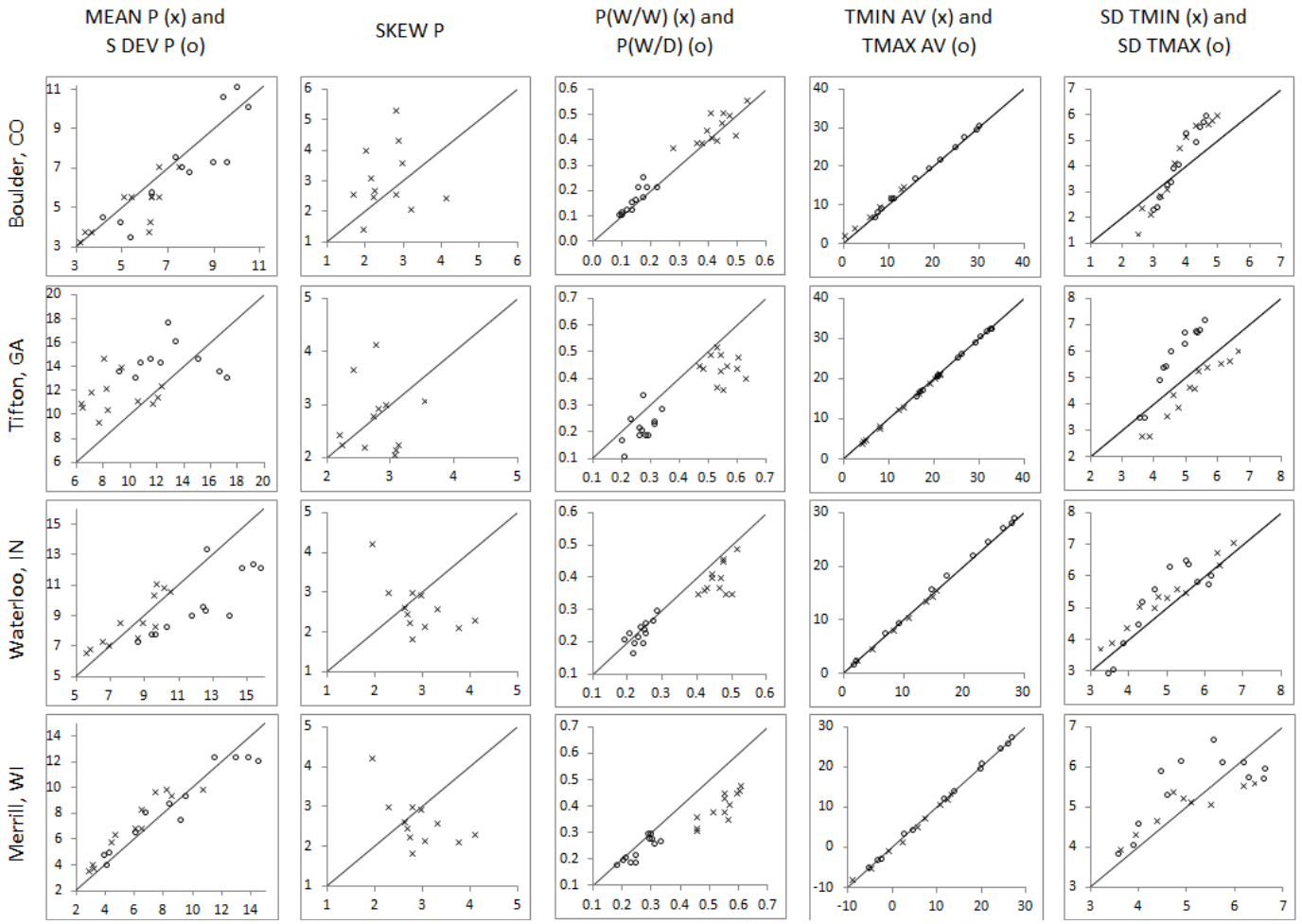

Figure 2.3: Selected Q-Q plots for MarkSim® baseline (horizontal axis) comparison to WEPP baseline (vertical axis) 20th century files. Units for precipitation in mm, temperature in degrees Celsius. 1:1 Line shown as solid black on each plot. For variable names, refer to Table 2.1.

WEPP erosion model outputs for hydrology and sediment loss were analyzed for each site under five climates: the WEPP Baseline, the MarkSim® Baseline, and MarkSim® forecasts for three future climates in 2050, 2070, and 2090. Hydrology was analyzed for total precipitation, total number of precipitation events, total number of runoff events, and the proportion of runoff events to precipitation events (Table 2.3). The proportion of runoff events to precipitation events gives an indication of whether the number of storms capable of producing runoff will change compared to the baseline climate. Comparison shows that total precipitation differences between MarkSim® baseline and WEPP baseline were low, while changes in the average annual number of precipitation events, number of runoff events, and proportion of precipitation versus runoff events were much greater. The MarkSim® baseline simulations show less precipitation events at the Boulder, CO site due to MarkSim® underpredicting the $P_{W/D}$ and $P_{W/W}$ for some months. Alternately, the MarkSim® baseline shows greater precipitation and runoff events for the other three locations due to an overprediction of $P_{W/W}$ to a much greater degree. The paradoxical increase in runoff events for the Boulder, CO site can be explained by the overprediction of summer rain-day depths, with most of the rain historically occuring during the summer months for that location. While the results of the hydrology values alone give an idea of the general climatic changes between potential climate scenarios, runoff and sediment results show the implications of these changes.

In general, each site examined showed substantial variation between the two baseline climates while showing more obvious trends when comparing the MarkSim® baseline to the three future periods (Table 2.3). Even at the site with the highest level of correlation between the MarkSim® baseline and the WEPP baseline climates (WI), the runoff and sediment loss results were different enough to question absolute evaluation of sediment loss when comparing the WEPP baseline with the three future periods. As such, it is recommended that the future climate inputs created by the macro be used to compare only *relative* changes in runoff, sediment loss, and precipitation due to climate change. In that case, one would compare the MarkSim® baseline to the three future periods, and avoid using the WEPP baseline climate when conducting impact studies.

Precipitation and runoff trends simulated by WEPP for the four representative locations (Figure 2.4) showed variations among sites which indicated that future climate impacts will be regional in nature. In the already arid region around Boulder, CO, precipitation decreases further, while an increase in total precipitation was observed for the Midwestern climates of IN and WI. While WI showed an increase in precipitation and runoff by 2090 (Table 2.2, Figure 2.4), the sediment yield increased by a much greater percentage (Table 2.4), implying that the frequency of intense, erosion-inducing storms will increase for this region. Unlike WI, GA shows a more direct correlation between rainfall, runoff, and erosion where all three variables decrease slightly with time. For the Waterloo, IN location, runoff frequency was predicted to increase by 23% to 51%, compared to an 8% to 31% increase in precipitation event frequency, implying that the frequency of runoff-inducing storms will increase.

Unlike the other three locations, the Boulder, CO location had a predicted decrease in all precipitation, runoff, and soil loss variables. A common theme at all four sites was a decrease in the number of snowmelt events and runoff depth from snowmelt. This is likely due to the increase in temperature at all four sites of almost 4°C, as shown in Figure 2.5. It is possible that the increase in runoff from rain at the IN site from 2000 to 2050 is due to less snowfall/snowmelt and more rainfall/runoff, although the same trend is not seen in the two later periods. Determining the replacement of one type of runoff with another would require additional analysis which is beyond the scope of this paper, so it may be more beneficial to compare total precipitation and the number of runoff events to simulated erosion to gain a better understanding of the frequency of erosion-inducing events (Table 2.4).

Table 2.3: Average annual precipitation and runoff results from WEPP v2012.8 for the four representative locations

Climate	Precipitation		Precipitation Events		Runoff Events		Precip as Runoff	
	Depth	Diff.	Storms	Diff.	Events	Diff.	% as Runoff	Diff.
	mm	%	Avg/Year	%	Avg/Year	%		%
Boulder, Colorado								
WEPP	439	-	85.9	-	1.1	-	1.27	-
MarkSim®	421	-4.1	71.7	-16.5	1.3	16.5	1.77	39.6
2050	422	-3.9	75.7	-11.9	1.0	-7.3	1.33	5.2
2070	407	-7.2	80.8	-5.9	1.0	-9.2	1.22	-3.4
2090	391	-10.8	86.3	0.4	0.8	-28.4	0.90	-28.7
Tifton, Georgia								
WEPP	1185	-	102.1	-	16.2	-	15.84	-
MarkSim®	1200	1.2	133.7	31.0	18.3	12.9	13.65	-13.8
2050	1152	-2.7	134.2	31.4	19.3	19.2	14.36	-9.3
2070	1134	-4.3	136.1	33.3	17.1	5.9	12.59	-20.5
2090	1165	-1.7	135.9	33.0	18.3	12.9	13.44	-15.1
Waterloo, Indiana								
WEPP	867	-	100.8	-	5.3	-	5.30	-
MarkSim®	890	2.7	109.3	8.4	6.6	22.7	5.99	13.2
2050	936	8.0	109.8	8.9	7.2	34.3	6.53	23.3
2070	957	10.4	110.6	9.7	7.2	33.9	6.46	22.0
2090	977	12.7	132.0	30.9	8.1	8.1	6.12	15.5
Merrill, Wisconsin								
WEPP	759	-	103.8	-	3.4	-	3.24	-
MarkSim®	819	7.9	128.9	24.1	4.9	44.3	3.76	16.3
2050	825	8.7	106.1	2.2	7.3	116.4	6.85	111.7
2070	879	15.9	106.1	2.2	7.2	113.7	6.77	109.1
2090	896	18.1	107.2	3.2	7.5	123.5	7.01	116.6

CLIGEN v5.3 generated weather inputs. Precip as Runoff category represents the percentage of the number of precipitation events which produce runoff. WEPP is WEPP baseline climate. MarkSim® is MarkSim® baseline climate. Diff. is change from WEPP baseline climate.

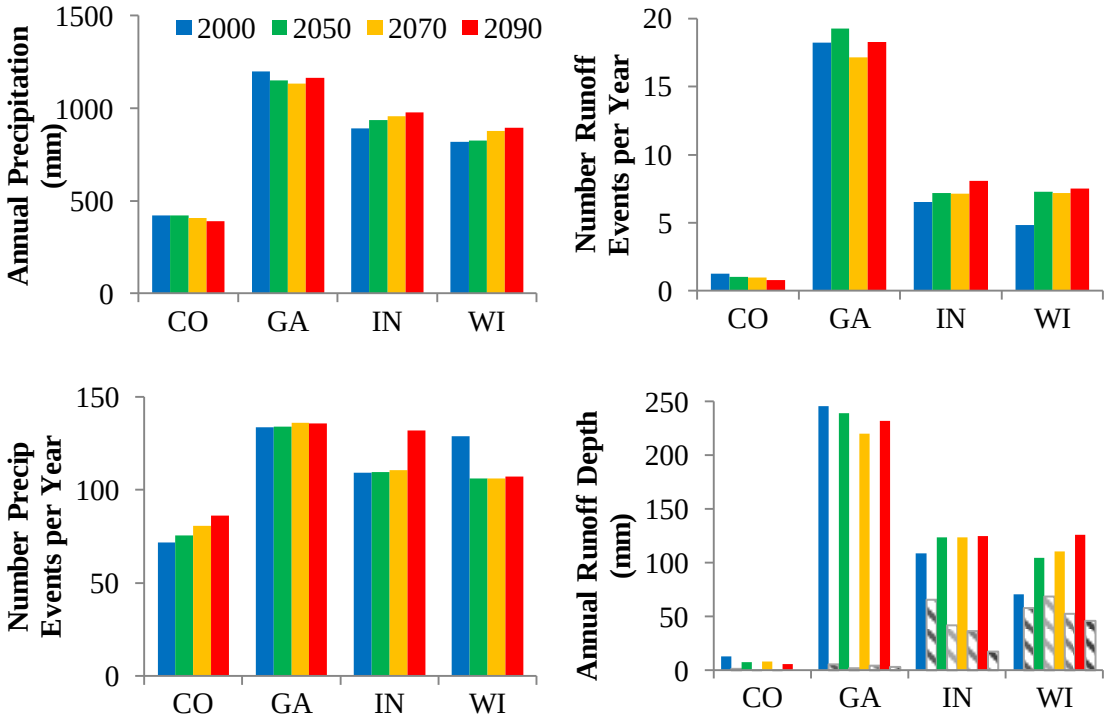

Figure 2.4: Average annual precipitation and runoff outputs from WEPP. Runoff depth from snowmelt appears as diagonal-filled bars to right of runoff depth from rain as solid bars.

Table 2.4 highlights the predicted changes in runoff, interrill detachment, and total detachment (soil loss) over the next century. Total runoff (from both rain and snowmelt events) was predicted to decrease between 5% and 19% at the Waterloo, IN location. Interrill and total detachment changes, however, were mixed, ranging from decreases in 2070 of 4.5% to 3.1%, respectively, to increases of up to 10% in 2050. Impacts of predicted climate changes in Merrill, WI were much more pronounced, with average annual runoff increases of up to 35% and average annual soil losses increasing between 33% and 54%. For both of these locations, decreasing snow cover and melt, and increasing runoff from rainfall were the main factors. At the Boulder, CO site, average annual runoff was predicted to decrease by 50% to 60%, and an associated soil loss decrease of 41% to 56%, indicating that at this semi-arid location future climate will become drier (and warmer, Figure 2.5), with lower risks of soil erosion by water. For the

Tifton, GA location, predicted average annual runoff decreased by 5% to 10% compared to 2000, while total soil loss was predicted to decrease by 3 to 9%. The slightly decreased average annual precipitation, combined with the increased temperatures at the GA site modified the water balance towards more evaporation and somewhat less runoff and soil loss.

Table 2.4: WEPP predicted average annual runoff, interrill detachment, and total detachment from the hillslope profile simulations at the four locations.

Climate	Precipitation		Precipitation Events		Runoff Events	
	Amt./Yr. mm	Diff. %	Amt./Yr. T ha^{-1}	Diff. %	Amt./Yr. T ha^{-1}	Diff. %
Boulder, Colorado						
2000	3.70	-	3.29	-	10.1	-
2050	1.97	-49.8	1.95	-40.7	5.34	-47.1
2070	1.97	-46.8	2.09	-36.5	5.95	-41.1
2090	1.47	-60.2	1.69	-48.6	4.43	-56.1
Tifton, Georgia						
2000	63.7	-	50.8	-	102	-
2050	60.8	-4.58	46.3	-8.9	98.5	-3.4
2070	57.0	-10.6	45.6	-10.2	93.2	-8.6
2090	59.6	-6.48	48.1	-5.3	98.6	-3.8
Waterloo, Indiana						
2000	44.2	-	15.6	-	74.9	-
2050	42.1	-4.80	16.5	5.8	82.4	10.0
2070	40.6	-8.10	14.9	-4.5	72.6	-3.1
2090	36.0	-18.5	16.1	3.2	76.2	1.7
Merrill, Wisconsin						
2000	32.6	-	12.0	-	48.8	-
2050	43.9	-34.9	15.1	25.8	65.6	34.4
2070	41.4	-27.1	14.1	17.5	65.0	33.2
2090	43.6	-34.0	17.3	44.4	75.1	53.9

MarkSim® is MarkSim® baseline climate. Diff. is change from MarkSim® baseline climate.

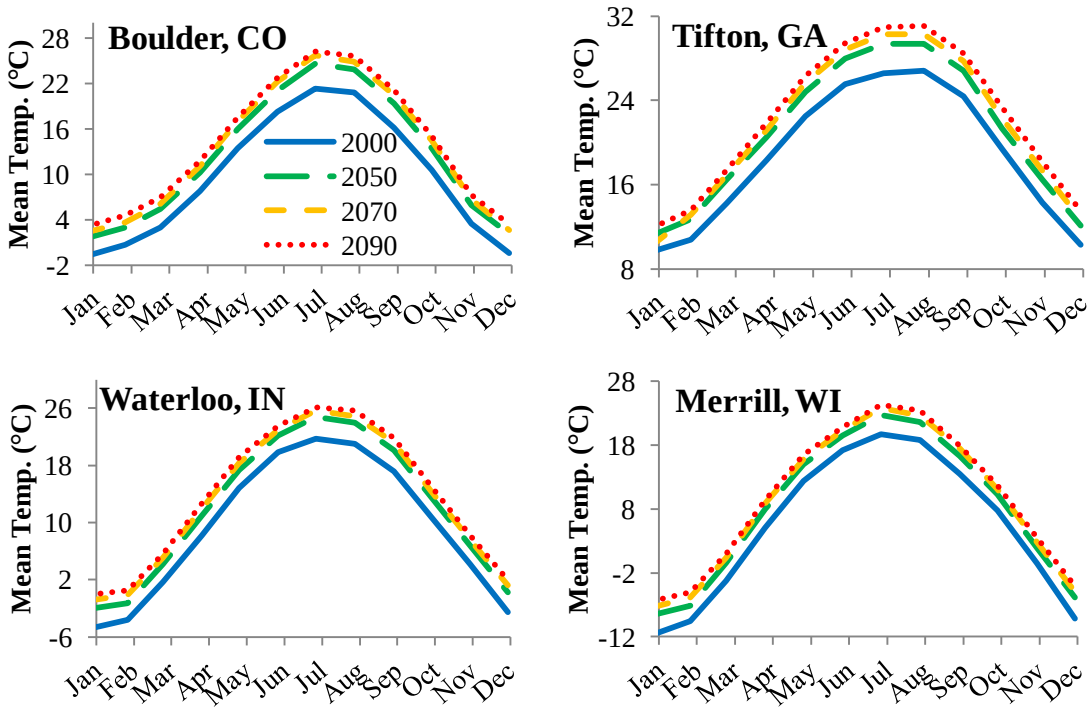

Figure 2.5: Mean monthly temperature at the four representative locations for the four simulated periods.

There are several advantages to the method outlined in this paper for obtaining future climate data for the WEPP model. A .par file ready for use with CLIGEN in WEPP takes less than 15 minutes to create on a modestly equipped computer, and the learning curve to use this method is virtually non-existent, since the MarkSim® application uses the familiar Google Earth interface and completes the downscaling, while the macro formats the file properly using automated scripts. The Microsoft Excel VBA Macro described in this paper is available free-of-charge from the internet (http://www.ars.usda.gov/Research/docs.htm?docid=24824) and includes a detailed step-by-step instructions manual for downloading the data from MarkSim® and creating CLIGEN/WEPP or SWAT input files.

As with all climate model downscaling, each GCM and/or downscaling technique may not be appropriate for some regions. A model developed in Europe may not adequately represent North America, while more heterogeneous landscapes may require more

advanced downscaling methods to adequately fit GCM output to a specific location. A verification tool is included in the Excel workbook to determine if the method demonstrated in this paper is suitable to a site. The verification tool consists of scatter plots showing the monthly CLIGEN parameters generated by the VBA macro using the MarkSim® baseline climate alongside the default WEPP .par file for the same location. In this way, users can obtain a rough idea of how well MarkSim® recreates historical climate at the site in question by comparing the scatter plots for both baseline climates. As has been shown here, more advanced downscaling methods may be required in regions where MarkSim® poorly replicated historical climates. The primary assumption with using this method lies in the accuracy of the MarkSim® downscaling model; however the verification tool can validate the MarkSim® baseline for specific locations. Another concern is raised with regards to the iterative aggregation and disaggregation of data inherent in MarkSim®; the MarkSim® weather generator aggregates GCM data, and then statistically reproduces daily time series. These replications of a statistical nature are then summarized by the macro and used as the input for another weather generator. This creates the possibility for compounding errors which originate in either the CLIGEN or MarkSim® weather generator. The differences in period of record for each site and the MarkSim® baseline climate cannot be ignored either, as the period of record for the MarkSim® historical climate is fixed from 1960-1990, while .par files which come with WEPP may have periods of record extending many years earlier and/or later than that 30-year window. However, recreating historical .par files based on observed NCDC weather station data did not substantially improve R^2 values at the 4 selected sites.

The method described here for climate inputs to WEPP was also modified to create continuous daily data for use with the Soil and Water Assessment Tool from the same spreadsheet (SWAT, Arnold et al., 1998), after a request from another researcher. This was accomplished by using portions of the macro used to create the WEPP .par file to string together multiple replicates of MarkSim® daily output, end-to-end, to create the 4 relatively simple climate input text files used by SWAT (daily precipitation, daily minimum air temperature, daily maximum air temperature, daily solar radiation). More

information and an example application with SWAT are described in Flanagan et al. (2014). Additionally, the VBA macro source code is unlocked, and can be edited by the user for adaptation to other climate data which is reported in a similar format to MarkSim®.

2.5 Conclusions

The MarkSim® DSSAT weather generator was used to generate downscaled future climate datasets for precipitation, minimum temperature, maximum temperature, and solar radiation values on a daily timescale. The data was then aggregated and formatted into parameter files for use with the CLIGEN weather generator via a user-friendly tool created using a macro-enabled Microsoft Excel Workbook. The macro makes obtaining future climate inputs for the WEPP model fast and simple. Additionally, the ability to create SWAT model climate input files was also added as an option with the tool.

Twelve locations throughout the contiguous United States were analyzed using Q-Q plots and R^2 values to determine that the WEPP baseline parameter files and those created by the MarkSim® baseline climate differed enough that only relative changes in erosion should be calculated using this downscaling method. WEPP outputs generated for four representative locations were compared for the two baseline climates as well as 3 future time periods and showed that regional variations in precipitation and temperature due to future climate change will have different impacts on water balance, runoff, and soil erosion depending on geographic location.

During the writing of this paper, a new version of the MarkSim® web application was released which generates future climate data based on the IPCC Fifth Assessment Report (5AR) data (http://gisweb.ciat.cgiar.org/MarkSimGCM/). The baseline MarkSim® climate generated using the IPCC AR5 data showed slightly better R^2 values at the four selected sites, but the improvement was not substantial enough to be considered different from the baseline climate comparisons made in this paper. The format of the files from

this updated application are identical to those referenced in the methods portion of this paper, and can be used in the same manner with the same macro.

CHAPTER 3. AN IMPACT ANALYSIS OF CLIMATE CHANGE FOR A SMALL AGRICULTURAL CATCHMENT IN THE UNITED STATES MIDWEST USING WEPP AND THE IPCC FIFTH ASSESSMENT REPORT

3.1 Abstract

The effects of predicted future climate change are variable from region to region, and the extent to which greenhouse gas emissions and temperature changes will affect precipitation, crop production, sediment loss, and runoff is still being examined. New methods for obtaining future climate data for use with natural resource models allows scientists and engineers to evaluate and design agricultural practices to adapt to predicted changes in climate change earlier, in order to mitigate the potential harmful effects of climate change or capitalize on opportunities for agricultural investment. Analysis of a small (6.7 acre, 2.71 ha) field site monitored as part of the USDA-ARS Conservation Effects Assessment Project in NE Indiana was conducted to determine the effect of climate change on agricultural resources. Precipitation, runoff, soil erosion, and crop growth were modeling using the Water Erosion Prediction Project (WEPP) model and the four Representative Concentration Pathway (RCP) scenarios from the Intergovernmental Panel on Climate Change (IPCC) Fifth Assessment Report (5AR) to determine the effectiveness of common agricultural Best Management Practices (BMPs) under predicted climate change. Decadal analysis of 21st century climate and model results showed that although precipitation will increase, sediment loss and runoff will decrease due to a reduction of concrete frost conditions during late winter. An increase in the amount of precipitation falling in spring and earlier soybean senescence will also lead to increased soil loss in early spring and fall, which favored field management practices which maximize ground cover during those periods. Overall, the best management option into the future will likely include in-field (no-till, grassed waterway) and edge-of-field (buffer strips) practices to reduce soil migration to lower slopes as well as filter fine

sediments from runoff and increase infiltration prior to discharging agricultural runoff to receiving waters.

3.2 Introduction

Potential impacts of climate change on agricultural production in the United States have been examined in-depth and are widely understood to vary from region to region (Howden et al., 2007; Hatfield et al., 2011, 2014). Elevated atmospheric CO_2 concentrations may increase yields (Southworth et al., 2002b; Karl et al., 2009; Hatfield et al., 2014), while additional spring soil moisture and an increase in the number of extreme precipitation events may delay and reduce crop planting and productivity (Rosenzweig et al., 2002; Hatfield and Prueger, 2004). Higher summer air temperatures could increase the frequency of heat stress and reduce soil moisture through increased evapotranspiration (Southworth et al., 2000, 2002a), and temporal redistributions of rainfall could cause plants to be water stressed during critical growing periods (Hatfield and Prueger, 2004). In addition to plant-growth impacts, changes in soil-water interactions under climate change are important to producers and present environmental concerns for receiving waters of non-point source pollution from farmlands (Nearing, 2001; Nearing et al., 2004). Shifts in the timing of rainfall and maximum temperatures, increases in the number of extreme precipitation events (Fowler and Hennessy, 1995; Lenderink and van Meijgaard, 2008) and a potential shift towards growing more corn and soybeans instead of wheat (Southworth et al., 2002a; O'Neal et al., 2005) also add to soil erosion mitigation practices losing effectiveness (Hatfield and Prueger, 2004). Timely and proactive adaptation is essential to preventing increased agronomic, nutrient, and soil losses as a result of climate change.

Agricultural production in the United States Midwest has come under increasing scrutiny due to hypoxia issues in the Gulf of Mexico where as much as 70% of nitrogen and phosphorus pollution originates from agricultural regions (Alexander et al., 2008) and the increasing severity of algal blooms in the Great Lakes (Michalak et al., 2013). Row crop agriculture must be supplemented with soil management to reduce soil erosion and

nutrient loss from fields. To increase understanding of the effects that agricultural BMPs have on off-site water quality, the United States Department of Agriculture (USDA) initiated the multi-agency Conservation Effects Assessment Project (CEAP) (Mausbach and Dedrick, 2004). The Agricultural Research Service (ARS) portion of CEAP examines fourteen benchmark watersheds in the US, including the 281,000 acre St. Joseph River Watershed in northeastern Indiana. Pesticide and nutrient pollution of drinking water in the city of Ft. Wayne has bolstered persistent monitoring of the watershed by the USDA-ARS National Soil Erosion Research Laboratory (Flanagan et al., 2003, 2008) since 2002. The sites monitored contain soils and agricultural management typical of the entire watershed, and portions of the Midwest by extension. Periods of records in the region are now reaching lengths required for detailed hydrological modeling (Flanagan et al., 2008; Heathman et al., 2008; Cechova et al., 2010; Ascough et al., 2012).

Concurrently, methods for obtaining projections of future climate are reaching the point that localized impact studies can be carried out using a variety of natural resource models. The IPCC has acknowledged that in the past a lack of coherence and quantity of impact studies may be a result of the difficulty associated with obtaining future climate data projections due to resource limitations of researchers (Wilby et al., 2004). In this paper, the WEPP model (Flanagan and Nearing, 1995; Flanagan et al., 2007) is used with the most recent observed data from a small field catchment in the St. Joseph River Watershed to assess the soil erosion mitigation effectiveness of several common agricultural BMPs and management practices under projected future climate. Future climate was defined by using an ensemble of the CMIP5 (Coupled Model Intercomparison Project Phase 5) model family (Taylor et al., 2012) under all four of the RCP scenarios used in the IPCC 5AR.

3.3 Materials and Methods

The WEPP model was used to simulate the impact of climate change on agricultural resources, including water balance, soil erosion, and crop growth, on a small 2.7 ha (6.7

acre) field in the Cedar Creek basin of the St. Joseph River Watershed. Cedar Creek is the largest tributary of the St. Joseph River, draining 707 square kilometers of land roughly three quarters of which is used for agricultural production (Flanagan et al., 2008). Geology in the region consists of poorly drained glacial till with a silt loam to clay loam texture on gently rolling topography with large amounts of surface water depression storage. The field site examined (AS2 in Figure 3.1, N40°27'29" W84°58'06") has been under agricultural management for over a century, and currently with a primarily corn-soybean rotation since monitoring of the site began in 2002. WEPP is a continuous simulation, physically based model, which uses four input files of climate, soil, slope, and management to calculate water balance, soil loss, and crop growth based on fundamental equations (Flanagan and Nearing, 1995).

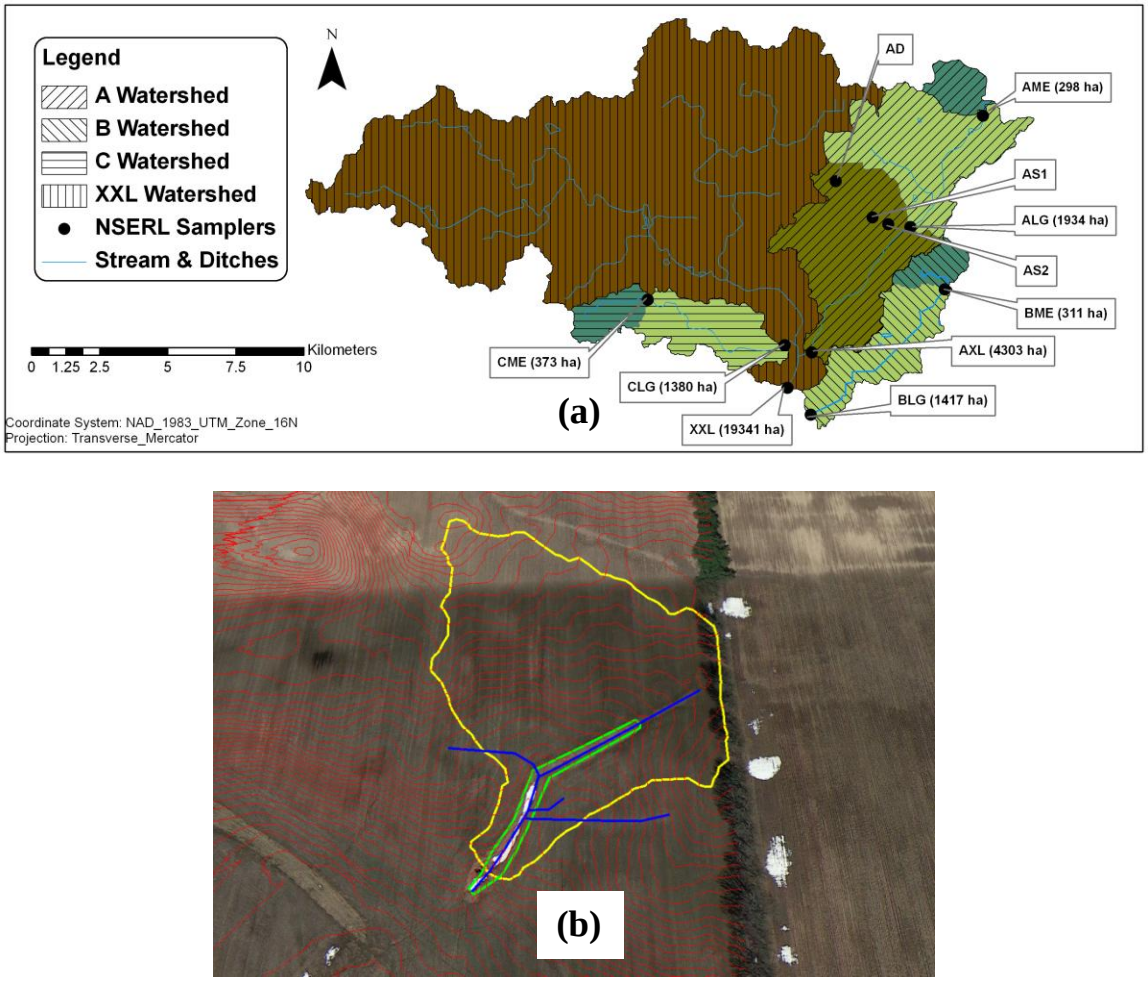

Figure 3.1: a) Map of Upper Cedar Creek, with NSERL monitoring sites from Flanagan et al. (2008). b) AS2 site closeup with waterway (green) and tile lines (blue) highlighted.

3.3.1 WEPP Model Inputs

GIS data were used to define the hillslopes' dimensions and determine flow paths for the watershed model. Subsurface tile drainage is present in the field, but is irregular and the tile condition is unknown; tile drainage routines were not used when building the model inputs.

Automated data collectors have monitored weather and water quantity/quality in a small concentrated flow channel which drains the field site since 2007. An adjacent field site (AS1) has been monitored since 2002, and weather data from the adjacent site was used when conducting calibration/validation of the WEPP model. Temperature and wind speed/direction data were obtained from the National Climatic Data Center (NCDC) (NOAA, 2014), but a reliable and easily accessible source for solar radiation data could not be identified. Since 2004 was outside of the calibration window (2007-2010), the solar radiation values were assumed based on the monthly averages from the period 2005-2011. Solar radiation, temperature, and wind data were taken from the NCDC for 2004 and from the adjacent field site for 2005-2011.

Management files were created based on the farmer's field logs which were provided for at least two years each for soybeans and corn during the calibration/validation window. The management for the field consisted of a corn-soybean rotation with use of harrow-spike tillage and a planter with double disk openers before corn and a no-till drill with single disk openers for soybeans without winter cover or residue management.

3.3.2 Calibration/Validation

Calibration/validation was conducted using the combined weather file from 2004-2011 to calibrate runoff and soil loss, in that order. The calibration window was 2007-2009, the validation window included 2010 and 2011, and 2004-2006 was used as a warm-up period since sediment data were not available for much of that period. Runoff was calibrated by varying the input effective baseline hydraulic conductivity, as well as the soil parameters associated with restrictive layers. The parameters of the restrictive layer

were used to roughly simulate any effects that the existing irregular tile drainage network may have had on hydrology. Specifically, the anisotropy ratio, which is a measure of the ratio of lateral versus vertical flow, was used to approximate the drainage effect of tile tiles. Measurements at the tile flow outlet indicated that the tiles are operable, but the exact depth and condition of the tiles are unknown. Additionally, the WEPP model uses parameters for artificial drainage more common to patterned tile networks, which are inappropriate for the irregular tiles present at the site. By using the anisotropy ratio, the lateral flow effect caused by the cone of depression made by the tiles could be approximated without knowing the exact size, depth and drainage coefficient required by WEPP for the drainage paramenter. While this is an unorthodox use of the anisotropy ratio, the effect of drainage tile on hydrology in poorly drained Midwestern fields was deemed too important to leave out entirely. Soil loss was calibrated by varying the erodibility parameters in the soil file. Soil and management files for all hillslopes were identical within each management scenario. Crop yields were calibrated to match farmer reported values for corn and soybeans.

3.3.3 Future Climate Data

The WEPP/SWAT Future Climate Input File Generator (Chapter 2CHAPTER 2) was used to format output from the MarkSim® DSSAT weather file generator (Jones and Thornton, 2013) web application. The web application allows selection of one of the four RCP scenarios, and an ensemble of one or more of the 17 CMIP5 GCMs. MarkSim® is a third-order Markov chain rainfall generator that predicts the occurrence of a rain day and has been modified to work as a GCM downscaler using stochastic downscaling and weather typing (Jones and Thornton, 2013). Future climate is defined by obtaining daily data for 5 future time slices directly from the GCMs, calculating monthly climate anomalies for each of the future time slices relative to the baseline climatology (1961-1990), and fitting a functional relationship to the future time slices to interpolate years in-between. Spatial downscaling is completed through the use of a climate record supplied by the WorldClim dataset (Hijmans et al., 2005). GCM differentials are calculated using the interpolation of the functional relationships and applied to the climate record using

inverse square distance weighting of the nine nearest GCM cells to create local future climate projections (Jones and Thornton, 2013).

The MarkSim® web application (http://gisweb.ciat.cgiar.org/MarkSimGCM/) produces daily cumulative precipitation, minimum and maximum temperature, and solar radiation in the form of text files. The WEPP/SWAT Future Climate Input File Generator was used to format these text files into a .par file for use with the CLIGEN weather generator (Nicks et al., 1995) in WEPP. CLIGEN was then used to create 100-years of simulated climate on a decadal basis for the 21st century for each of the 4 RCP scenarios from the AR5 CMIP5 model family. Tools in the WEPP/SWAT Future Climate Input File Generator were used to analyze the default WEPP climate files for Waterloo, IN to determine if the WorldClim climate record matched the observed precipitation and temperature data from the region closely enough that the modeled WEPP results could be used to evaluate absolute changes in soil loss, precipitation, and runoff generated by WEPP. Fifty replicates for each decade and RCP scenario were downloaded from the MarkSim® application and formatted using the WEPP/SWAT Future Climate Input File Generator, for a total of 29 .par files including the baseline climate. Each .par file generated by the macro therefore represents a statistical mean for the five years preceding and succeeding each 0-year (i.e. 2030 would represent 2025-2034). The total dataset represents the potential climate from 2015-2094 for each of the four RCP scenarios, plus the historic climates generated by MarkSim® (the MarkSim® Baseline), which represents the years 1960-1990. The .par files were used to generate 100 years of continuous weather data using CLIGEN version 5.3 with a Fourier interpolation method.

3.3.4 Management

Ten potential land-management scenarios were modeled using the calibrated WEPP model (Table 3.1). BMP and conservation practice effectiveness were simulated by modifying the management parameter files within WEPP. The management simulations were divided into three groups. The first group examined the differences between various tillage practices representing the best, middle, and worst case scenarios in terms of

disturbance levels. The second group covered the implementation of common agricultural BMPs used on flatter croplands under the baseline tillage system. The third group included a combination of BMPs and two conservation management options. Grassed waterways were modeled to reflect those which were recently installed at the site.

3.4 Results and Discussion

3.4.1 Calibration/Validation

Flow values which corresponded to dates in which the channel was frozen or the flow was outside of the instrument's readable range were removed from the record obtained from the field site. Runoff peaks were observed on 269 days over 31 months from 2007-2011. A thaw and snow melt event from March 27-31, 2008 resulted in instrument malfunction and was removed from the record.

Table 3.1: List of management scenarios assessed at the Indiana location

Management	Description
Control	Repeated 2-year corn-soybean rotation with spike tooth harrow before corn.
Tillage Managements	
No-Till	Transition to no-till planters for corn and soybeans.
Fall Moldboard	Control management with fall moldboard plowing.
Spring Chisel	Control management with spring chisel plowing.
BMP Managements	
Grassed Waterway	Control management with the addition of 6m wide grassed waterways.
Buffer Strips	Control management with 15m long edge-of-field grassed buffers.
Rye Cover	Control management with rye cover crop planted in the fall.
Conservation Managements	
Alfalfa	Conservation management with low-impact tillage and a corn-soybean followed by a 4-year alfalfa rotation.
Combination	Combination of the No-Till, Rye Cover, Grassed WW, and Buffer managements.
Prairie	Conversion of all fields to continuous brome grass.

Sediment data from the field site are available during events which were field or auto-sampled. A total of 63 sediment loss events were recorded from 2007-2011; however no data were available for 2008. Sediment data were recorded every 30 minutes, so to determine daily sediment totals for each day, the ten minute flow data for the periods corresponding to sediment measurements were used. Since sediment levels in streams are proportional to discharge, the 30-minute sediment concentrations were interpolated over the 10-minute flow data to obtain 10-minute resolution sediment discharge rates. These were then multiplied by the interpolated time step, to obtain total sediment loss over that time step. All sediment losses over each time step during each day were summed to obtain total daily sediment loss.

Optimal calibration results for AS2 were obtained by optimizing the three model quantitative statistics (NSE – Nash-Sutcliffe efficiency, PBIAS – percent bias, and RSR – ratio of the root mean square error to the standard deviation of measured data) outlined in Moriasi et al. (2007). Their conditions state that a model can be considered good if total NSE > 0.50, total RSR is at most 0.70, PBIAS is within 25% for runoff, and PBIAS is within 55% for sediment. All criteria were not met for runoff, as NSE was maximized at 0.481 and RSR total was minimized at 0.721. PBIAS for runoff was 2.05%, indicating that the model tended to only slightly overestimate runoff on the average. Sediment yielded very poor calibration NSE when the calibration window was considered from 2007-2009 (Table 3.2). Sediment data were not available for 2008.

When the calibration/validation window was reduced to only include the initial validation period (2010-2011), sediment modeling efficiencies increased, likely due to the small sample size (26) in the reduced window. Attempts were made to expand the validation window to include 2012 and 2013, but these years only contained 2 and 4 sediment loss events, respectively. Multi-parameter calibration would likely yield better sediment calibration using the larger window, however an extreme runoff event occurred in 2009 which resulted in atypically high sediment yields during the next several observed storms.

Table 3.2: Calibration/validation results for WEPP watershed model

Observation Period		'07-'11	'10-'11
Soil File	K_i (kg s m^{-4})	2.72E+06	2.72E+06
	K_r (s m^{-1})	3.281E-03	3.281E-03
	τ_{crit} (Pa)	5.267	5.267
Mean Daily Sediment Loading	Calibration	98.33	268.18
	Validation	201.71	146.33
	Total	151.23	201.71
Results	NS CAL	-0.062	0.908
	NS VAL	0.809	0.673
	NS Total	0.114	0.809
	RSR Total	0.941	0.438
	PBIAS Total (%)	51.85	7.93

3.4.2 Note on Crop Parameters under Future Climate

The general assumptions of an unchanging crop planting schedule and no change in plant cultivars is unrealistic. Changes in temperature and atmospheric CO_2 concentrations will be important factors in determining future cultivars and management options for farmers. While increasing annual temperatures may make frost tolerance for corn a non-issue in the future (Southworth et al., 2000), maximum daily temperatures above 33.3^o C in August and July have been shown to be negatively correlated to corn yield, and temperatures above 37.7^o C can cause severe damage to corn (Rosenzweig et al., 2002). Southworth et al. (2000) found that rising temperatures could shift corn planting dates to later in the year by 14-39 days by 2050, while Southworth et al. (2002a) found that winter wheat yields would be optimized by planting as early as September 2. Overlap of harvest and planting dates caused by these type of shifts have been speculated to create competition for time in the field (Southworth et al., 2002a) and economic analyses related to yields under higher temperatures have found that wheat may be eliminated from crop rotations in all but the southernmost regions of the Midwest by 2050 (O'Neal et al., 2005). Farmers in the North and Central Midwest may not require soybean cultivar changes to deal with temperature changes, while southern regions will require more heat-resistance (Southworth et al., 2002b). Soybean yields are also very sensitive to CO_2 concentrations, with planting dates for optimal growth and increased soybean yield found to be 50 days later in Eastern Illinois by 2050 (Southworth et al., 2002b).

A very simple analysis of crop yield impacts was conducted using the WEPP model to determine if changing planting and harvest dates would have a significant impact on sediment loss rates. Crop yields were calibrated to the MarkSim® baseline climate using a simplified identical 2-year rotation to match NASS 5-year average statistics for DeKalb County, IN. The Biomass Energy Ratio (BER), a parameter within the WEPP management file which determines growth rate based on photosynthetic activity (Flanagan and Nearing, 1995) was varied to adjust the crop yield. A BER of 62.34 kg/MJ for the 125 bu/ac Jefferson corn management file brought average corn yields up to modern yields, while the soybean biomass energy ratio remained unchanged. These biomass energy ratios were also used when assessing changes due to future climate in sections 3.4.4 and 3.4.5.

Two climates were used in the assessment, the MarkSim® Baseline and the RCP 8.5 2090 climate. The RCP 8.5 climate was chosen for comparison because it showed the greatest deviation in average annual temperature from the baseline condition, and would therefore likely see the greatest change in crop growth given that average annual precipitation and monthly distribution of precipitation were similar for all scenarios by 2090. Crop growth parameters within WEPP were not changed when assessing the future climate, which is to say that the cultivar was not changed for the baseline climate. Planting and harvest dates were shifted earlier and later in the year, while keeping the total time spent in the field unchanged from the baseline condition.

In this manner, average annual crop yield was maximized according to Table 3.3. The purpose of this research was not to assess crop growth changes under future climate, but to determine if soil erosion losses would change in the future. Therefore, the objective of examining optimal crop growth was to determine if changing planting and harvest dates to optimal times would also alter sediment losses. Average annual corn yields by 2090 were 11% higher than in the baseline climate using the same planting dates. Optimal yields were modeled when the growing season was shifted 22 days earlier (April 1), but

yields were only 1% higher than the initial planting dates. Further adjustment of the harvest date resulted in negligible changes to corn yield. Adjusting planting dates later than the baseline did not produce higher yields, regardless of harvest date.

Table 3.3: Comparison of baseline and optimal crop yields obtained by shifting planting dates.

Crop	Planting Date	Harvest Date	Yield
Corn	April 27	November 10	1.28 kg/m^2 (158 bu/ac)
Soybeans	May 10	October 20	0.27 kg/m^2 (40.5 bu/ac)
Corn (2090)	April 27	November 10	1.41 kg/m^2 (174 bu/ac)
Soybeans (2090)	May 10	October 20	0.22 kg/m^2 (31.9 bu/ac)
Corn (Opt. 2090)*	April 10	October 25	1.43 kg/m^2 (177 bu/ac)
Soybeans (Opt. 2090)*	April 1	September 10	0.24 kg/m^2 (35.5 bu/ac)

*Opt. 2090 represents highest modeled yields obtained by shifting planting dates.

Planting and harvest dates were shifted for soybeans in the same manner as corn. Average annual soybean yields by 2090 were 22% lower than in the baseline climate using the same planting dates. Optimal yields were modeled when the growing season was shifted 40 days earlier (April 1), but yields were only increased by 11% over the initial planting dates, or 12.5% lower than the baseline climate using initial planting dates. Further adjustment of the harvest dates resulted in negligible changes in yield. Adjusting planting dates later than the baseline did not produce higher yields, regardless of harvest date. Additionally, changing planting date alone could not bring soybean yields to those simulated under the baseline climate.

For the RCP 8.5 2090 climate, using optimal planting conditions for corn and soybeans in the same management file reduced average annual sediment loss by only 0.2 g/m^2 (0.10%) compared to the future climate using the initial planting and harvest dates. The RCP 8.5 2090 climate represents the most extreme scenario for changes in crop growth, so the degree of shift in optimal planting date, and the subsequent effects on sediment

loss will decrease with reduced scenario severity. Thus, the minimal sediment loss differences between the baseline and optimal condition shown here did not merit the adjustment of cropping dates when assessing BMP effectiveness to reflect a changing climate.

The increase in average annual sediment loss under the 2090 climate was not significantly greater than under the baseline climate ($p>0.05$) when equal cropping practices were applied, but the fact that the differences in future baseline and optimal cropping practices showed little absolute differences indicated that factors other than the cropping practices are affecting sediment loss from the site. Additionally, the optimal planting dates found here contradict previous publications which found that these dates will likely move further into the future (Southworth et al., 2000, 2002b). The differences could be due to those studies' use of the AR4 GCM data, use of crop growth models which also account for increased atmospheric CO_2 levels, or the fact that they also investigated the possibility of cultivar changes in the future.

For this sediment loss study, the modification of planting dates for the most extreme future scenario and time period did not affect sediment losses to a degree which merits the modification of the less severe scenarios and time periods. As such, the baseline cropping practices were maintained for all future climates and time periods. Future research work should look at the potential changes in yields and sediment loss due to cultivar changes using the WEPP model, as well as potentially including effects of increased atmospheric CO_2 levels in future WEPP crop growth equations.

3.4.3 Comparison of MarkSim® Output to Historical CLIGEN .par Files

The MarkSim® and CLIGEN baseline climates were compared using the tools in the WEPP/SWAT Future Climate Input File Generator (Table 3.4). Generally good correlations between the two baseline climates were found for mean precipitation and precipitation probability variables. Differences in mean rain day precipitation and precipitation skew showed no significant variation ($p>0.05$), while the difference in

precipitation S.D. between the two baselines was significant at all confidence intervals. MarkSim® generally underpredicted mean rain day precipitation by an average of 0.53 mm/day (~5% in summer) and overpredicted precipitation S.D. by almost 2.54 mm on average (~20% in summer). While precipitation skew was not significantly different ($p>0.05$) between the two baseline climates, it did show great variability between months. $P_{w/d}$ showed a nearly-perfect correlation in most months both graphically and statistically ($p=0.451$). Differences in $P_{w/w}$ were significant ($p<0.05$), with MarkSim® overpredicting this probability by 0.058 on average.

For non-precipitation variables, temperature showed poor correlations, with significant differences in Mean T_{max} and T_{min} S.D. ($p<0.05$), while differences in Mean T_{min} were only significant when raising the confidence interval to 99.9%. T_{max} S.D. barely met the criteria at the 95% confidence interval ($p=0.064$). MarkSim® consistently underpredicted Mean T_{max} and T_{min} for all months. Temperature standard deviations varied less than the Means, but were underpredicted in all but three months for T_{max} and all but one month for T_{min}. Solar Radiation exhibited great variability, with MarkSim® underpredicting the mean in late winter, and overpredicting the mean during the rest of the year. Summer solar radiation was overpredicted by MarkSim® by 40% above the CLIGEN baseline climate.

3.4.4 Climate Change Impact Assessment

100-year climate files were created using CLIGEN for each decade and RCP scenario from .par files obtained through the MarkSim® DSSAT weather generator and the WEPP/SWAT Future Climate Input File Generator (Chapter 2). Each climate was used as input for 100 years of continuous simulation in WEPP under the baseline management scenario. By fixing all other inputs, differences among climate scenarios were assessed to identify changes in water balance and soil loss resulting from the predicted climate change.

Predicted precipitation under all four RCP scenarios showed similarities with one another in the future (Figure 3.2). When considering all RCPs together, average annual precipitation was predicted to increase by 7-10% by 2100, with the majority of this increase (4-8%) taking place by 2030. From 2030 to 2090, precipitation increased by 2-5%. The highest decadal precipitation occurred in 2070 under the RCP 8.5 scenario at 1006 mm while the minimum occurred in 2040 under the RCP 6.0 scenario at 932 mm. The greatest divergence among scenarios was predicted to occur in 2040, with a difference of 56.3 mm, while the smallest divergence was predicted in 2080 (15.1 mm). The RCP 8.5 scenario had the greatest precipitation totals of any scenario to 2070.

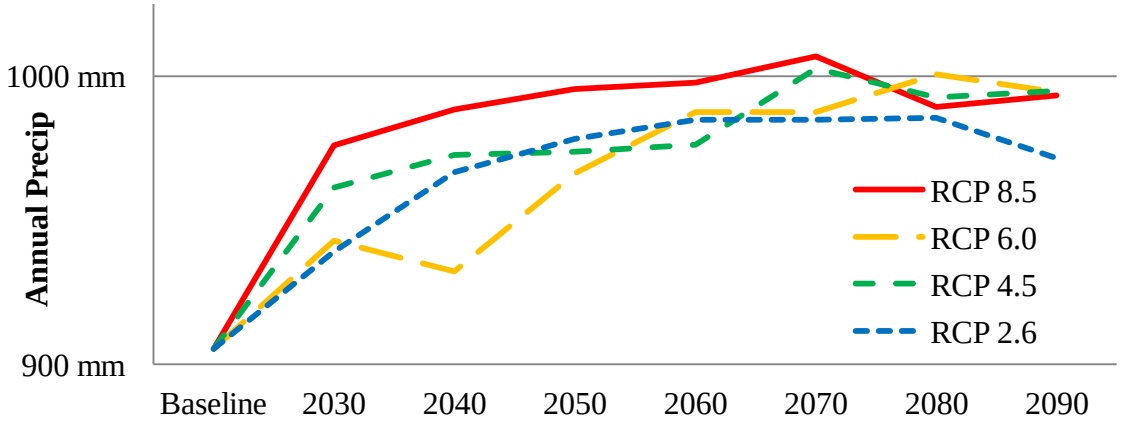

Figure 3.2: Average annual precipitation predicted under all four RCP scenarios for Waterloo, IN.

The extreme jump from the baseline to 2030 for some scenarios was questioned initially, but analysis of NCDC data from Ft. Wayne, IN (the nearest long term weather record available, Figure 3.3) showed that the mean annual precipitation for the area from 1960-1990 was 905 mm, which is within 1 mm of the predicted baseline precipitation produced by MarkSim®. Additionally, extending linear trend lines for the mean annual precipitation from 1960-2014 and 1940-2014 showed that the precipitation was predicted to be between 1000 mm and 1100 mm by 2030, which is a greater value than from any RCP projection used here. This has another implication, in that the increase in average annual precipitation may be slowing for all possible scenarios, and that the largest

increases in annual precipitation for this region may have already occurred by 2030 for most scenarios. Only the RCP 6.0 scenario shows a much larger increase from 2030 on, which was not examined further. Predicted monthly precipitation averaged for the entire future period is shown in Figure 3.4. May had the largest increase in predicted precipitation (>25%), while November showed no change when averaging all decades. June through December showed minimal increases of between 0% and 4% over the future period, while the late winter and spring months had predicted increases of between 9% and 28%.

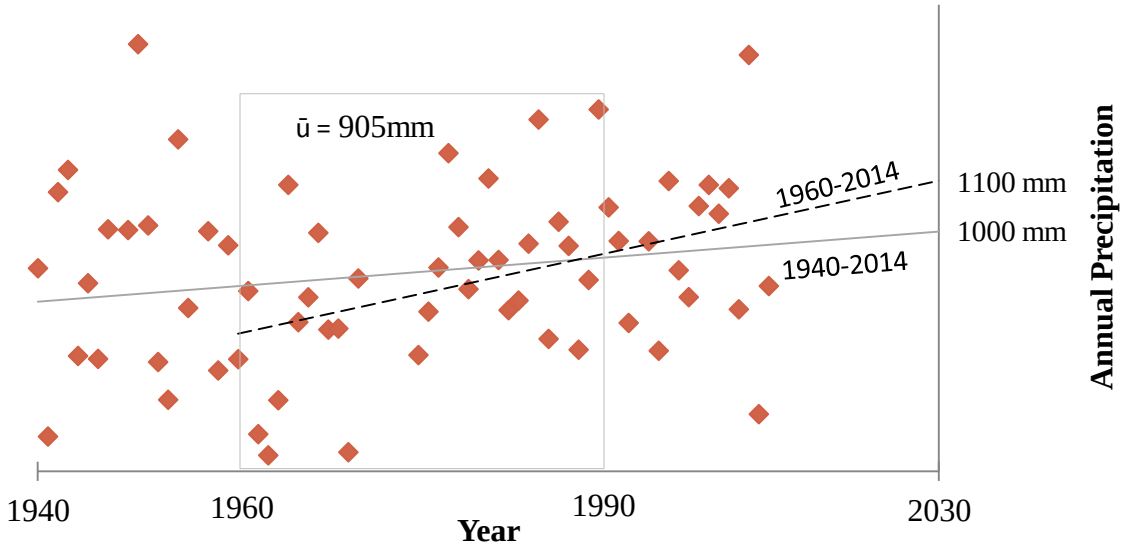

Figure 3.3: Annual observed precipitation totals for Fort Wayne, IN. 1940-2013

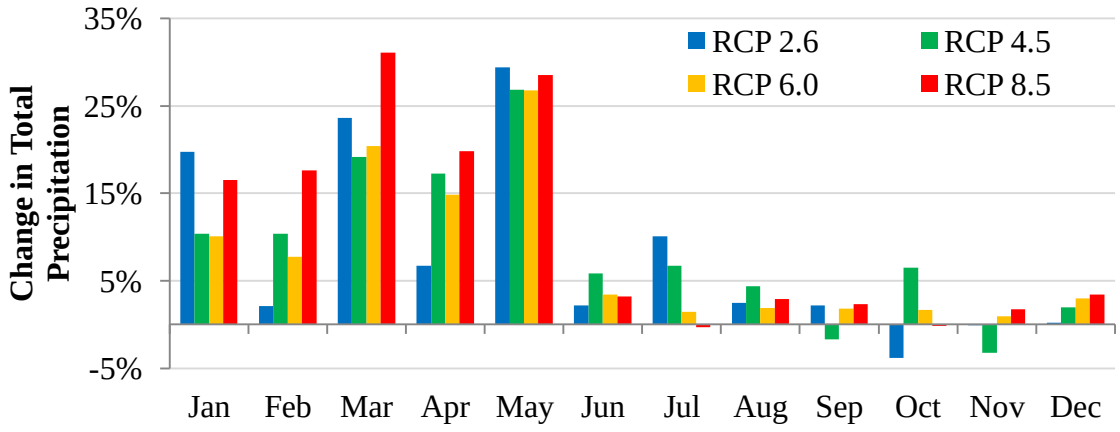

Figure 3.4: Predicted change in average monthly precipitation for 21st century for Waterloo, IN.

Modeled runoff results indicated that factors other than precipitation affected the predicted changes in runoff into the future (Figure 3.5). Of interest was the observation that runoff dropped in the early century, peaked in mid century, then decreased towards the late-century. The RCP 8.5 scenario decreased to the lowest level of any scenario by 2090, which could indicate that temperature had some effect on runoff generation. Average monthly runoff analysis (Figure 3.6) indicated runoff changes which were not obviously correlated to precipitation changes. Of note is the decrease in runoff for February and increase in runoff for spring and fall. As with precipitation, this scenario had only a marginal impact on runoff volumes, while the divergence between scenarios was greater here than it was for precipitation.

Table 3.4: Comparison of MarkSim® and CLIGEN baseline CLIGEN parameters for Waterloo, IN.

	Month	Jan.	Feb.	Mar.	April	May	Jun	July	Aug.	Sep.	Oct.	Nov.	Dec.
CLIGEN baseline climate parameter values (1959-1995)	Mean P (mm)	6.60	6.86	7.37	8.38	8.64	10.92	11.18	10.67	10.41	8.64	7.62	7.11
	SD P (mm)	7.87	7.37	7.87	9.14	9.65	12.19	12.45	12.19	13.46	9.40	9.14	8.38
	$P_{w/w}$	0.36	0.35	0.35	0.46	0.49	0.35	0.37	0.37	0.40	0.41	0.45	0.40
	$P_{w/d}$	0.22	0.21	0.25	0.30	0.26	0.27	0.23	0.20	0.20	0.17	0.23	0.24
	Mean T_{max} (°C)	-0.18	1.89	7.76	15.75	22.22	27.35	29.19	28.26	24.68	18.32	9.50	2.52
	SD T_{max} (°C)	6.08	5.88	6.54	6.37	5.24	3.92	3.01	3.12	4.52	5.64	6.42	5.80
	Mean T_{min} (°C)	-9.34	-8.13	-3.19	2.71	8.24	13.64	15.78	14.56	10.62	4.83	-0.53	-6.12
	SD T_{min} (°C)	7.08	6.76	5.51	5.32	5.02	4.39	3.73	3.93	5.04	5.38	5.61	6.37
MarkSim® baseline climate parameter values (1960-1990)	Mean P (mm)	5.32	6.05	6.43	9.44	7.98	9.86	9.72	10.64	9.38	8.03	8.84	6.29
	SD P (mm)	9.89	8.55	8.39	13.41	11.54	14.84	15.15	14.98	13.71	12.55	11.62	9.29
	$P_{w/w}$	0.42	0.39	0.49	0.47	0.49	0.45	0.43	0.46	0.45	0.45	0.49	0.47
	$P_{w/d}$	0.23	0.19	0.24	0.27	0.25	0.28	0.25	0.23	0.23	0.20	0.22	0.25
	Mean T_{max} (°C)	-0.40	1.32	6.78	14.40	21.28	26.33	28.11	27.60	23.84	14.01	8.98	1.79
	SD T_{max} (°C)	6.03	5.80	5.62	5.01	4.32	3.82	3.47	3.52	4.26	4.71	5.51	6.08
	Mean T_{min} (°C)	-9.49	-8.45	-3.57	2.05	8.05	13.38	15.28	14.51	10.61	4.66	-0.64	-6.90
	SD T_{min} (°C)	6.62	6.34	5.82	4.95	4.57	3.91	3.24	3.46	4.27	4.84	5.19	6.34

Mean P is mean daily precipitation on precipitation days, SD is standard deviation.

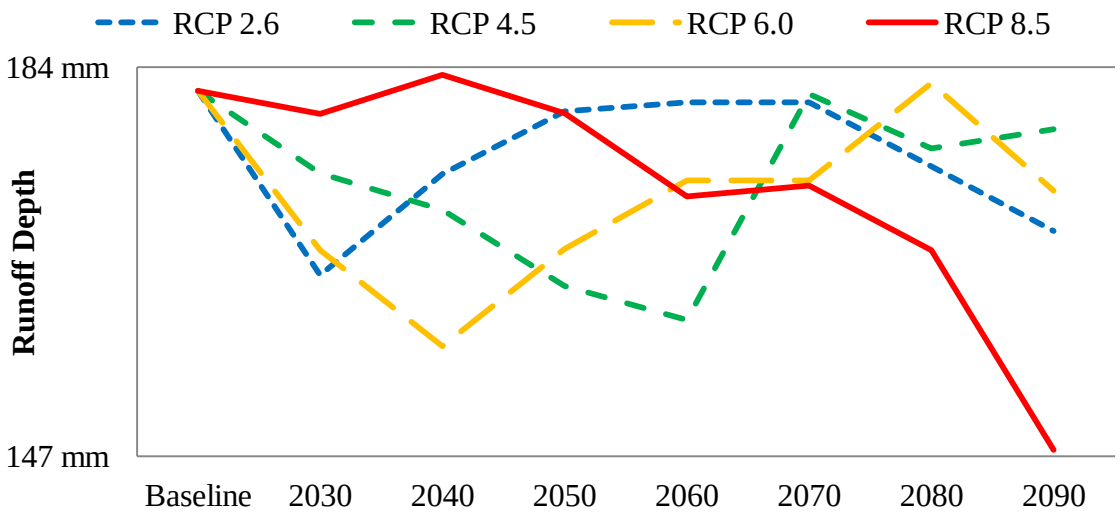

Figure 3.5: Predicted annual runoff under baseline management at Waterloo, IN.

February runoff was predicted to decrease by 35-56% by 2030, and decrease another 10-31% between 2030 and 2090 (Figure 3.7) for a total decrease of 57-68% from the baseline condition by 2090. This decrease in runoff by 2090 contrasts with the 8-22% predicted increase in precipitation for February. Storm frequency and intensity, changes in snowmelt timing, frequency, and intensity, and frequency and intensity of rain on snow events were initially suspected, but could not be correlated to the increase in runoff either alone or together. A condition known as concrete frost may have a significant impact on runoff and erosion from open landscapes in colder regions (Zuzel et al., 1982; Shanley and Chalmers, 1999). Concrete frost is the condition in which a layer of near-surface soil is close to saturation and freezes, reducing effective hydraulic conductivity to zero. Precipitation intensity is not a factor in runoff generation or sediment loss when this condition existed, as rainfall energy is dissipated by overlying snowpack. If a snowpack is absent, sediment loss and runoff are higher during rainfall events due to the low infiltration rates. However, when the soil surface thaws quickly, there is the potential for increased infiltration, and less runoff and sediment loss.

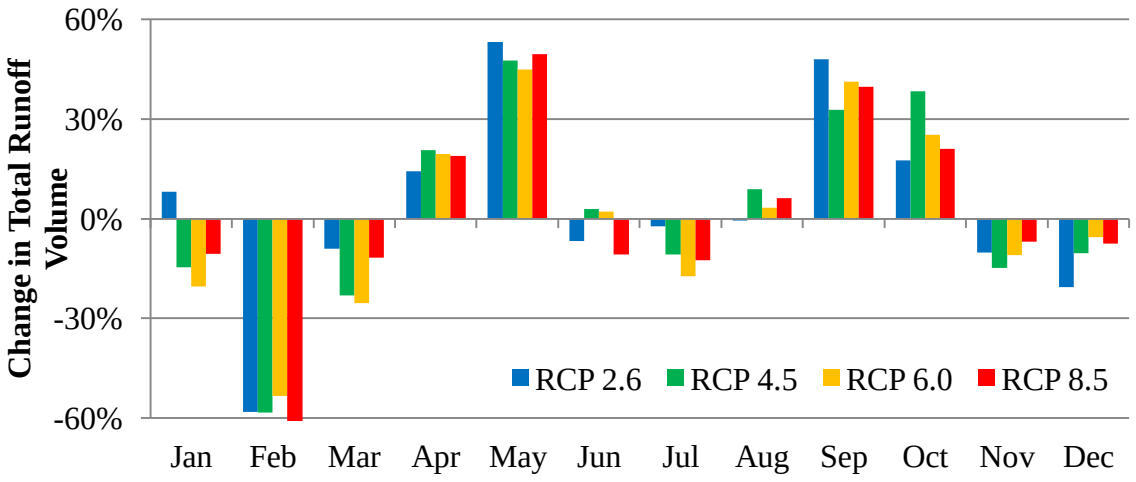

Figure 3.6: Predicted change in average monthly runoff for 21st century at Waterloo, IN.

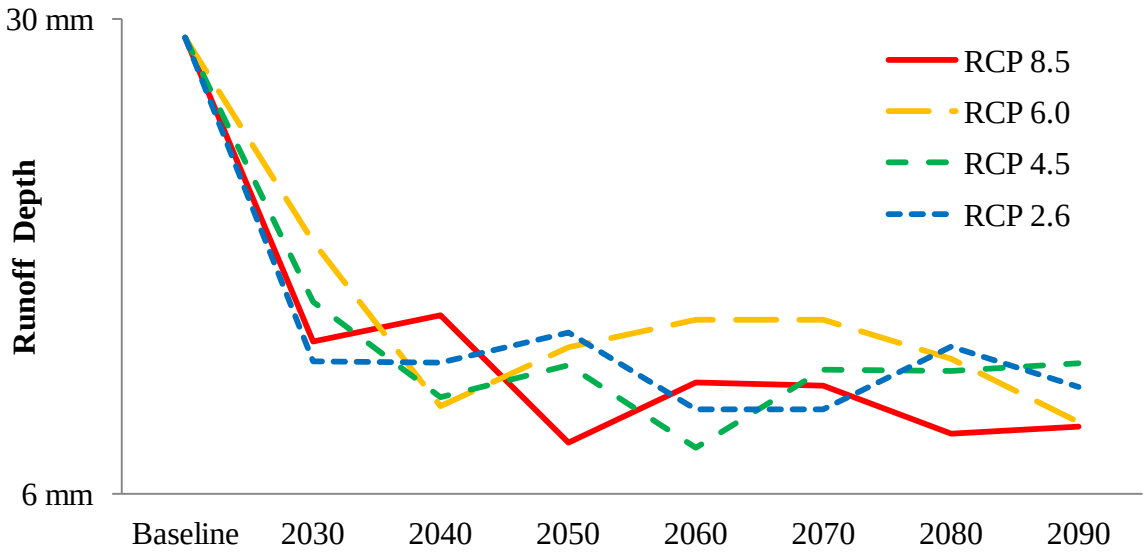

Figure 3.7: Predicted mean runoff depth in February for 21st century at Waterloo, IN.

Analysis of modeled baseline February runoff events for the catchment in this study showed that frozen soil runoff events were visually distinguishable from events in which soils were thawed (Figure 3.8). Additionally, those events which occurred when frozen soils were present showed a direct linear correlation between incident precipitation (rainfall reaching the ground + snowmelt) and runoff, which would be expected if infiltration was zero. Similar trends were observed for all future scenarios. There was a large reduction (67-82%) in the number of events falling on frozen soils in the future.

This transition from frozen to thawed soils resulted in a reduction in runoff (Figure 3.9). The RCP 8.5 scenario showed no frozen soil runoff events larger than 1000 m^3, which were numerous in the baseline climate. Since the thawed events already showed lower runoff volumes per mm of incident precipitation than frozen events, the increase in thawed soil runoff events did not generate enough runoff to replace the larger events coming from frozen soils, leading to the reduction in runoff for February. A similar trend was found in the other winter months and March, which explains the increase in runoff but decrease in sediment for those months as well.

The increase in September runoff was interesting because other months with similar small increases in precipitation showed no or limited increases in runoff. Additionally, canopy cover is at its highest during this period, and therefore, there should be minimal runoff from the fields during this time. As with February, the change in precipitation, runoff, and soil loss by 2030 was to a much larger degree than from 2030 to 2090, and typically peaked in the early to mid century before decreasing towards the end of the century. Years planted in corn saw limited change in runoff from the baseline condition (9-15%), while runoff for soybean years increased by 84-121%. This indicated a crop-specific effect which was causing runoff to increase. Increased air temperatures resulted in more rapid accumulation of growing degree days, and earlier crop senescence. Soybean biomass accumulation was also slightly depressed due to somewhat greater temperature stress, resulting in lower yields and less residue cover. Examining the date of initial senescence showed that senescence shifted back 10-15 days to August 13 or earlier (Figure 3.10). This caused the soybeans to already be fully senesced by September 1, whereas before they did not fully senesce until the middle or end of September. Senescence reduced canopy cover by 90% as well as terminated all plant transpiration. RCP 2.6 produced the lowest average annual runoff for 2030 while RCP 4.5 produced the highest average annual runoff. Average storm intensity and frequency were mostly unchanged from the baseline condition, however the number of storms greater than 40 mm increased sharply in the RCP 4.5 scenario (24%) compared to the baseline and RCP 2.6 scenarios (10% and 15%) (Figure 3.11). This shift also appeared in the form of a

lower cumulative probability plot for RCP 4.5 (Figure 3.12). These larger precipitation depths were tied to runoff volumes greater than 400 m^3 (14.8 mm) from the AS2 catchment, which increased from 6% to 22% of all storms from RCP 0.0 to RCP 4.5.

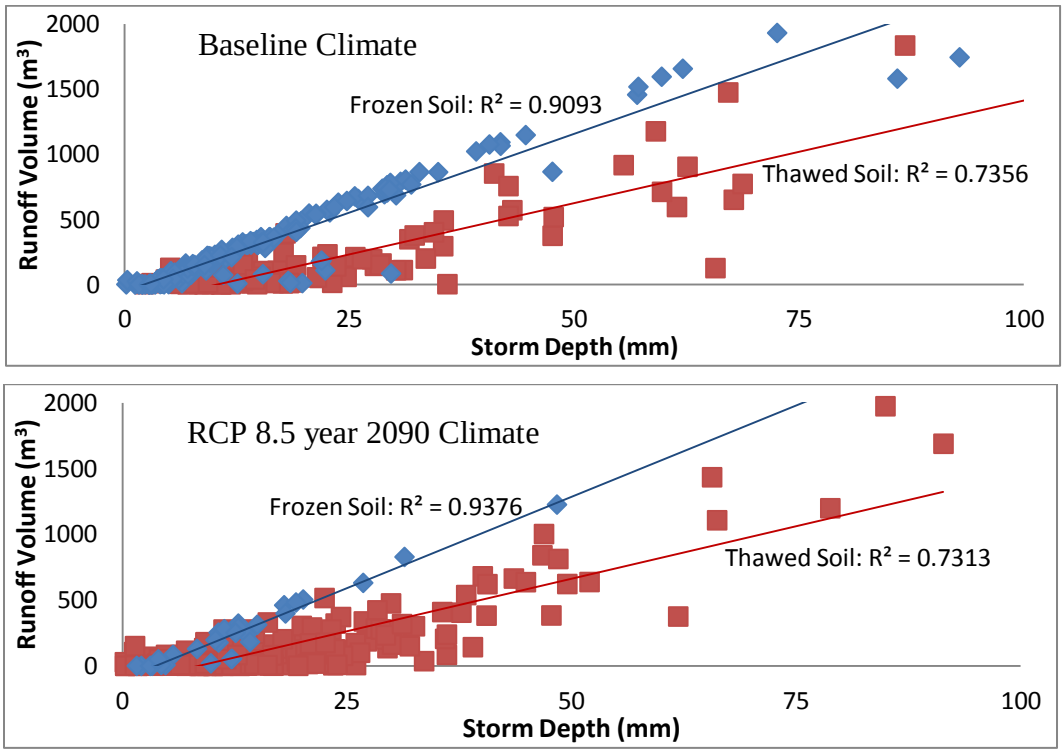

Figure 3.8: Simulated runoff events in February comparing those on frozen (blue) vs. thawed (red) soils for baseline (top) and RCP 8.5 2090 (bottom) climates. Events based on 100 years of weather simulated for each climate. Linear trend lines with coefficient of determination values shown for each soil condition.

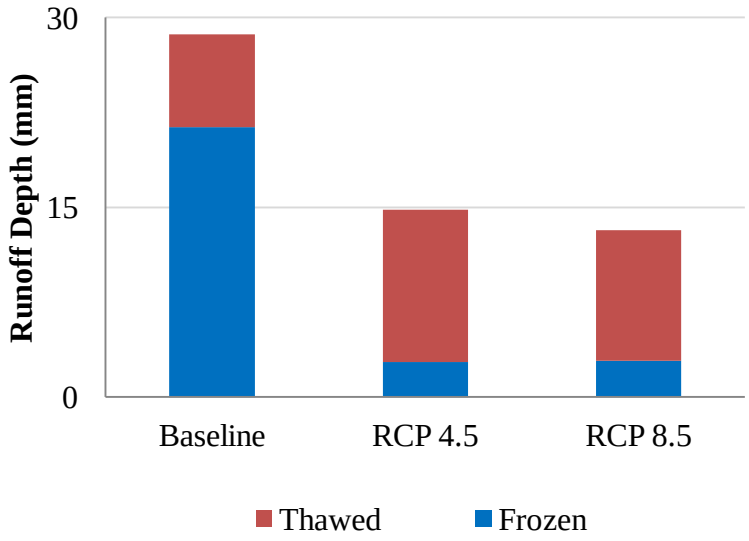

Figure 3.9: Predicted mean February runoff depth for Waterloo, IN, from thawed and frozen soils.

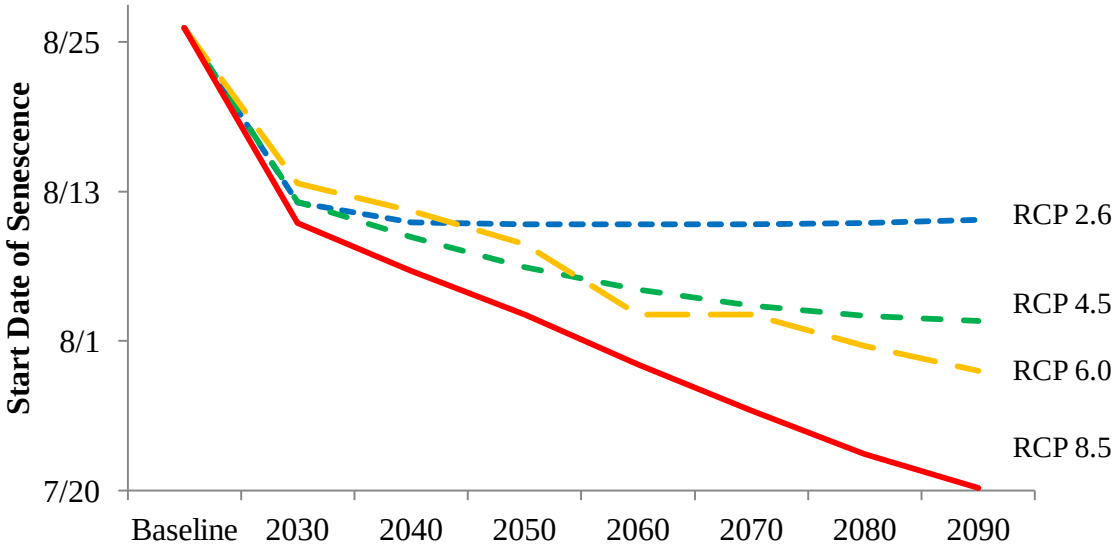

Figure 3.10: Average start date of soybean senescence.

Increases in spring runoff were initially suspected to be due in part to a 15% increase in precipitation. Evidence could not be found for any other contributing factors. Unlike September, the distribution of storm depths and runoff volumes did not change significantly ($p>>0.05$) with regards to the scenario (±1%). Additionally, with crops

planted in late April, canopy cover was not sufficiently established until late May or early June for either soybeans or corn. ET was analyzed, but showed an increase into the future for all scenarios. The increase in precipitation was greater than the increase in ET. The increase in total precipitation for April was also found to be the primary contributing factor to the increase in runoff for that month as well.

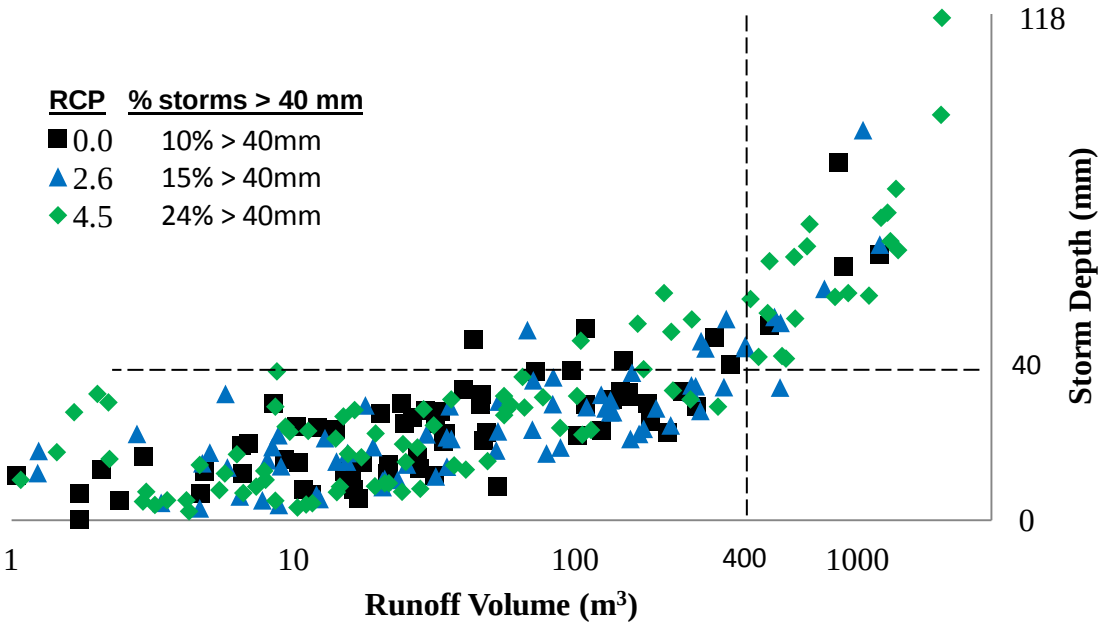

Figure 3.11: Runoff producing precipitation events for September at Waterloo, IN. Events based on 100 years of weather simulated for each climate. 0.0 is baseline climate, 2.6 and 4.5 are RCP 2.6 2030 and RCP 4.5 2030 climates.

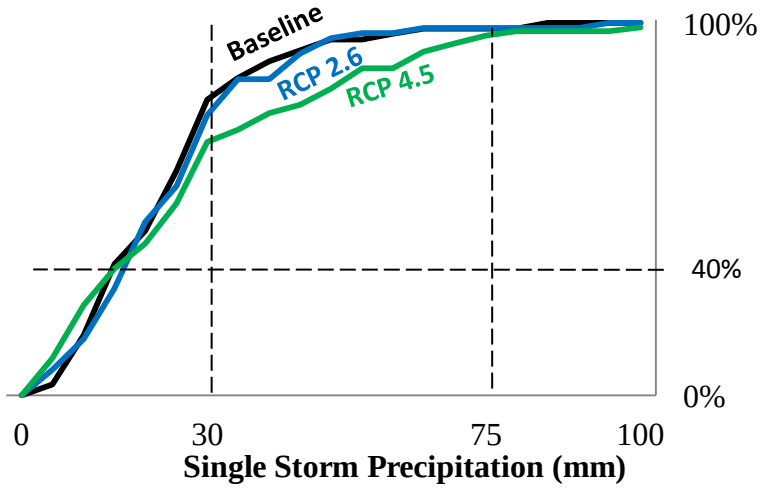

Figure 3.12: Cumulative probability plot for storms from Figure 3.11 (5 mm bin size).

3.4.5 Assessing BMP Effectiveness under Potential Future Climate

BMP effectiveness into the future was compared in two ways. In section 3.4.6, comparisons are made to the baseline climate for all managements, including the control, where percent change is defined as the difference between the average of 21st century climate simulations and the baseline condition for each RCP scenario. That is, each management was assessed for its effectiveness compared to the baseline climate through the 21st century. In section 3.4.7, comparisons are made to the control conditions for all managements using only those model results from the 21st century forecasts, and not to the baseline climate. That is, each practice was examined for its effectiveness compared to the control management through the 21st century. In both comparisons, we found that examining results for each decade presented variability between decades which clouded the overall results and made it difficult to determine the effectiveness of different practices. When considering the average of all decades, more obvious trends could be observed. However, the selection of scenario did have a greater effect on soil loss and runoff than in the previous sections, and these differences will be highlighted.

3.4.6 Comparison to Baseline Climate

Predicted 21st century average annual soil losses for all management are shown in Figure 3.13. Total soil losses were lowest for all BMP management as well as the combination and prairie management, and greatest for the fall moldboard and spring chisel management. Figure 3.14 shows that the alfalfa management had the greatest predicted reductions (18-36%), while the no-till showed the greatest predicted increases (20-68%) in average annual soil loss. The combination of practices had the lowest predicted soil loss under both the baseline and 21st century climates. While the no-till management showed the largest percent increases in predicted soil loss into the future, the absolute changes were less than those for the other two tillage managements. Average predicted soil losses for the 21st century were not significantly different from the baseline climate for the control, grassed waterway, buffer strip, or combination scenarios ($p>0.05$).

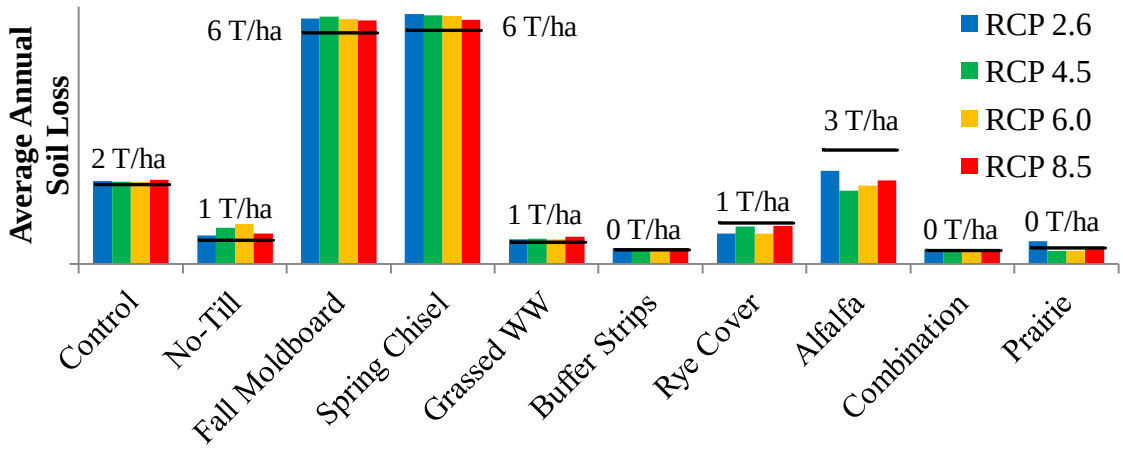

Figure 3.13: Average annual sediment yields for the average of all future decades. Baseline values are shown as dotted black lines over RCP bars.

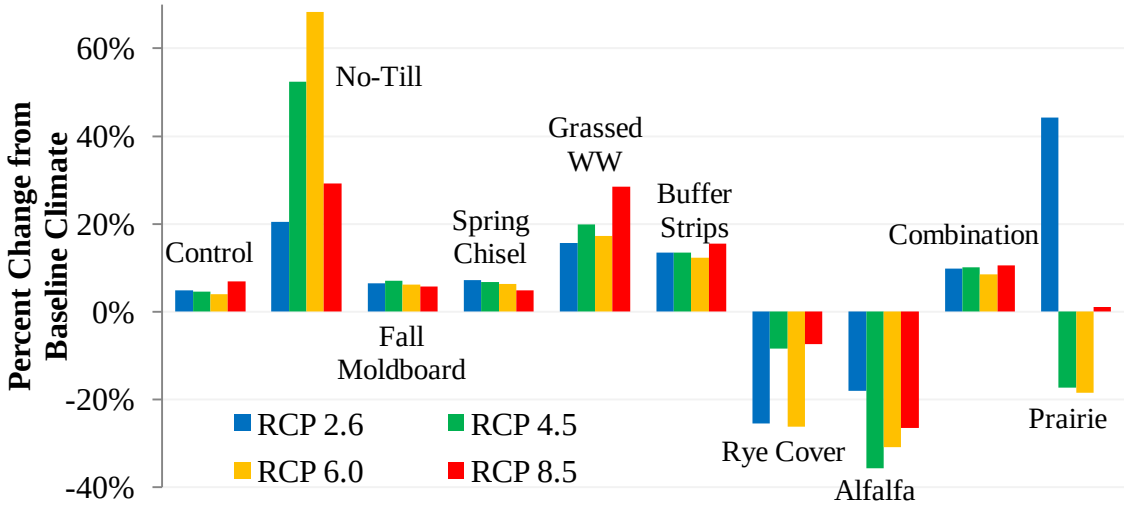

Figure 3.14: Percent change in average annual sediment yields under 21st century projected climates compared to baseline climate for Waterloo, IN, for ten different management scenarios

Runoff results were similar to those for soil loss, with the BMPs that had greater predicted soil loss also having greater predicted runoff volumes. However, all managements except for fall moldboard plow under the RCP 2.6 scenario showed lower runoff volumes compared to the baseline climate (Figure 3.15). This was due in part to the reduction in frozen soils during spring snowmelt events referred to in the previous section. Changes in runoff volume and variation among managements were to a lesser

degree than with soil loss (Figure 3.16). Runoff yield also decreased with increasing RCP (RCP 2.6>RCP 4.5>RCP 6.0>RCP 8.5) for seven of the ten managements examined in this study. The alfalfa and prairie managements showed the greatest predicted reduction in runoff in the future, with both decreasing by an average of 19-20%.

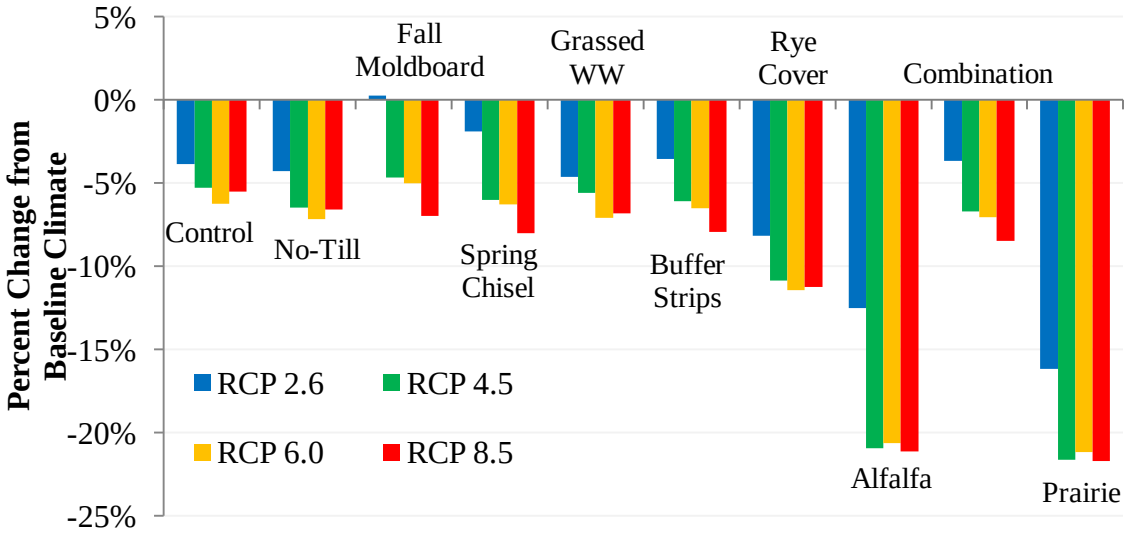

Figure 3.15: Percent change in average annual runoff for 21st century. Forecasts compared to baseline climate at Waterloo, IN for ten different management scenarios.

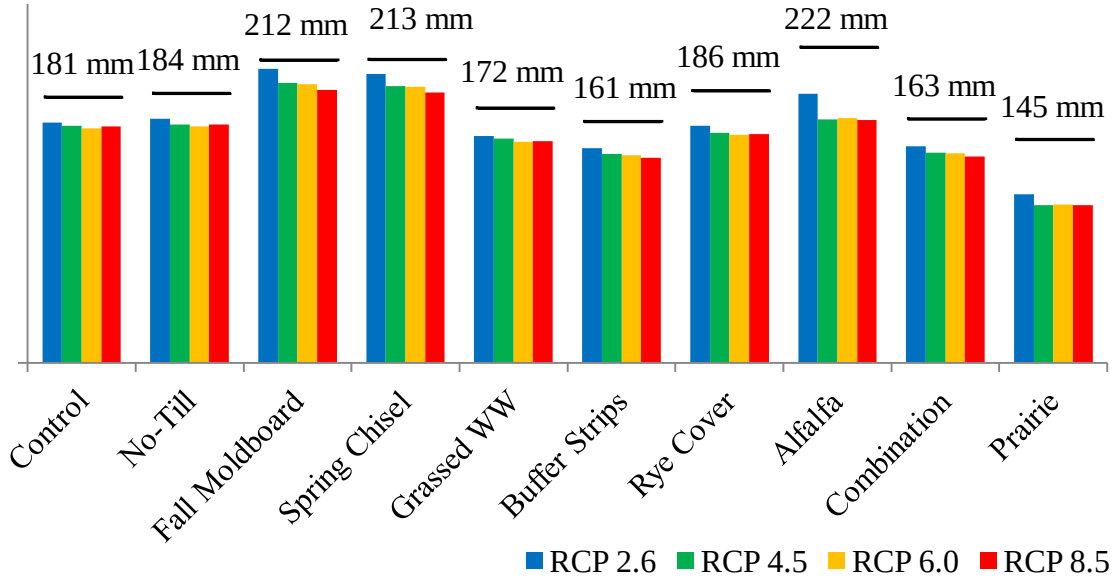

Figure 3.16: Average annual runoff for 21st century forecasts. Baseline values are shown as dotted black lines over RCP bars.

3.4.7 Comparison to Control Management

Predicted soil losses for the no-till, BMP management, and conservation management were lower than the control management for the 21st century climate scenarios (Figure 3.17). Predicted runoff volumes were lower for the BMP management as well as for the combination and prairie conservation management (Figure 3.18). Those scenarios which showed higher or similar sediment losses (fall moldboard, spring chisel, and alfalfa) also showed higher runoff volumes compared to the control management. No-till deviated from this trend by showing minimally greater runoff but over a 50% reduction in soil loss compared to the control. Soil losses for the seasonally plowed management were around 200% higher over the 21st century future climate scenarios compared to the control management, with all management other than alfalfa having greater than 50% decreases in soil loss. The prairie management had the greatest predicted reduction in runoff, while the combination management had the greatest predicted reduction in sediment losses. The combination of grassed waterways, buffer strips, and rye cover crops was only marginally more effective (82% reduction) at reducing sediment losses than the buffer strips alone (81% reduction). The prairie condition had the greatest predicted reduction in runoff, but did not show significantly different ($p<0.05$) soil loss when compared to the combination scenario.

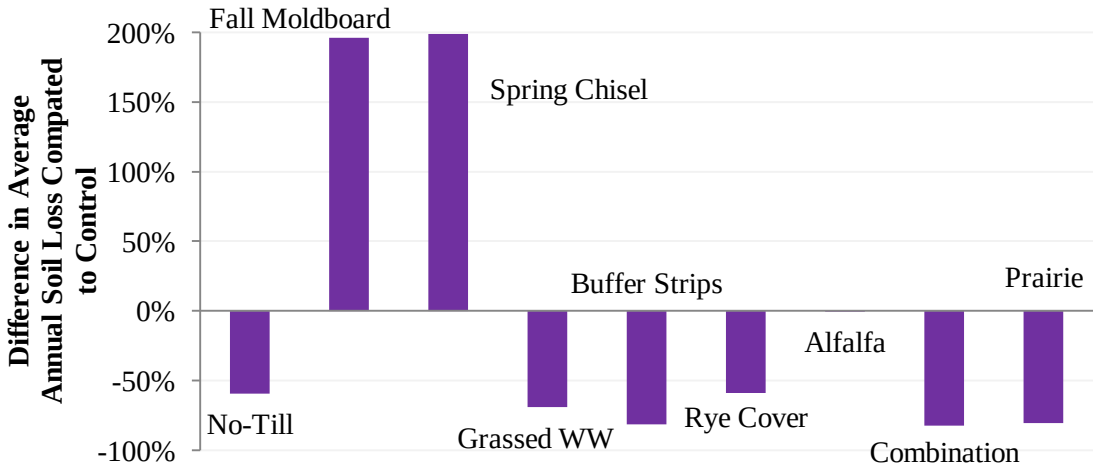

Figure 3.17: Percent difference in soil loss from each management compared to control management. Average results from all RCPs shown.

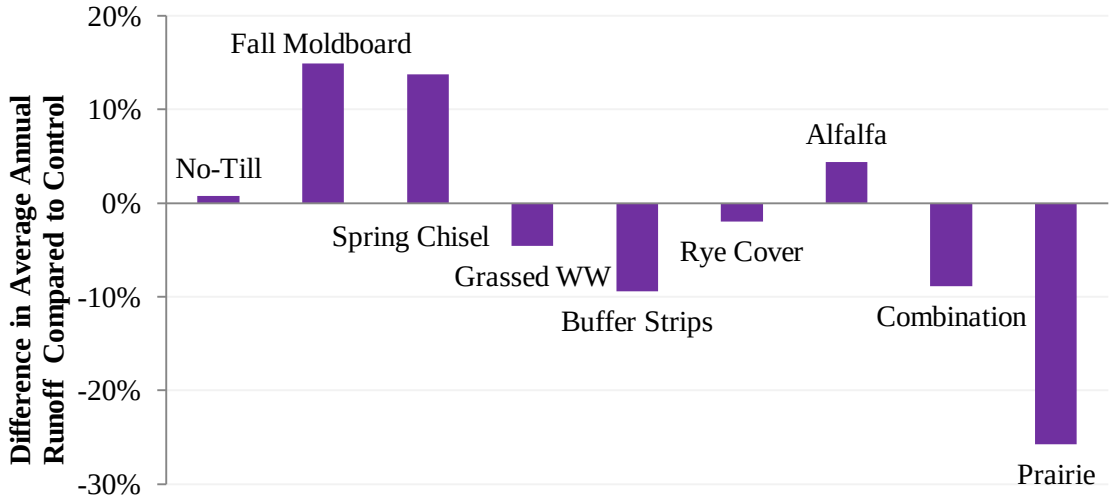

Figure 3.18: Percent difference in predicted average annual runoff from each management compared to control management. Average results from all RCPs shown.

3.5 Conclusions

Predicted changes in runoff, precipitation, and sediment losses were analyzed under a continuous minimally-tilled corn-soybean rotation for a small agricultural field catchment in Northeastern Indiana. Findings indicated that changes due to climate change will be most pronounced in late winter, late spring, and early fall. Precipitation was predicted to increase in the first five months of the year, with minimal changes from June-December. Increasing temperatures were predicted to cause runoff and sediment loss to decrease substantially in late winter due to a reduction in the number of days in which rainfall and snowmelt are incident on frozen soils. Runoff and sediment loss were predicted to increase in late spring due to a 15-25% increase in precipitation coupled with a lack of vegetation in the early growing season. With soybean cultivars unchanged, runoff and sediment loss were also predicted to increase in early fall for years planted to soybeans due to earlier senescence as a result of more rapid crop maturity.

These predicted changes, however, are likely to be mitigated to some degree as a result of farmer adaptations in the form of earlier planting dates and changes in cultivars, especially in the late spring and late fall months. However, the predicted relative

increases in sediment losses and runoff in the late spring have greater implications for agrochemical transport to receiving waters. Unmentioned here also is the potential for increased heat stress and crop failure in the late summer months, which could affect soil loss similar to that seen in September.

Results found here were similar to those by other authors using WEPP, specifically Pruski and Nearing (2002), where precipitation and soil loss were predicted to increase from 1990-2099 while runoff decreased due to dissimilar changes in precipitation and runoff from month to month. They reported a similar projected increase in precipitation in April and May, resulting in increased runoff and soil loss. However, Pruski and Nearing (2002) found a projected decrease in precipitation in June through September, leading to reductions in runoff and soil loss. The net effect in their study was a decrease in the runoff and sediment loss under soil, slope, and cropping conditions similar to those modeled herein. The increases in temperature resulting in earlier senescence of soybeans have also been noted by other authors using WEPP at a site in Indiana (Savabi and Stockle, 2001). Unlike previous studies, the observation here that a reduction in concrete frost reduced runoff in early spring is unique to this study.

The buffer strips provided the same or better predicted filtration of sediments as the grassed waterways while maintaining a sediment trap during the fallow period, the combination of both being more effective than using a rye cover crop alone. However, the fallow and spring cover provided by the rye cover crop means that the sediments are retained further up on the hillslope, while the use of only grassed buffers would build up sediment deposits on the toeslope. In practice, buffer strips in this type of terrain will likely be accompanied by grassed waterways, and simulation of grassed waterways and buffer strips without rye cover would likely show less runoff, but may result in higher soil losses due to increased detachment compared to the combination scenario modeled here.

Based on these findings, producers will first need to identify the most critical type of nonpoint source pollution from their fields before selecting a BMP which will be most effective into the future. If soluble nutrient loss requires the most attention, then management practices which reduce total runoff (buffer strips and conversion to rotations that include multiple years of sod/hay) should be considered, while if off-site sediment loss or soil-bound nutrients are of most concern then practices such as grassed waterways or buffer strips should be considered. Overall, the best management options into the future will likely include in-field (no-till) and edge-of-field (grassed waterways and buffer strips) to reduce soil migration to lower slopes as well as filter fine sediments from runoff and increase infiltration prior to discharging agricultural runoff to receiving waters.

CHAPTER 4. AN IMPACT ANALYSIS OF CLIMATE CHANGE ON AGRICULTURAL RESOURCES IN THE UNITED STATES SOUTHEASTERN COASTAL PLAIN USING WEPP AND THE IPCC FIFTH ASSESSMENT REPORT

A small agricultural hillslope managed by the USDA-ARS in the Southern Coastal Plain of the United States was modeled using the Water Erosion Prediction Project (WEPP) model under current and future climates to assess the effect of predicted future climate change on soil erosion, runoff, and BMP effectiveness. Future climate data reflected the four Representative Concentration Pathways (RCP) scenarios used with the CMIP5 model family as part of the IPCC Fifth Assessment Report, and represent a spread of potential radiative heating increases through the 21st century. Simulation results showed that runoff and soil loss changed for most months under the existing conventional management, with these changes typically accompanied by similar changes in total rainfall. Predicted climatic shifts caused soil loss and runoff to be reduced in the first three months of the year, while little change was modeled during the growing season. Late fall and early winter months, when ground cover is low, had increases in predicted soil loss and runoff which corresponded with an increase in total late-year precipitation. Increased temperatures resulted in the winter cover crop growing faster and unhindered by frost in the early months of the year, reducing soil loss during this traditionally low-cover period. Soil loss was also predicted to increase prior to harvest as a result of the reduction in canopy cover caused by the earlier senescence of cotton under warmer temperatures. Increased runoff in March and more ET in July from temperature-enhanced crop growth also increased irrigation demands in the growing season under the baseline management. Of the ten management systems examined under the future climate, the combination of no-till, rye cover crop, and riparian buffer increased in effectiveness into the future, while all other management systems had either similar or slightly reduced

effectiveness under predicted future climate. In general, the effectiveness of the various practices did not change much into the future.

4.1 Introduction

Agriculture in Georgia's Coastal Plain is primarily rain-fed by convective summer thunderstorms (Bosch et al., 1999), with supplemental irrigation during periods of drought being common. Climate stationarity is no longer a valid assumption, and a better understanding of future rainfall patterns throughout the year will help land planners prepare for not only rainfall changes which could influence crop growth, but also determine if conservation practices meant to reduce runoff and soil loss need to be bolstered or altered. Temperature changes may also influence crop growth and lead to short and long-term growth promotion and/or reduction. The use of natural resource and crop growth models with future climate data can expose strengths and weaknesses in current agricultural systems which can be addressed by farmers through adaptations to land management and BMP implementation.

The runoff and erosion occurring on agricultural lands are important processes that must be understood in order to prevent sediment, nutrient, and agro-chemical losses which can contaminate receiving waters. The benefits of conservation land management and tillage practices have been well documented in the Coastal Plain. Studies in the region have traditionally focused on the effectiveness of riparian buffers (Lowrance et al., 1984, 1985, 1986, 2000; Cooper et al., 1987; Phillips, 1989; Welsch, 1991; Bosch et al., 1994; Daniels and Gilliam, 1996; Sheridan et al., 1999) and, more recently, strip-tillage (Potter et al., 2004, 2010; Bosch et al., 2005, 2012; Feyereisen et al., 2008). Only a few studies (Suttles et al., 2003; Cho et al., 2010a) have compared multiple BMPs or land covers. Additionally, these studies have all used observed data which assumes climate stationary and were not designed to assess the effectiveness of these practices under a variable climate.

The lack of research in the region assessing the effects of projected future climate change on soil erosion, nutrient, or agrochemical losses present a key knowledge gap which exists due to the lack of prediction tools which account for rainfall erosivity and cropping changes (Delgado et al., 2013) and the difficulty in creating site-specific future climate data for impact assessments (Wilby et al., 2004). Detailed climate change impact studies on a site-specific basis will provide farmers and conservationists with projections required to implement BMPs and cropping changes to prevent losses in the future. This study aims to provide a general climate assessment, as well as a comparison of various Best Management Practices (BMPs) under observed historical and projected future climate to depict the general climatic changes and agro-environmental changes that can be expected in the region over the next 100 years using a combination of the current GCM projections to the end of this century, detailed site specific experimental and agricultural records, and an advanced natural resource model. This research uses methods developed in the previous chapters to show their applicability to an important agricultural location in the US.

4.2 Materials and Methods

4.2.1 Site Description

The Water Erosion Prediction Project (WEPP) model was used to simulate runoff, soil loss, and crop growth on a typical US Southern Coastal Plain hillslope under current and future projected climates. WEPP is a physically-based model founded on fundamental equations of water balance, soil erosion, and plant growth to model the agro-environmental effects of various farming, rangeland, and forestland practices (Flanagan and Nearing, 1995). The hillslope selected for this study was located on the University of Georgia Gibbs Farm in Tift County, Georgia (Figure 4.1, Bosch et al., 2005, 2012). Extensive management records, including tillage, cropping and irrigation, as well as surface runoff and erosion measurement systems make the plots ideal for calibrated soil erosion modeling. A conventional tillage plot was selected for calibration/validation of soil erodibility and hydraulic conductivity parameters to represent a baseline condition. Once calibrated, the management and climate files were varied to simulate different

combinations of alternative land management and future predicted climates, while fixing the base hillslope and soil input files to the calibrated values.

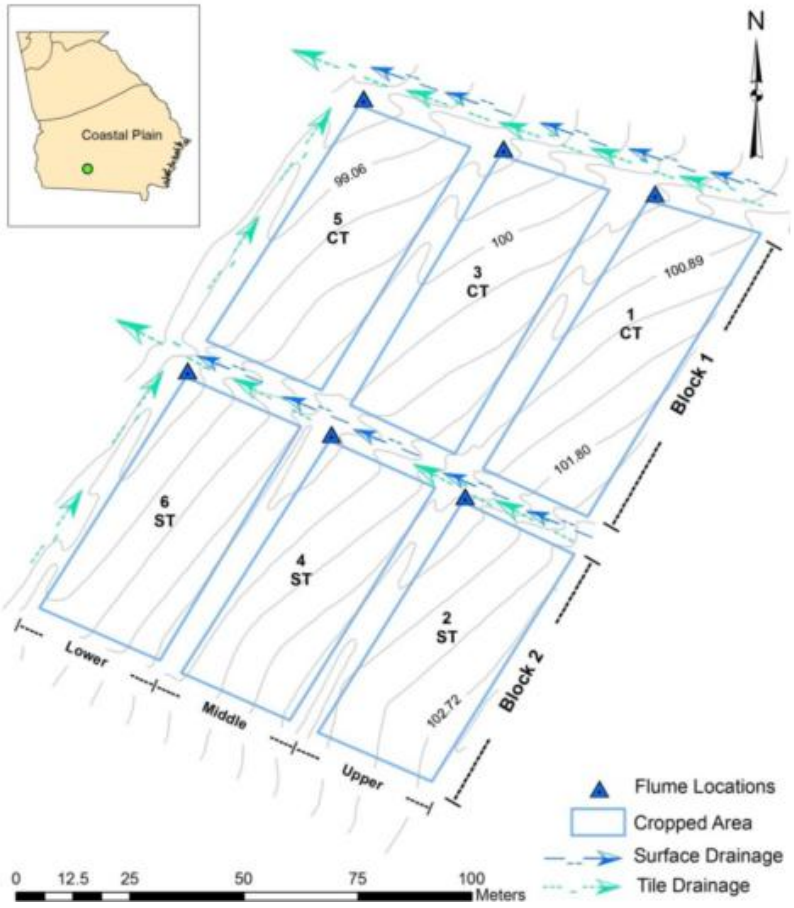

Figure 4.1: Layout of the Gibbs Farm experimental site. Inset map shows location within the Southeastern Coastal Plain in Georgia, USA (Endale et al., 2014)

4.2.2 Calibration/Validation

Observed data from 2000-2009 for one of the three conventional tillage plots, referred to as plot 3 in prior research (Bosch et al., 2005, 2012; Endale et al., 2014), at the Gibbs Farm was used for calibration/validation. The 0.2 ha plot had a slope gradient of ~3.5%, and the soil was a Tifton loamy sand. Detailed descriptions of soils and instrumentation at the site can be found in Bosch et al. (2005). A continuous WEPP management file was created to reflect the reported management practices on plot 3 (Endale et al., 2014). This management file consisted of 196 management operations, including tillage, planting,

harvest, irrigation, shredding/cutting, killing, and initial conditions. Cropping consisted of a cotton-peanut rotation with spring disk and fall chisel plow tillage. Irrigation was applied from 2000-2009 at a rate of 11.5 mm h^{-1} on 66 occasions with application depths ranging from 6.3 mm to 25.4 mm, using the fixed-date scheduling irrigation scheduling option in WEPP.

Runoff and sediment were collected from each plot through a system of weirs, berms, and data loggers. Weather data were measured at a weather station immediately adjacent to the plots. More details on management and data collection equipment during this period are provided in Endale et al. (2014). Soil loss and hydrology were calibrated to attempt to meet the model performance standards described by Moriasi et al. (2007), wherein a hydrologic/erosion model can be considered satisfactory if NSE>0.50, RSR≤0.70, PBIAS±55% for sediment, and PBIAS±25% for runoff[1]. WEPP model calibration was conducted by varying the baseline interrill erodibility and effective hydraulic conductivity within the soil parameter input file. No rill erosion is evident on the plots, so input baseline critical shear values were set at a high level (47.88 Pa) to prevent rill erosion simulation. All observed runoff events were used for calibrating/validating hydraulic conductivity for runoff prediction, while all recorded sediment loss events were used for soil erodibility.

In addition to calibration for runoff and soil loss, irrigation scheduling needed to be incorporated into the simulations assessing potential future climates. Sprinkler irrigation scheduling can be designated in WEPP inputs by specifying minimum and maximum irrigation depths and the percentage of the irrigation requirement to be applied (Kottwitz, 1995), as well as start and end dates of irrigation, and irrigation rate. In order for the future irrigation to be considered equivalent to the observed irrigation, roughly the same number of events must occur per year and the soil water content at the beginning and end of the irrigation events must be similar. A two-sample t-test was used to determine if the

[1] NSE – Nash-Sutcliffe model efficiency (Nash and Sutcliffe, 1970); RSR - ratio of the root mean square error to the standard deviation of measured data (Singh et al., 2005); PBIAS – percent bias (Gupta et al., 1999).

soil water content under the irrigation scheduling specified for a 30-year continuous simulation of the MarkSim® baseline climate was similar to the irrigation patterns from the 10-year observed record. The mean water content of the soil profile before and after irrigation was extracted from the calibration/validation model outputs.

4.2.3 Future Climate Data

Projected future climate information was obtained from the MarkSim® DSSAT weather file generator (Jones and Thornton, 2013) web application (http://gisweb.ciat.cgiar.org/MarkSimGCM/) that allows users to download up to 99 replicates of potential single-year realizations of future climate on a daily timescale, representative of one of the CMIP5 GCMs from the IPCC fifth assessment report. Fifty replicates representing the baseline climate based on the WorldClim dataset (Hijmans et al., 2005), plus seven decades in the 21st century from 2030-2100, were downloaded from the web application for each RCP scenario, centered on the location of the Gibbs Plots (31° 26’ 13” N, 83° 35’ 17” W). The WEPP/SWAT Future Climate Input File Generator (Chapter 2) was used here to convert the output from the MarkSim® web application for use with the CLIGEN weather generator (Nicks et al., 1995). CLIGEN version 5.3 was used with the Fourier interpolation method to generate 100 years of continuous data for each decade, resulting in 29 unique climate inputs to be used with WEPP.

4.2.4 Management

Ten land management scenarios (Table 4.1) with the potential for implementation in the Southeastern Coastal Plain of the US were modeled under each of the 29 future climate scenarios by modifying the input WEPP management file. The scenarios were divided into three groups. The first group represented heavy, moderate, and light tillage. The second group examined implementation of common agricultural BMPs used on flatter croplands together with the baseline tillage system. The third group simulated combination or conservation managements, including the conversion of all land to native Loblolly Pine. The conversion to Loblolly Pine would be expected to yield the lowest soil loss of any scenario due to its persistent cover.

Table 4.1: List of management scenarios assessed at the Tifton location

Management	Description
Control	Repeated 2-year cotton-peanut rotation with Spring disk and Fall chisel plowing.
Tillage Managements (Control Rotation)	
No-Till	No-till planters and standing residue in Fall.
Strip-Till	Strip-tillage in Spring.
Moldboard	Control management with Fall moldboard plowing.
BMP Managements	
Contouring	Control management with rows planted on 0.5% contours.
Riparian Buffer	Control management with edge of field riparian buffer.
Rye Cover	Control management with rye cover crop planted in the fall.
Conservation Managements	
Sorghum	Cotton-Peanut-Sorghum conservation rotation with winter wheat.
Combination	Control rotation with rye cover crop, no-till, contouring, and riparian buffer.
Loblolly Pine	Conversion of all land to Loblolly Pine.

Three of the management scenarios were based on the experimental plots at the Tifton site. The control management was reflective of the actual conventional tillage practice, wherein spring disking and fall chisel plowing are conducted every year. The strip-till management simulated the conservation practice being used on an adjacent plot in the same experimental set (Endale et al., 2014), which includes spring strip-tillage (similar to no-tillage, except that a 0.15 m wide strip of soil is cleared of residue by coulters on the planter, into which seeds are planted) with no fall tillage. For these two scenarios, the rye cover crop present on the actual experimental plots was excluded so that the rye cover could be examined independently as a BMP. The baseline management, used for the independent climate assessment in section 4.3.3, was dissimilar to the future management and included spring disk and fall chisel tillage as well as a winter rye cover crop.

4.3 Results and Discussion

4.3.1 Calibration/Validation

Input files for calibration/validation of the WEPP hillslope model were created using reported crop management and observed weather data. Weather and irrigation data collected at the site between 2000 and 2009 were used to create a continuous breakpoint

format input WEPP climate file. Statistics for these climate years are shown in Table 4.2. Average annual precipitation from 1981-2010 at the nearby city of Tifton was 1201 mm (NOAA, 2014), while the average for this location was 1165 mm from 2000-2009. 2005 was a wet year with ‘08 and ‘09 being moderately wet, and ‘01 and ‘07 being dry. 2007 had the most sprinkler irrigation events. 2006 and ‘07 also had the fewest runoff and sediment loss events, while ‘03 and ‘04 had the most. 2000-2001 was selected as the warmup period, with 2002-2004 for calibration and 2005-2009 for validation. The calibration and validation windows were selected to provide a roughly even distribution of storm events, runoff depths, and sediment yields.

Crop yield was calibrated first, followed by runoff and soil loss. The default plant parameter files for cotton and peanuts distributed with the WEPP model were used as a starting point for calibration of plant growth and crop yields. Using these files, modifying the Biomass Energy Ratio (BER) resulted in cotton yields at about 450% above observed yields. The “optimum yield under no stress conditions” parameter is typically set to zero in other plant parameter files, but here was set to 1 kg m^{-2} in the cotton file. Changing this parameter to zero and the BER for cotton to 5.581 kg MJ^{-1} optimized cotton yield to 0% difference, but the Leaf Area Index (LAI) at maturity was then very low at just over 2. Based on this conflict, it was determined to be more appropriate to calibrate LAI, rather than yield, and adjusting BER to roughly match typical mature LAI levels. A BER of 7.524 kg MJ^{-1} resulted in a LAI at maturity of between 5 and 6, which was considered adequate. Changing the harvest index (HI) to 23% resulted in a 1% difference in predicted and observed average annual cotton yield from 2000-2009. An uncalibrated LAI at maturity of 4 for peanuts was found to be adequate, as LAI for peanuts have been reported to be between 4 and 7 (Kiniry et al., 2005).

Runoff and soil loss from the hillslope were calibrated by varying the baseline effective hydraulic conductivity in the WEPP soil input file until the three qualitative model statistics (NSE, RSR, PBIAS) were satisfied. Results are shown in Table 4.3. Hydrology statistics were optimized and satisfied for all but PBIAS, using a hydraulic conductivity

of 12.7 mm h^{-1}, which resulted in NSE of 0.542, RSR of 0.697, and PBIAS of 25.5%. Soil loss was optimized with a baseline interrill erodibility of 7.628×10^{5} kg s m^{-4}, resulting in NSE of 0.537, RSR of 0.681, and PBIAS of 24.2%.

Table 4.2: Climate, runoff and soil loss summary for model calibration/validation periods

Year	Storms	Precip. (mm)	Irrigation Events	Precip + Irrigation (mm)	Runoff Events	Runoff Depth (mm)	Soil Loss Events	Sediment Yield (t/ha)
2000	93	1042	5	1148	31	125	15	0.485
2001	102	886	9	1115	49	171	30	0.676
2002	124	1145	7	1323	87	417	37	3.069
2003	132	1246	1	1271	58	529	41	2.344
2004	122	1131	6	1258	34	197	17	0.944
2005	123	1487	4	1564	33	275	19	1.259
2006	98	1113	7	1259	12	128	9	1.175
2007	95	903	16	1205	22	32	8	0.092
2008	107	337	9	1547	26	169	15	0.255
2009	125	1360	5	1442	25	310	18	4.428
Average	112	1165	7	1313	38	235	21	1.473
’00-‘01	195	1928	14	2262	80	296	45	1.161
’02-‘04	378	3522	14	3852	179	1143	95	6.357
’05-‘09	548	6199	41	7017	118	914	69	7.209

Table 4.3: Calibration/validation results for WEPP hillslope model.

Parameter		Calibrated Value	
Soil File Parameters	K_i (kg s m^{-4})	7.628×10^{5}	
	K_r (s m^{-1})	3.281×10^{-3}	
	τ_{cr} (Pa)	47.88	
	K_b (mm h^{-1})	12.7	
	Period	Runoff (m^3)	Soil Loss (kg)
Observed Mean Event Loading	Calibration	8.27	8.54
	Validation	10.11	13.48
	Total	9.00	10.61
Modeled Mean Event Loading	Calibration	3.64	5.35
	Validation	11.40	11.79
	Total	6.70	8.04
Results	NS CAL	0.474	0.452
	NS VAL	0.542	0.551
	NS Total	0.514	0.537
	RSR Total	0.697	0.681
	PBIAS Total (%)	25.47	24.16

A two-sample t-test was used to determine if the soil water contents simulated under the irrigation scheduling specified for a 30-year continuous simulation of the MarkSim® baseline climate were similar to the irrigation patterns from the 10-year observed record. The optimal irrigation schedule is shown in Table 4.4. During the 10-year window, irrigation was typically applied on the plots from April through August to a depth of 25.4 mm over 138 minutes. The minimum depth was set to 12.7 mm and the maximum to 25.4 mm, since irrigation depths in the field varied between those values during the 10-year window.

Table 4.4: Optimal irrigation scheduling parameters and t-test results

	Schedule		Depletion
	System		Stationary
	Minimum Depth (mm)		12.7
	Maximum Depth (mm)		25.4
Irrigation	Start Date		April 1
Parameters	End Date		Sept. 1
	Rate (mm/hr)		11.54
	Depth Ratio		1.73
	Max Ratio		0.35
	Nozzle Energy		0.6
		Observed	Simulated
Average # events per year		*7*	6.7
Starting	Mean	*366.00*	365.89
Water	Variance	*844.13*	735.05
Content	P(T<=t) two-tail		0.977
Ending	Mean	*382.31*	378.44
Water	Variance	*725.86*	478.96
Content	P(T<=t) two-tail		0.281

Confidence Level of 95%

Calibration was conducted by adjusting the WEPP input irrigation Depth Ratio and Max Ratio. The Depth Ratio is the ratio of irrigated depth to depth of water needed to bring the soil to field capacity, while the Max Ratio is the depletion ratio at which irrigation will occur. The timing of irrigation was found to be more sensitive to the Depth Ratio, while the Max Ratio could be adjusted to reduce or increase the variance of the mean starting soil water depth. These two values were adjusted until the simulated 30-year average annual number of irrigation events closely matched the observed 10-year average annual

number, and the p-value of the two sample t-test was maximized for both the starting and ending soil water depth. The irrigation schedule shown in Table 4.4 resulted in mean starting and ending soil water depths during the 30-year simulation which were not statistically different from the 10-year mean (p=0.997 and p=0.281, respectively). The nozzle energy was left at the default value, as it was found that changing this parameter had no effect on soil erosion or runoff results using the stated intensity and maximum irrigation depth.

4.3.2 Comparison of MarkSim® Output to Observed CLIGEN .par File

The CLIGEN parameter files were compared to the default WEPP parameters files for the same location using tools within the WEPP/SWAT Future Climate Input File Generator (Table 4.5). The comparison of MarkSim® generated and historical CLIGEN monthly means showed poor correlations for many variables. Mean precipitation differences were significant at the 99.5% confidence level, while $P_{w/w}$, mean and S.D. for solar radiation, and mean T_{Min} and T_{Max} differences were significant at all confidence levels.

While mean precipitation trends were similar for both baseline climates, MarkSim® underpredicted monthly mean rain day precipitation by between 3 and 10 mm. The same was true for rain day precipitation S.D., although the mean difference between the baseline climates for this variable was not found to be statistically significant ($p>0.05$). Q-Q plots also showed poor correlations for precipitation mean and standard deviation. $P_{w/d}$ showed good correlation both statistically ($p>0.05$) and graphically (results not presented in this paper). Precipitation skew also correlated well in the summer months, when convective thunderstorms provide the majority of intense storms to the region (Bosch et al., 1999)

Table 4.5: Comparison of MarkSim® and CLIGEN baseline climates for Tifton, GA.

Month	Jan.	Feb.	Mar.	April	May	Jun	July	Aug.	Sep.	Oct.	Nov.	Dec.
CLIGEN baseline climate parameter values (1959-1995)												
Mean P (mm)	12.45	12.19	13.97	14.73	11.94	11.43	10.92	11.18	10.41	10.67	9.40	10.92
S.D. P (mm)	14.99	16.26	17.78	20.32	14.48	13.21	13.72	14.73	14.73	13.72	14.48	13.21
$P_{w/w}$	0.45	0.45	0.40	0.37	0.44	0.49	0.52	0.48	0.49	0.44	0.36	0.43
$P_{w/d}$	0.22	0.24	0.23	0.19	0.19	0.25	0.34	0.29	0.19	0.11	0.17	0.21
Mean T_{max} (°C)	15.96	17.58	20.97	25.43	29.31	32.05	32.73	32.65	30.83	26.39	21.16	17.03
SD T_{max} (°C)	6.02	5.61	5.35	4.09	3.31	2.86	2.38	2.44	3.43	3.97	4.97	5.77
Mean T_{min} (°C)	3.77	4.88	8.22	12.30	16.50	20.11	21.42	21.12	19.03	12.98	7.79	4.44
SD T_{min} (°C)	6.04	5.68	5.23	4.19	3.16	2.16	1.42	2.42	2.89	4.77	5.64	5.84
MarkSim® baseline climate parameter values (1960-1990)												
Mean P (mm)	11.99	8.27	9.29	7.96	6.89	11.89	11.97	10.39	8.02	6.00	7.65	6.58
SD P (mm)	19.81	13.62	12.56	11.66	10.42	16.87	16.96	14.93	11.21	9.00	11.81	10.56
$P_{w/w}$	0.49	0.54	0.62	0.53	0.58	0.49	0.54	0.60	0.54	0.49	0.55	0.53
$P_{w/d}$	0.26	0.31	0.32	0.27	0.30	0.23	0.27	0.33	0.27	0.20	0.21	0.27
Mean T_{max} (°C)	15.67	17.21	20.57	24.88	28.71	31.31	32.03	32.45	30.04	25.78	20.68	16.60
SD T_{max} (°C)	4.54	4.38	4.07	3.72	3.40	3.14	3.00	3.05	3.46	3.63	4.25	4.55
Mean T_{min} (°C)	3.61	4.42	7.99	11.73	16.31	19.78	21.03	21.10	18.78	12.98	7.74	3.97
SD T_{min} (°C)	4.92	4.74	4.19	3.65	3.36	2.87	2.50	2.57	3.19	3.89	4.23	4.83

Mean P: mean precipitation event depth, SD P: standard deviation of precipitation events, $P_{w/w}$: probability of a wet day following and wet day, $P_{w/d}$: probability of a wet day following a dry day, Mean and SD for temperatures are calculated from daily data.

Solar radiation means and standard deviations differed significantly at all confidence intervals, with means being overpredicted and S.D. being underpredicted. The two baseline means differed most during the growing season, which could have a noticeable impact on crop growth simulation for the region. Means for both T_{Max} and T_{Min} also differed at all confidence levels, however MarkSim® underpredicted T_{Max} by only 0.55^{o} C on average, and T_{Min} by only 0.29^{o} C on average. These differences were also less than the average difference in the late winter and early spring, when soil temperature and any potential thaw or frost-kill would impact crop growth in the early growing season. Temperature S.D. were not significantly different ($p>0.05$).

4.3.3 Climate Change Impact Assessment

Continuous 100-year climate files were created using CLIGEN for the four RCP scenarios of the IPCC 5AR using the MarkSim® DSSAT weather generator web application and the WEPP/SWAT Future Climate Input File Generator. A conventional tillage management file, reflecting the typical two-year cotton-peanut rotation which existed during the 10-year observed period, was used to assess the impact of a changing climate on a typical Southern Coastal Plain agricultural plot. By fixing all other inputs, differences among climate scenarios were assessed to identify changes in water balance and soil loss that may result from projected climate change.

Figure 4.2 shows the changes in average monthly precipitation, runoff, and soil loss modeled under the four RCP scenarios for the 21st century. Total annual precipitation increased slightly, while runoff and soil loss were marginally affected. Predicted runoff and soil loss changed for most months, with these changes typically accompanied by similar changes in total rainfall. The RCP 8.5 scenario usually had the greatest change in runoff and soil loss over the entire future period, while RCP 4.5 had the greatest change in precipitation for most months. Soil loss and runoff were reduced in the first three months of the year, while growing season months (May-August) had little change from the baseline climate. September, October, and December all had significant predicted increases in soil loss and runoff ($p<0.05$) with a corresponding increase in precipitation.

November had relatively small changes in all three variables under all but the RCP 8.5 Scenario. Some months in particular (February, April, July, and September) exhibited behavior which was explained by further analysis, such as increased rainfall but reduced soil loss. A more detailed analysis follows.

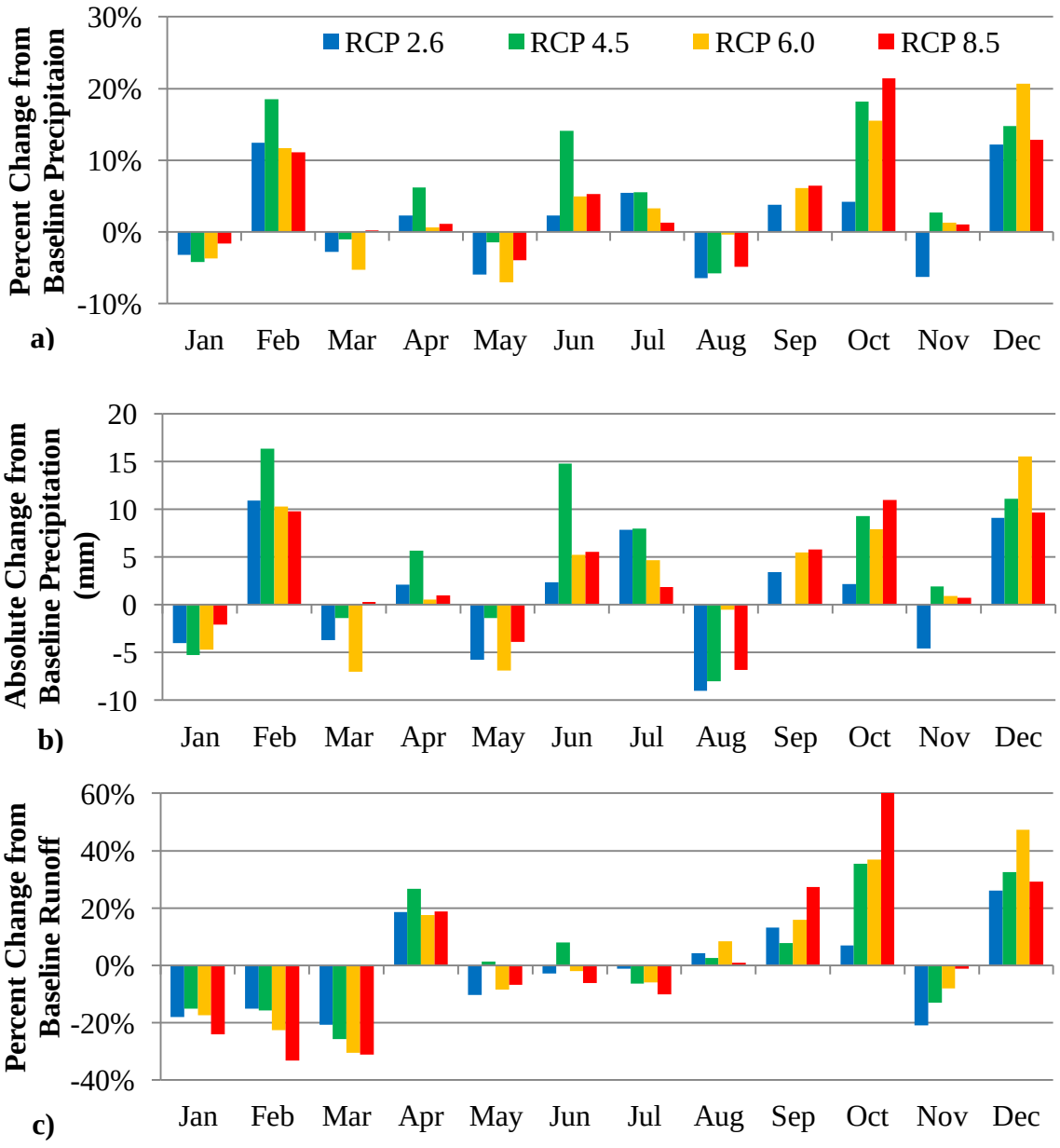

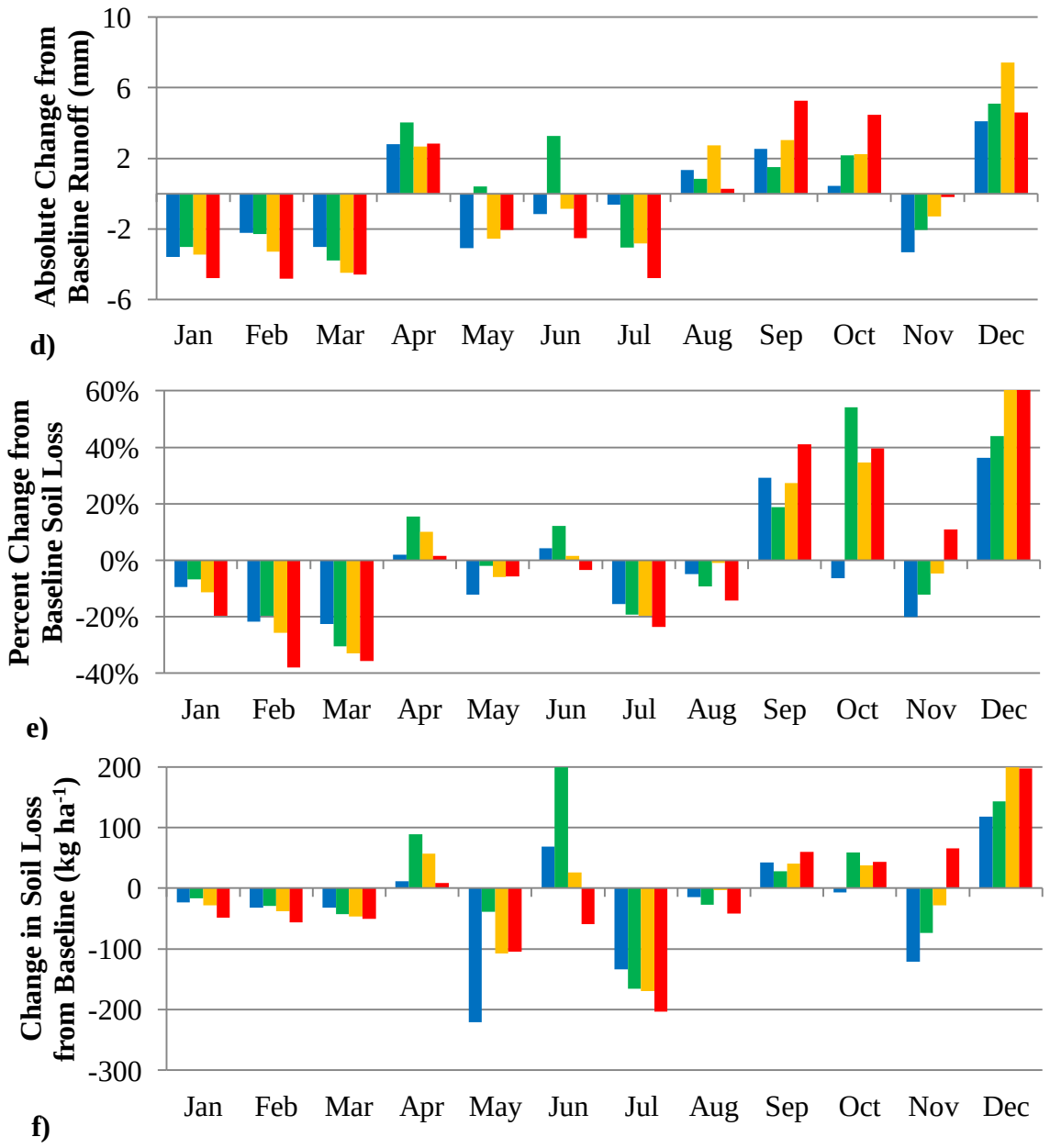

Figure 4.2: Predicted mean monthly precipitation (a,b), runoff (c,d), and soil loss (e,f) for the 21st century at Tifton, Georgia, due to projected climate change.

4.3.4 February Soil Loss Decreased, Despite Increasing Precipitation

The roughly 20% reductions in runoff and soil loss in the month of February do not appear to make sense with the over 10% increase in precipitation for that month. However, growth of the rye cover crop was found to be enhanced by the higher

temperatures of the future climates, which explained why the RCP with the greatest temperature change (RCP 8.5) also had the greatest reduction in predicted runoff and soil loss. Increasing temperatures promoted crop growth in the coldest months, particularly. While temperatures never fell below -5^{o} C in any of the 100 years of the baseline climate, approximately 75% of those years had temperatures which fell below 0^{o} C in December or January. In those years, predicted rye growth was stunted for anywhere between three days and several weeks, which resulted in reduced LAI in February. Under all projected RCP scenarios in the 21st century, however, fewer or no stunted growth periods were simulated in December and January, resulting in drastically higher rye growth (Figure 4.3).

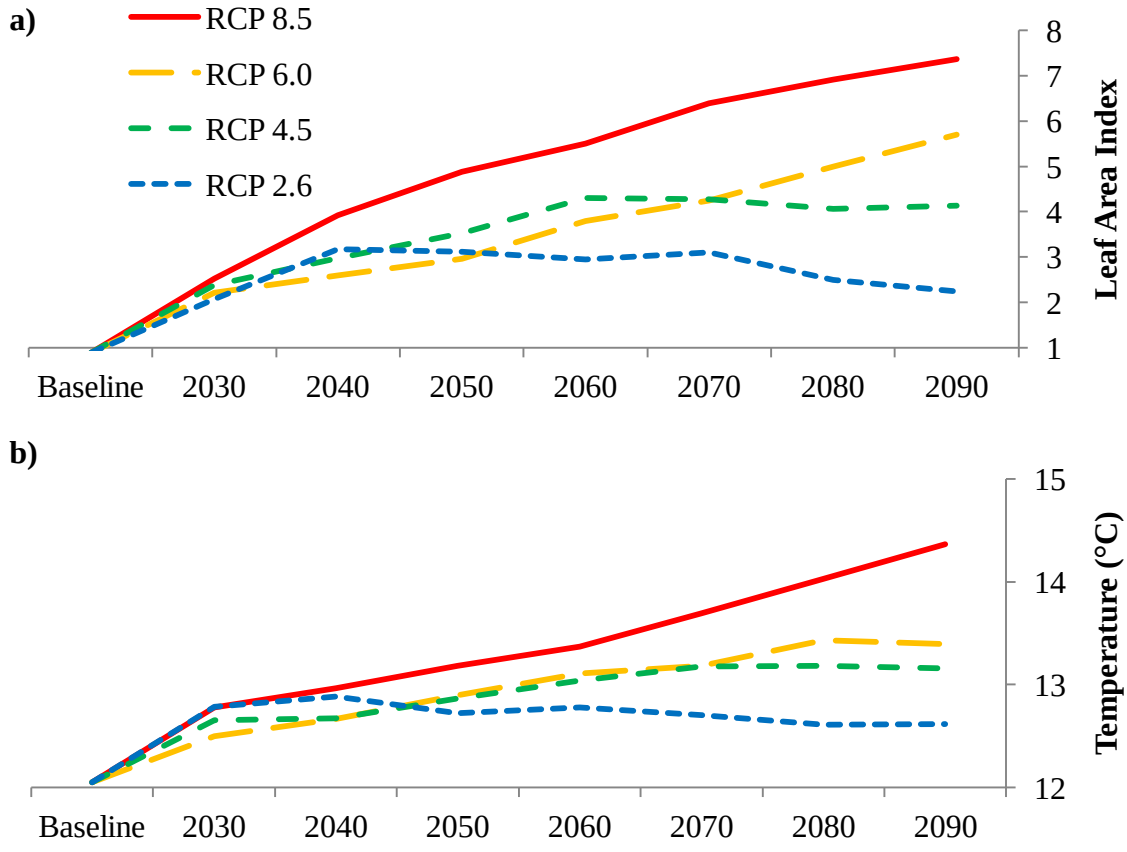

Figure 4.3: Predicted February rye cover crop LAI (a) and February mean temperature (b) under the baseline management at Tifton, Georgia, due to projected climate change.

4.3.5 Increases in April Runoff and Soil Loss Could Not be Readily Explained

Rye is killed at the end of March, followed by 2 disk tillage operations designed to incorporate the dead biomass fully into the soil. With the increase in biomass produced by the rye and subsequently higher levels of surface and buried residues, it would be expected that runoff and soil loss would be reduced in April; however, higher runoff and soil loss was simulated. Predicted runoff was 18-27% greater over the future period, while predicted soil loss was 2-15% greater for the month of April. The total water balance for April (calculated as precipitation – runoff + irrigation - deep percolation - ET) did not change significantly into the future ($p>0.05$). ET increased by less than 10% or 2 mm, irrigation increased by 57-84% or 3-5 mm, and deep percolation increased by 18% or 3 mm; the combination of which could not explain the increase in runoff. While the average depth of storms increased absolutely, the change was not significant ($p>0.05$). When considering all 100 years simulated for all 5 scenarios in 2070, the number of large storms resulting in 60 mm or more of precipitation increased by 3-10 storms per 100 years. Of these, the largest storms for the RCP 6.0 and 8.5 scenarios were nearly twice as large as in the baseline climate. The number of precipitation events resulting in runoff increased in April over the course of the 21st century, but did not appear to correspond to the increase in runoff. Adjusted interrill erodibility also decreased slightly into the future, further obscuring the cause of the changes.

In other months, the changes in runoff and soil loss appeared to correspond in a linear manner to changes in precipitation depth. April did not exhibit such a linear response, with runoff increasing to a much greater degree than precipitation changes. Further investigation of individual precipitation variables generated by CLIGEN revealed that storm characteristics, such as average peak intensity, storm depth, and storm frequency, did not change to a degree that would explain the greater increase in runoff and soil loss. However, combined together all these changes apparently caused enough variation to result in the noticeable increases in runoff and soil loss.

4.3.6 July Runoff Decreased, Despite Increased Precipitation

July, like February, showed an increase in precipitation but a decrease in runoff and soil loss (Figure 4.4). However, most of the change in precipitation for February occurred by 2030, and remained around 100 mm per year throughout the entire future period. In July, precipitation peaked by 2030, and gradually decreased to 1-8 mm above baseline levels by the end of the century. Runoff, on the other hand, gradually decreased starting in 2030, with 2090 levels being 1-6 mm below the baseline level. LAI, while decreasing at the end of the century for RCP 8.5, increased significantly ($p<<0.05$) for all scenarios in 2030 (Fig. 2a). Therefore, the initial jump in precipitation appears to have been offset by an initial increase in LAI; since the LAI did not change through the future period, the gradual reduction in precipitation explained the corresponding reductions in runoff. This was also supported by the numbers from 2030, when RCP 6.0 had a slight reduction in predicted runoff and no change in precipitation.

4.3.7 Earlier Senescence of Cotton Increased Soil Loss

Earlier senescence of cotton was predicted to occur into the future, with senescence occurring 9 days earlier by 2090 under the RCP 2.6 forcing, and a full month earlier by 2090 under the RCP 8.5 forcing. Precipitation also increased significantly ($p<0.05$) under all but the RCP 2.6 scenario. The combination of increased precipitation and earlier senescence reduced canopy cover and increased runoff, resulting in increased predicted soil loss in September and October. Insignificant ($p>0.10$) changes in precipitation, coupled with greater levels of biomass in the soil from increased crop growth, reduced soil losses in November under all but the RCP 8.5 scenario. Precipitation was predicted to increase in December by 12-21% over the 21st century, and this resulted in more soil loss events under all scenarios.

4.3.8 Irrigation Requirements Increased in the 21st Century

One important aspect of agriculture in the Southeastern Coastal Plain is the requirement for many row crops planted in the sandy loam soils to be irrigated during the summer months, when precipitation is heavily dependent on unpredictable convective

thunderstorms. Assuming irrigation scheduling does not change into the future, predicted total irrigation depths and frequency were forecast to increase for the growing season through the 21st century. Irrigation requirements in June were reduced, while requirements in April, May, and August were simulated to increase.

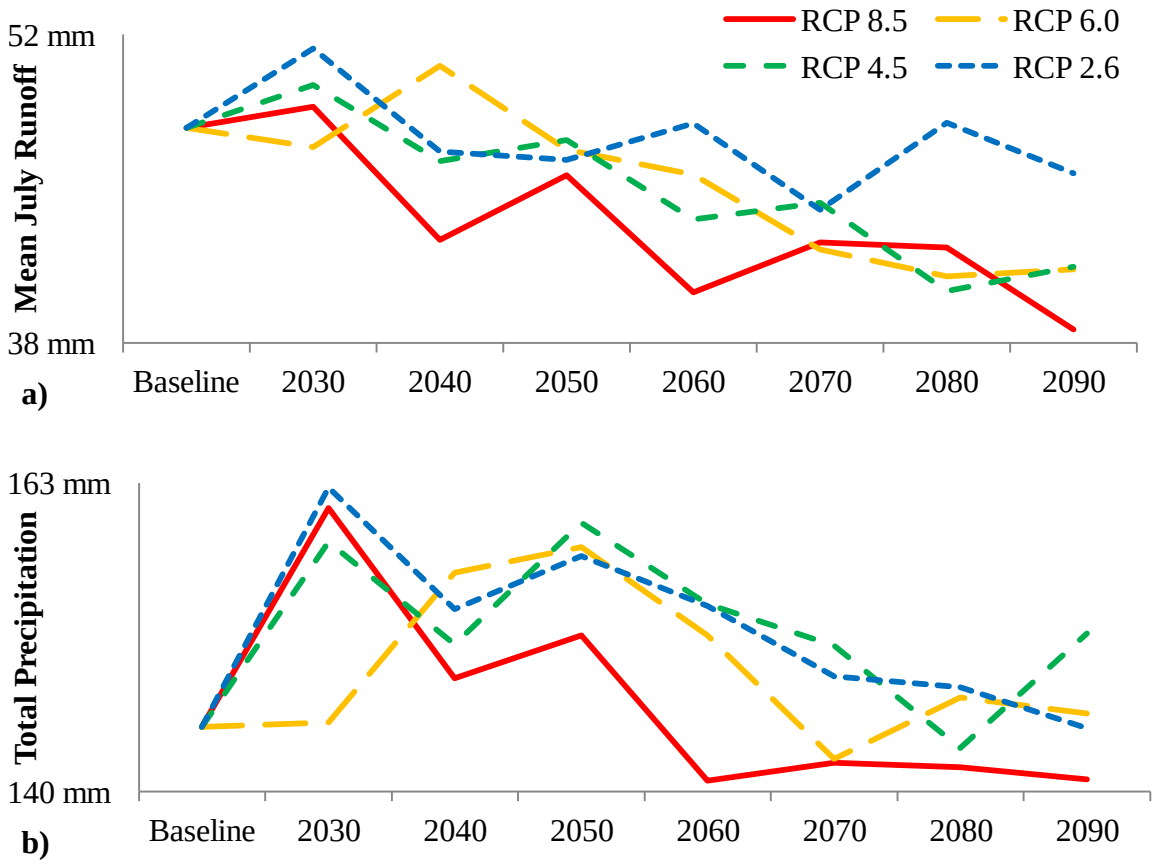

Figure 4.4: Predicted runoff (a) and precipitation (b) for July under the baseline management at Tifton, Georgia, due to projected climate change.

The increase in the total water budget for April, previously mentioned, was primarily a result of the reduction in deep percolation losses for that month, while irrigation increased to offset the reduction in net soil moisture for the first day of the month caused by increased ET and runoff in March. The reduction in irrigation requirements for June were a result of differences in soil water content at the beginning of the month being statistically and absolutely insignificant between the baseline and future climates ($p>>0.5$, ±2 mm). While July had the greatest increase in ET of any month (12-22 mm),

due to both higher temperatures and the related increase in crop growth associated therewith, this increase in ET was offset in all but the RCP 8.5 scenario by an increase in precipitation, reduction in deep percolation losses, and a slight reduction in runoff. This resulted in no significant change in irrigation for July. August, however, saw the largest increase in irrigation requirements due to a reduction in precipitation coupled with a reduction in the soil water content at the beginning of the month of 2-10 mm. The increase in ET for August was offset by a reduction of deep percolation losses. Irrigation changes in May and September were insignificant ($p>0.05$).

4.3.9 Assessing BMP Effectiveness under Potential Future Climate

Effectiveness of individual land management systems changed into the future (Figure 4.5). Results showed that using conservation tillage options (strip-till and no-till) were the most effective in reducing soil loss into the future, while systems that included riparian buffers had the greatest predicted reductions in runoff into the future. Results also showed that the rye cover and combination management systems were more effective in the future compared to under the baseline climate.

One of the most interesting findings is that the combination management, which was a combination of the no-till, riparian buffer, and rye cover systems, had only a slightly lower total predicted soil loss compared to just the no-till management, but had an increase in effectiveness into the future, which neither the no-till nor the riparian buffer managements exhibited individually. The combination management system was the only one, out of the ten examined, to have a significant decrease in predicted soil loss in the future compared to the baseline climate. The combination management also had the lowest predicted future total runoff. However, predicted runoff did not differ significantly ($p>>0.05$) when comparing the baseline and future climates for any management system.

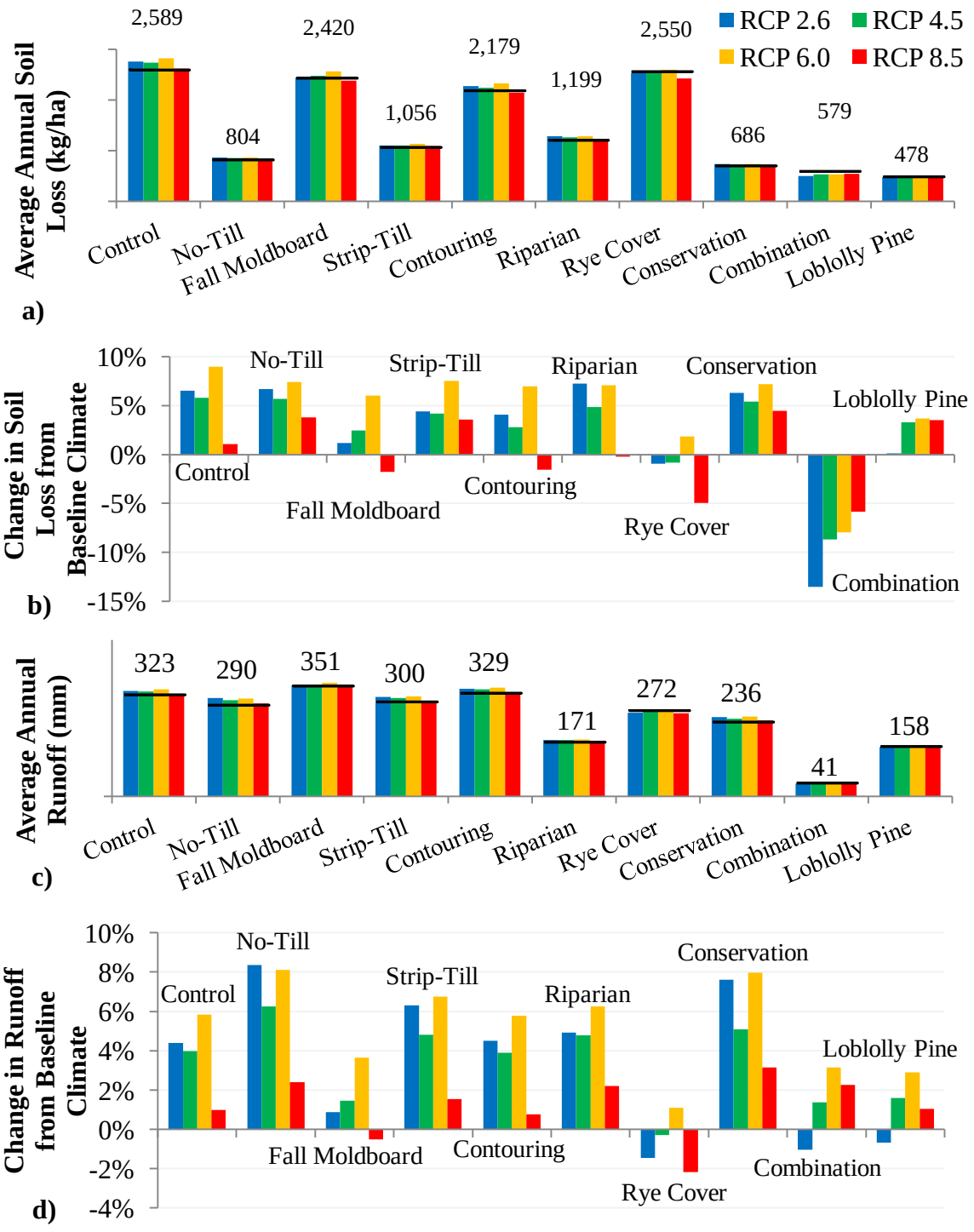

Figure 4.5: Predicted soil loss (a,b) and runoff (c,d) under the ten management scenarios for the 21st century. Black lines in the bar graph show baseline climate levels.

Overall, effectiveness of different management systems did not show much change into the future. The conversion to Loblolly pine had the lowest predicted soil loss of any management system, while the control had the highest, followed by rye cover and fall moldboard plowing. The fact that the baseline and rye cover management systems did not differ into the future indicated that little erosion occurs in the months preceding sowing or harvest, when temperature-related crop promotion was most drastic. This was also reinforced by the fall moldboard plow management, which omitted the double disk spring plowing, and having only marginally lower predicted soil loss than the control. The inclusion of a riparian buffer alone was not enough to limit soil loss on a plot, and was only made effective with the inclusion of no-till and a rye cover crop. A separate analysis (not shown) of various grasses in the buffer zone closest to the field also indicated that the type of cover in that zone of the buffer was not as important in soil loss mitigation as the presence of the zone itself. Strip-till, a practice being adopted in this and other regions, was also effective in limiting soil losses from the field, with about only a third of the total losses compared to the baseline management.

4.4 Conclusions

A small, experimental, agricultural hillslope managed by the USDA-ARS in the Southeastern Coastal Plain of the United States was modeled using WEPP under current and projected future climates to assess the effect of predicted future climate change on runoff, soil erosion, and BMP effectiveness. Simulation results showed that runoff and soil loss changed for most months under the existing conventional management, with these changes typically accompanied by similar changes in total rainfall. Predicted climate change caused soil loss and runoff to be reduced in the first three months of the year, while limited change was modeled during the growing season. Late fall and early winter months, when ground cover was low, had predicted increases in runoff and soil loss which corresponded with an increase in total late-year precipitation. Increased air temperatures resulted in the winter cover crop growing faster and unhindered by frost in the early months of the year, reducing predicted soil loss during this traditionally low-cover period. Soil loss was also predicted to increase prior to harvest as a result of the

reduction in canopy cover caused by the earlier senescence of cotton due to the projected warmer temperatures. Increased predicted runoff in March and more ET in July from temperature-promoted crop growth also increased irrigation demands during the growing season under the baseline management. Ten management systems were examined under the future projected climate scenarios, and effectiveness of the combination of no-till, rye cover crop, and riparian buffers was the only one that increased into the future. All other management systems had either similar or slightly reduced effectiveness. In general, the effectiveness of the various land management practices did not change much into the future.

This study has several drawbacks which may limit the use of results for management decisions, separate from limitations which have previously been noted regarding the method of future climate data acquisition (Section 2.5). First, an important and largely unpredictable measure of adaptation in agriculture which has not been detailed here is the gradual selection and change-over to crop cultivars better suited for future altered temperature and precipitation patterns. These cultivar changes were not assessed in the current study, and limitations in the predictability of economic drivers for crop viability make speculation and simulation of these changes difficult. As modeling technologies improve, the effect of cultivar changes will need to be assessed alongside BMP implementation to determine the interplay of each to natural resource management. Second, the size of the hillslope examined was small, limiting the extrapolation of results to a larger geographic area. On the other hand, the small controlled area allowed for high resolution records to be obtained for climate, soil, topography, management, and observed runoff and soil loss, resulting in high calibration/validation prediction efficiencies and providing high levels of confidence in the WEPP model results and projections.

Despite these limitations, the results from this study indicate that current conservation practices and BMPs being implemented at this location will likely be sufficient for mitigating soil erosion and runoff into the future.

CHAPTER 5. FIRE RISK ASSESSMENT UNDER FUTURE CLIMATE FOR THE BLACKWOOD CREEK WATERSHED IN THE LAKE TAHOE BASIN, CALIFORNIA/NEVADA

5.1 Abstract

The Blackwood Creek watershed, a tributary of Lake Tahoe in California, was assessed for potential changes in climate and fire risk under 21st century climates projected by the Intergovernmental Panel on Climate Change (IPCC) Fifth Assessment Report (5AR). While total precipitation varied by decade, the portion of precipitation falling as snow decreased by as much as 26%, and projected air temperatures increased by as much as 3.4°C by 2090. Total soil water (TSW) predictions by the Water Erosion Prediction Project (WEPP) model indicated that fire ignition in the Sierra Nevada region from 1984-2013 coincided with simulated minimum TSW. Risk categories based on simulated TSW changed under projected future climate, with an increase in the number of high risk days defined by TSW less than 40 mm. Simulated TSW in the Blackwood Creek watershed at the time of nearby historic fires also indicated that the Keetch-Byram Drought Index (KBDI) was correlated to TSW ($R^2 = 0.59$) when KBDI was less than 500. Corrections to the aggregated WEPP model used here as well as retooling of KBDI to be more applicable to lands in the Western US would likely provide better datasets to assess fire risk in the Lake Tahoe Basin.

5.2 Introduction

The Blackwood Creek watershed is a 2900 hectare watershed that is located on the western shore of and is a tributary to Lake Tahoe in California, USA. This watershed has a history of logging and gravel mining which cleared and altered the forest stand in much of the watershed prior to 1960 (Coats et al., 2008). Logging in the 19th century has been attributed to the promotion of a fire deficit in many western regions (Taylor and Beaty,

2005; Westerling et al., 2006), with current fire frequency being at its lowest point in thousands of years (Beaty and Taylor, 2009; Marlon et al., 2012). In addition to fuel accumulation, a changing climate may also have an effect on fire risk, with recent increases in wildfire severity being linked to earlier spring snowmelt and higher spring and summer temperatures (Westerling et al., 2006). Climatic change in the basin has already been observed in the historical record as increases in air temperature, less precipitation as snowfall, earlier spring snowmelt, and increased rainfall intensity (Coats, 2010).

No wildfires are known to have occurred in the Blackwood Creek basin since Euro-American settlement in the 18th century. A large fire there or in other large watersheds along the western shore of Lake Tahoe could have major impacts on suspended sediment loads into the lake. Currently, most of the sediment loadings in Blackwood Creek come from channel degradation (Gavigan and Curtis, 2007), but the volcanic soils which make up 14.9% of the watershed deliver 65.8% of the total sediment load (Brooks et al., 2010). The combination of channel degradation due to logging activities on the hill slopes and gravel mining in the river (Gavigan and Curtis, 2007) no doubt contribute to Blackwood Creek having higher observed sediment loads than other nearby watersheds (Nolan and Hill, 1991). Wildfires leading to the clearing of vegetated lands which buffer the streams in the watershed from highly erodible badlands at the higher elevations of the Blackwood Creek and nearby Ward Creek watersheds (Stubblefield et al., 2009; Brooks et al., 2010) could further increase sediment loadings and threaten the clarity of the lake.

The Keetch-Byram Drought Index (KBDI) is a commonly used metric for fire risk in the US which uses a simple relationship between temperature and precipitation to budget soil moisture deficits on a daily timescale (Keetch and Byram, 1968). While the initial publication which presented this method emphasized that it was not a substitute for more established fire criteria, such as the National Fire Danger Rating System (Bradshaw et al., 1984), the KBDI was intended as a reference for deep-drying which can be used for planning fire control operations (Keetch and Byram, 1968). As such, it provides a

benchmark for other fire risk assessment tools which are developed from relatively simple datasets, such as those available from future climate projections by GCMs.

The KBDI has been used elsewhere to assess historical and future fire likelihood at global and local scales. McKelvey and Busse (1996) used the KBDI to assess twentieth century forest fires on federal lands with a specific emphasis on the Sierra Nevada Mountains in California. They found that periods of drought consistent with those which occurred in the twentieth century cause a significant increase in the likelihood of large wildfires. They also found that KBDI can be used to accurately describe risk zones in the Sierra Nevada, but their results indicated that Tahoe City had much lower KBDI values compared to other stations in the region. On a larger scale, KBDI was used by Liu *et al.* (2010) to assess trends in wildfire potential due to climate change under scenarios defined by the Special Report on Emission Scenarios from the IPCC 4AR (IPCC, 2000). Liu *et al.* (2010) found that fire potential will increase in the United States and globally, with fire seasons lengthening by 2 to 8 months. They also noted that the degree of increase in fire potential was sensitive to GCM and emission scenario.

The IPCC is the scientific intergovernmental authority on climate change research, using the latest science and technology to publish regular assessment reports which detail the current understanding of climate change. The latest Intergovernmental Panel on Climate Change (IPCC) Fifth Assessment Report (AR5, IPCC 2014) used projections from the Coupled Model Intercomparison Project (CMIP5, Taylor *et al.* 2012) under the four Representative Concentration Pathways (RCP, Moss *et al.* 2010). The RCP scenarios from the AR5 represent four possible radiative forcings by 2100, with the number of each scenario corresponding to the global radiative forcing in W/m^2 (Taylor et al., 2012). RCP scenarios have been used by a number of scientific institutions to drive General Circulation Models (GCM). GCMs are mathematical atmospheric and oceanic models which predict atmospheric conditions such as precipitation and temperature at various spatial and temporal scales. These projections have been made available through the IPCC for use in further research, particularly impact assessments.

WEPP is a physically-based soil erosion model founded on fundamental equations of water balance, soil erosion, and plant growth to model the agro-environmental effects of various farming, rangeland, and forestland practices (Flanagan and Nearing, 1995) at hillslope and small watershed scales. The WEPP model has been continuously developed since 1985 as a replacement to more simplistic soil erosion prediction technologies so that engineers, scientists, and government agents can be better informed on potential on-site erosion and off-site sediment losses (Flanagan et al., 2007). WEPP is capable of modeling forestland erosion and water balance (Elliot and Hall, 1997; Elliot, 2004; Dun et al., 2009) and has been used in the past to evaluate soil, water, and vegetative processes in post-fire forest landscapes (Soto and Díaz-Fierros, 1998; Robichaud, 2000, 2005; Covert et al., 2005; Spigel and Robichaud, 2007). CLIGEN is a stochastic weather generator provided with WEPP which uses monthly statistics for precipitation, temperature, wind patterns, and solar radiation to generate daily weather which can then be used to conduct simulations with the WEPP model (Nicks et al., 1995).

Understanding factors which can help predict the likelihood of wildfire occurrence is important for forest fire prevention, but the precipitation and temperature changes associated with climate change are likely to alter how forest managers assess fire risk. Additionally, the relationships which govern empirically derived models for drought and fire risk assessment may change as the atmosphere changes and vegetative responses to those changes occur. The Angora (2007) and Gondola (2002) fires in the Lake Tahoe basin have increased local concerns of fire safety and the effects that post-fire increased sediment loadings could have on the clarity of the waters of Lake Tahoe.

The goals of this study were to characterize the nature of climate change in the Blackwood Creek basin, as well as determine if changes in wildfire likelihood would occur under current projected future climate. To accomplish these goals, the latest IPCC AR5 projections from the CMIP5 under the four RCP scenarios were used to assess potential changes in annual precipitation, snowfall, Total Soil Water (TSW), and fire risk defined by TSW and KBDI in the Blackwood Creek watershed of the Lake Tahoe basin

using the WEPP model and the CLIGEN weather generator. This research also presents the first example of downscaling future climate projections to a specific watershed in the Lake Tahoe basin, as well as the first use of the IPCC AR5 data in an impact assessment in the region.

5.3 Materials and Methods

The Water Erosion Prediction Project (WEPP) model was used to simulate water balance in the Blackwood Creek watershed of the Lake Tahoe Basin (Figure 5.1) under current and projected future climates. An extension of WEPP, referred to as the WEPP-UI approach in Brooks *et al.* (2010) and herein as the 626 hillslope model, was used to simulate and aggregate 626 individual hillslope profiles, which as a whole represent the Blackwood Creek watershed. The 626 individual hillslopes each contain up to 19 overland flow elements which are defined by slope, vegetation, and soil input files derived from GeoWEPP, an ArcGIS extension which allows users to define the input files for and run a WEPP watershed model based on publically available landcover, soil survey, and topographical databases (Renschler and Harbor, 2002).

Annual precipitation in the Blackwood Creek watershed has been reported to average around 1500 mm over the entire basin with 90% of precipitation falling as snow (Tetra Tech, 2001) and the remainder falling as a result of infrequent summer thunderstorms (Stubblefield, 2002). A daily breakpoint weather file, provided by Tetra Tech for the Lake Tahoe Total Maximum Daily Load (NDEP, 2011) report, was obtained for 1988-2006 at the Tahoe City Natural Resources Conservation Service (NRCS) Snow Telemetry (SNOTEL, http://www.wcc.nrcs.usda.gov/snow/) station. This climate file was used to run a 626 hillslope model simulation to obtain the baseline total TSW characteristics used for the fire risk assessment.

Figure 5.1: Map showing location of Blackwood Creek on the Western shore of Lake Tahoe. Inset shows location of Lake Tahoe on Eastern border of California, USA. Image modified from Stubblefield et al. (2009)

Projected future daily weather patterns from a variety of GCMs using the AR5 RCP scenarios were obtained from the MarkSim® DSSAT weather file generator (Jones and Thornton, 2013) web application (http://gisweb.ciat.cgiar.org/MarkSimGCM/) and formatted for use with WEPP using the WEPP/SWAT Future Climate Input File Generator (Chapter 2). MarkSim® is a weather generator which works as a GCM downscaler by using stochastic downscaling and weather typing (Jones and Thornton, 2013). Future climate is created using daily data created by GCMs for five future time periods, calculating monthly climate anomalies for each time period relative to the baseline climate (WorldClim, Hijmans *et al.* 2005), and interpolating years in-between by fitting a functional relationship to the future time periods. Spatial downscaling is completed through regression of synoptic atmospheric variables to local weather events from the WorldClim dataset (Hijmans et al., 2005). CLIGEN version 5.3 was used with the Fourier interpolation method to generate 100 years of continuous data for each decade

of the four RCP scenarios used in the IPCC AR5, resulting in 29 unique future climate inputs.

A modeling challenge identified by Brooks et al. (2007) when working in the Tahoe basin is accurate representation of the spatial variability in climate. Climate in the basin varies by region as well as elevation, and no weather stations exist within the Blackwood Creek watershed, requiring information for use within the watershed to be scaled from a nearby weather station. For this purpose, 800 m resolution Parameter-elevation Relationships on Independent Slopes Model (PRISM, Daly *et al.*, 2008) maps of average monthly precipitation, minimum temperature, and maximum temperature were used to scale climate data from Tahoe City, California, to each hillslope (Brooks et al., 2010). The same scaling factor was used for the 626 hillslope model under both the historical SNOTEL climate as well as the future RCP climates, which assumes that the relationship between precipitation and temperature at the Tahoe City SNOTEL location and the rest of the Blackwood Creek watershed will remain the same into the future.

Fire risk was assessed by comparing the timing of fires in the Sierra Nevada region with TSW modeled by WEPP and the KBDI. Timing of fires was obtained from the Modeling Trends in Burn Severity Project (Eidenshink et al., 2007), which has a useful web tool which allows users to download data on wildfires by region or state (http://www.mtbs.gov/). The data is available from 1984-2013, which contains the period for which observed SNOTEL weather data exists. The MTBS data for the Western US includes only burned areas larger than 400 ha, which excludes the Gondola fire which occurred in the Lake Tahoe Basin in 2002 and burned an estimate 280 ha. The Gondola fire was included in the fire assessment herein.

A representative hillslope was selected from the 626 hillslope model to compare TSW and KBDI during the period of record coincident with the observed SNOTEL weather data. The timing of wildfires in the region was compared to TSW and KBDI to identify three fire risk categories. These fire risk categories were then applied to the future climate

data to assess changes in the fire risk categories into the future. KBDI is an estimation of moisture deficit in a landscape based on the assumption that the available water at field capacity in the zone where drought occurs is equal to 8 inches (Keetch and Byram, 1968). The calculated value of KBDI is equivalent to the estimated water deficit of the soil in hundredths of an inch and ranges from 0 to 0.800 inch. KBDI is a function of precipitation and temperature, and was calculated using the equation from Janis *et al.* (2002):

$$DF_t = \frac{(800-KBDI_{t-1})(0.968e^{0.0875TMAX_t+1.5552}-8.30)\times 10^3}{1+10.88e^{-0.0174R}} \quad (5.1)$$

where DF_t is the drought factor on the current day, $KBDI_{t-1}$ is the drought factor on the preceding day, $TMAX_t$ is the daily maximum temperature (°C), and R is the mean annual rainfall (cm). The mix of English and metric units is presented here, as it was in Janis *et al.*, (2002) because KBDI is traditionally represented in English units, while the weather data used to calculate KBDI was provided, and presented here, in metric units. The drought index for the current day is calculated by subtracting the net precipitation from the previous 24 hours from the preceding day's KBDI and then adding the calculated value of DF_t. KBDI is a continuous calculation, so the first day in the calculated series has a KBDI equal to zero. As such, it is important to start the calculation on a date in which the ground is assumed to be saturated (Keetch and Byram, 1968), such as after spring snowmelt or several days of rain. Herein, the calculation was started in September of 1988, when reliable weather records begin, so that the KBDI reached zero after the spring snowmelt in 1989.

Several conditions apply to KBDI regarding temperature and days with consecutive precipitation. First, solving the numerator of Equation 5.1 shows that the drought factor is equal to zero when the maximum daily temperature is less than 6.79^{o}C. Second, only the amount of precipitation over 0.51 cm should be subtracted from the current day's KBDI. Third, when there are consecutive rain days, only the portion of net rainfall greater than 0.51 cm which fell on the previous day can be subtracted for the current day's KBDI calculation. Fourth, when snow is considered to be covering the fire fuel layer, there is no drying and all precipitation is considered as net precipitation.

The fourth condition presents some confusion when calculating the drought factor on days with snow cover which had not been addressed in the literature to this point, and must be considered in climates such as Lake Tahoe, where snowfall is the dominant precipitation. Keetch states that all precipitation can be transferred to the net rainfall columns of the KBDI worksheet in the event that no drying of the fuel cover occurs, which would be the case in the event of snow accumulation. A literal translation would therefore mean that when snow exists, the net rainfall is not reset to zero following dry spells. This means that rain-on-snow events would result in all precipitation counting towards net rainfall and the precipitation depth subtracted from the drought factor. While there are likely to be a very limited number of such instances which occur in a given year, and the total cost of such an omission would be at most 0.51 cm on any single day, the wording with regards to this is vague, likely due to the fact that this index was developed for the southeastern US forests where snowfall accumulation is rare. Another question is whether or not the drought factor will increase during dry spells if there is snow on the ground. This possibility is not explicitly addressed in any of the literature or the original documentation. However, it is highly likely that low temperatures will be limiting during these periods, and thus cause the drought factor to be zero except in the case of a multi-day thaw event. In fact, this same assumption was made but not stated in Liu *et al.* (2010) (Yongqiang Liu, personal correspondence, 3/16/2015). In such an event, fire cover would not increase in dryness until all of the snow has melted. As such, we assumed that the drought factor would be equal to zero at any point that snow is evident on the ground. Again, it is highly unlikely that snow presence will limit the drought factor, since temperature should almost certainly be limiting in this case as well. For this study, net rainfall was assumed to continue to accumulate during dry spells when snow is present, but resets to zero as soon as a dry spell occurs without snow cover. The presence of snow was determined using the water output from WEPP model simulations using a breakpoint precipitation format climate input file of the Tahoe City SNOTEL weather record. The mean annual rainfall in the KBDI equation was set equal to the annual precipitation under the MarkSim® baseline climate.

5.4 Results and Discussion

The complete SNOTEL record for 1988-2006 at the Tahoe City, California, station includes large sections at the beginning and the end of the record which are missing weather data. The record was therefore trimmed to include the years 1989-2006 with the exception of the last 15 days of 2006, for which weather data was unreliable. A SNOTEL station exists in the Ward Creek watershed, a watershed immediately adjacent and to the north of the Blackwood Creek basin. However, the Tahoe City station was selected to be consistent with the location of downscaled data obtained from MarkSim®; the Global Historical Climate Network Dataset (GHCND; Peterson and Vose, 1997) includes a weather station in Tahoe City but not one in the vicinity of Ward Creek. Additionally, the SNOTEL record used herein at both Ward Creek and Tahoe City have a period of record which overlaps with the period of record using in the GHCND from 1989-90 only.

Initially, water balance, soil loss, and fire risk were going to be assessed for the entire Blackwood Creek basin for this research. However, running 100-year long simulations of the 626 hillslope model revealed that there is a problem in the winter water balance processes which results in a net accumulation of TSW equivalent to about 1% of total precipitation in the basin. By the end of the 100-year simulation, this resulted in an extra 1.27 m of TSW in the water balance for the watershed. A similar trend was not observed in the individual hillslope outputs, pointing towards the aggregation processes in the 626 hillslope model output processing as the source of the error. Further identification and remedy of this error was beyond the scope this study. Additionally, re-simulation with the 626 hillslope model using the 29 different climates assessed in this study would have required additional time and digital storage volumes exceeding those allocated to this research. Water balance and fire risk were therefore assessed using representative hillslopes taken from the individual WEPP outputs of the 626 individual hillslopes.

WEPP outputs for three representative hillslopes were inspected to determine which hillslope in the Blackwood Creek watershed would give the most representative results. Elevations varied from 1920 m at the outlet to 2598 m at the highest point, and it was

found that hillslopes of similar elevation at the highest and lowest elevations also experienced similar weather, regardless of the proximity of the hillslopes to one another. According to the PRISM adjustments, lower elevations had the lowest average annual precipitation and higher temperatures while higher elevations had more precipitation and lower temperatures. Using this knowledge, representative hillslopes were selected based on elevation, with the three categories representing a hillslope near the bottom of the elevation spectrum, one near the top, and one near the median elevation (2166 m). Hillslopes were selected which had forested cover and only a single overland flow element (OFE). Overland flow elements are used in WEPP to represent heterogeneity in soil type and land cover within a single hillslope. A hillslope with only one OFE has uniform soil and land cover, making the model structure and the outputs generated simpler. Several hillslopes meeting these criteria existed near the median elevation, so the hillslope which also had average annual precipitation near the median value (1508 mm/year) was selected.

5.4.1 Assessment of Future Climate

Mean annual temperatures in the basin (Figure 5.2) were projected to increase by 1.2-1.7^{o}C by 2030, with mean temperatures diverging depending on the scenario thereafter. The RCP 2.6 scenario did not increase substantially from 2030-2090, while the RCP 8.5 scenario increased by nearly 6^{o}C over the baseline climate by 2090. The RCP 4.5 and 6.0 scenarios projected temperature increases of roughly 3^{o}C over the baseline climate by 2090.

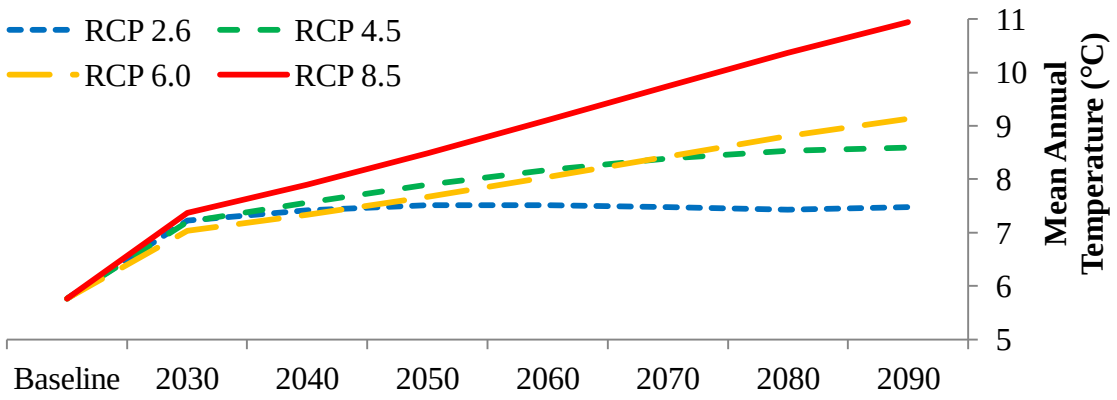

Figure 5.2: Mean annual temperatures at Tahoe City, California, under projected future climates with the four RCP scenarios

Annual precipitation depths are shown in Figure 5.3. Precipitation depths in 2090 were 5% lower compared to the baseline in the RCP 8.5 scenario, and 6% higher by 2090 in the RCP 2.6 scenario. Decadal variations were evident for annual precipitation depth, with a general decrease in RCP 8.5 scenario after 2060. The highest precipitation totals were at the higher elevations, while the lowest were found closer to the Lake Tahoe shoreline.

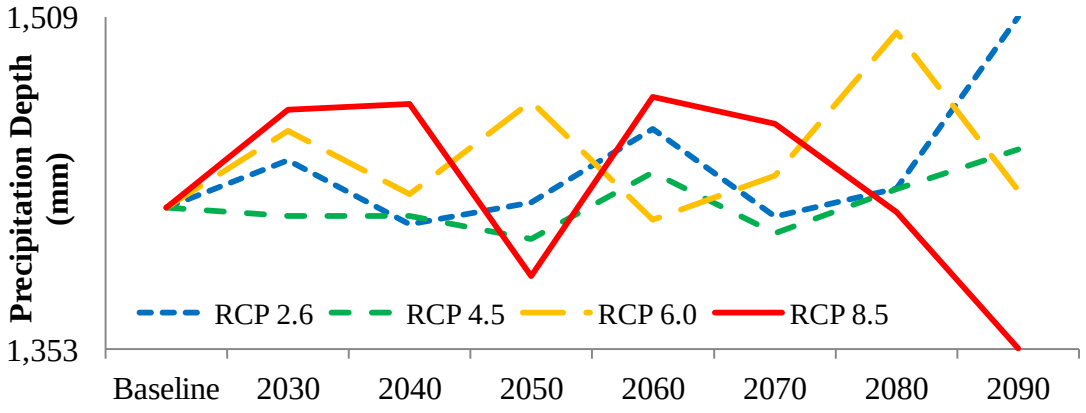

Figure 5.3: Mean annual precipitation depths at the median hillslope under the four RCP scenarios

Annual snowfall depths showed only slight differences when comparing the low elevation hillslope with the two higher ones (Figure 5.4). In general, the snowfall tended to decrease with increasing RCP severity, with RCP 8.5 projecting a 44% reduction in the

fraction of precipitation falling as snow. Under the RCP 8.5 scenario, snowfall at the higher elevation hillslope decreased from the baseline level of 1037 mm (63% of total precipitation) to 564 mm (47% of total precipitation) by 2090. The other two elevations were similar, with the lower elevation decreasing from 436 mm (45%) to 222 mm (24%) of snowfall, and the medium elevation dropping from 640 mm (55%) to 482 mm (41%) of snowfall under the RCP 8.5 scenario. Since average annual precipitation varied by less than 100 mm at the highest elevation through the 21st century, the majority of this snowfall reduction is likely due to temperature increases.

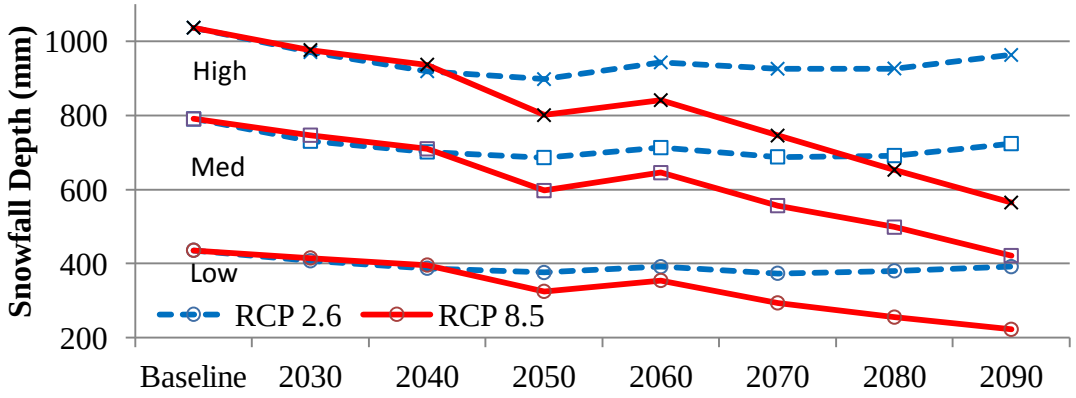

Figure 5.4: Predicted snowfall trend at the three representative hillslopes (high, medium, and low elevations) for the RCP 2.6 and RCP 8.5 scenarios

5.4.2 Fire Risk

Around 2400 wildfires were reported in the MTBS from 1984-2013 in the states of Nevada and California combined. Of these, approximately 258 occurred in and around the Sierra Nevada Mountains, burning a total of 908,614 ha. Approximately 48 of the 258 occurred within 50 km of Lake Tahoe (defined as having a center at 39.010N, 120.033W), burning 129,620 ha. Of those 48, 20 occurred to the west of the lake center, burning 48,610 ha. During the period which coincides with SNOTEL weather data, 150 fires occurred on 126 days during the period of complete SNOTEL data from 1989-2006, burning 434,828 ha. Of the 150 fires, 29 occurred within 50 km of the lake, burning 92,825 ha. For these 29 fires, 14 occurred to the west of the lake center, burning 41,842 ha.

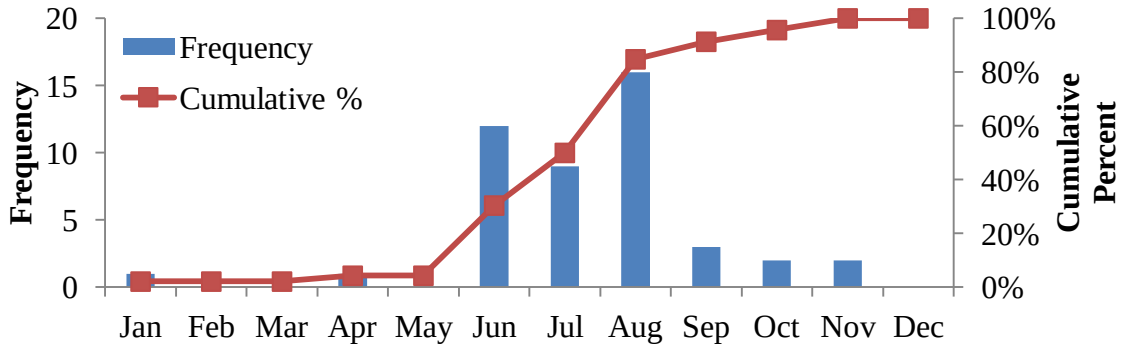

Figure 5.5: Histogram of fires near Lake Tahoe sorted by month (1984-2013)

For the Sierra Nevada Mountains (Figure 5.6), there was a higher instance of fire in the period from 2000-2008, with 56% of the fires in the region occurring during 27% of the observed period. The timing of fires within years was similar when comparing the Sierra Nevadas with fires near Lake Tahoe, with nearly 80% of fires occurring during the summer months. The most active month both in the Sierra Nevadas as a whole and near Lake Tahoe was August, with more than a third of all fires taking place in this month. August had both the highest total area burned (492,618 ha) and the highest average area burned per fire (5,131 ha) (Figure 5.5). September had the second largest average area (4,356 ha) and the third most total area burned (130,706 ha) compared to July which had the third highest average area (2564 ha) and the second most total area burned (151,288 ha). Put another way, while there were more fires started in July, the fires which started in September were more severe and burned more land per fire.

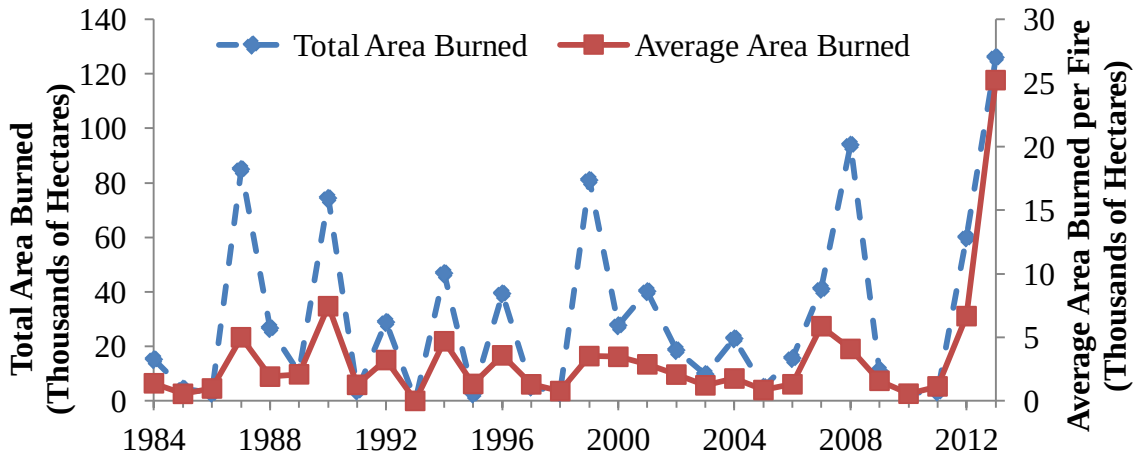

Figure 5.6: Total area burned by fires and average area burned by fires in the Sierra Nevada mountain range by year (1984-2013)

TSW and KBDI were calculated for the period 1988-2006 using the WEPP model and Equation 5.1, respectively. The TSW simulated at the high elevation hillslope was consistently at the minimum level of 8 mm, with TSW rapidly dropping to the minimum level following all precipitation events. This was likely a result of the steep slope and shallow restrictive layer assigned to that hillslope. Similar results were found for all hillslopes at a similar elevation. Due to the consistent low TSW, the high elevation hillslope was deemed unacceptable for assessing fire risk due to TSW. Additionally, KBDI was ruled to be an unsatisfactory metric for fire risk at these elevations due to the fact that the hillslopes with persistent low TSW coincided with highly erosive, sandy soils underlain by bedrock and bare of vegetation referred to as “badlands” in the upper reaches of the Blackwood Creek watershed (Leonard et al., 1979; Stubblefield, 2002; Stubblefield et al., 2009). The low elevation and median elevation hillslopes had similar TSW graphs (not shown), while the lower elevation hillslope had consistently higher KBDI values due to lower precipitation and higher mean annual temperatures. Only results for the median elevation hillslope are presented here, as it was considered to be most representative of the entire Blackwood Creek watershed.

Of the 150 fires which occurred in the Sierra Nevada range from 1989 to 2006 (Figure 5.7), 78 (62%) occurred when TSW was simulated at the median hillslope to be below 40 mm. An additional 36 fires (29%) occurred when TSW was between 40 mm and 220 mm, and the remaining 12 fires (9%) occurred when TSW was greater than 220 mm. Based on these observations, three fire risk categories were defined based on the TSW listed above: low risk (220 mm < TSW), moderate risk (40 mm < TSW ≤ 220 mm), and high risk (TSW ≤ 40 mm). The number of days in each year matching these criteria was compared between the observed climate, baseline MarkSim® climate, and projected future climate to determine changes in the length of fire risk seasons.

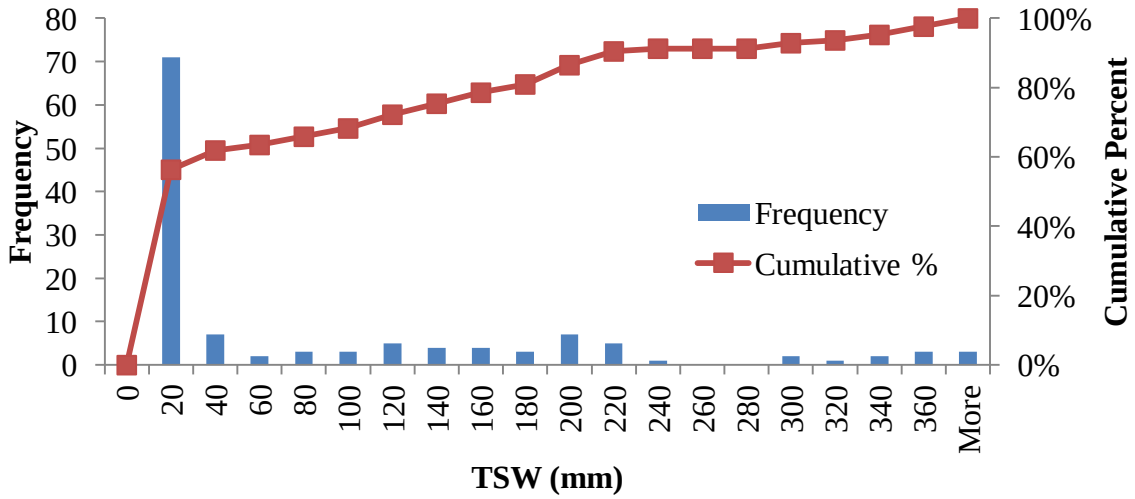

Figure 5.7: Histogram of fires sorted by WEPP simulated Total Soil Water (TSW) content (1989-2006)

The risk seasons were found to be markedly different for all three fire risk categories when comparing the MarkSim® baseline climate and the observed climate. The high risk season was 20% shorter (9 days), the moderate risk period was 29% shorter (45 days), and the low risk period was 56% longer (65 days) under the MarkSim® baseline climate compared to the observed 17-year record from 1989-2005. This difference can most immediately be attributed to the difference in period of record between the MarkSim® baseline climate (1960-1990) and the observed SNOTEL weather file (1989-2006). This may also be due to the fact that MarkSim® generated more frequent probabilities of a wet

day following a wet day ($P_{W/W}$) precipitation during the summer compared to the observed climate at Tahoe City. As such, the results for the moderate and low risk categories must be interpreted with caution.

KBDI results showed correlation between fire occurrence and KBDI when KBDI was less than 500, with an R^2 of 0.59 (Figure 5.8). The cumulative probability plot of KBDI on the day of fire ignition was linear with constant bin size. However, over 50% of all fires occurred when KBDI was greater than 500, almost all of which take place when TSW is at a minimum, making this correlation difficult to use. Since the correlation between fire occurrence and soil moisture was more apparent, TSW was used as a metric for fire risk instead of KBDI. KBDI was not correlated with fire size.

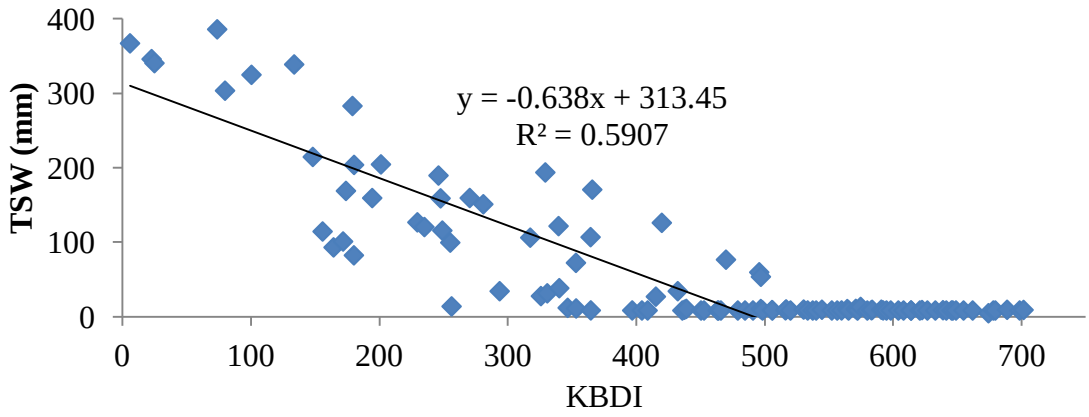

Figure 5.8: TSW predicted by WEPP versus KBDI, with linear regression equation and coefficient of determination shown for KBDI $\leq$ 500

The number of high risk days per year was projected to increase under all scenarios and time periods, with the exception of RCP 8.5 in the 2040s. Upon closer examination, it was found that solar radiation reported by MarkSim® was abnormally low from October to December for this scenario and decade combination. The error appears to be in the MarkSim® web application, as recreation of CLIGEN .par files yielded similar results. Similarly, this underprediction of solar radiation also caused the low risk days for the same time period and scenario to be projected to increase. The number of high risk days

(Figure 5.9) increased by 13-30 days, the number of moderate risk days decreased by 16-18 days, and the number of low risk days was mostly unchanged (±3 days), except for the RCP 8.5 scenario which had a decrease of 14 low risk days by 2090.

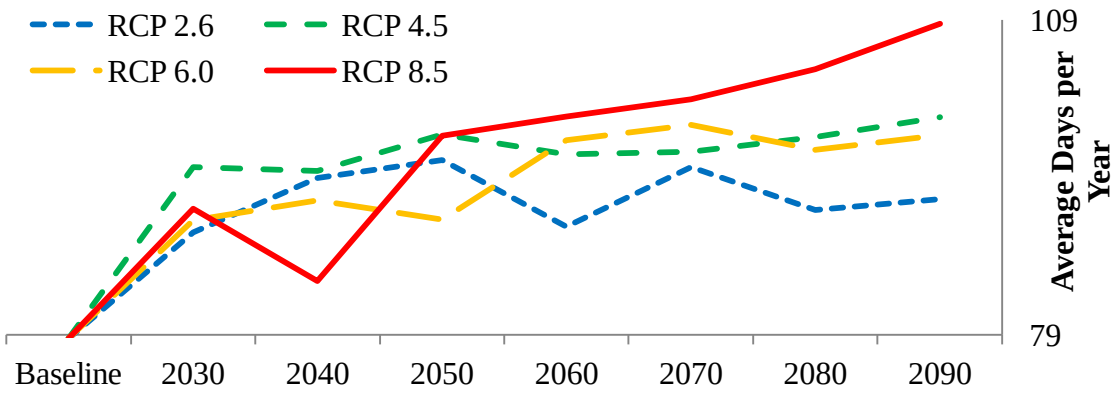

Figure 5.9: Average annual number of high risk days (TSW < 40mm) through 21st century

Several trends were observed regarding the three risk categories defined previously. A typical risk year (2004, Figure 5.10) is shown as an example. This highest risk season was identified to be when soil moisture was at a minimum, typically around 10 mm, during the summer months. The majority of the low risk season occurred during the spring, when infiltration of snowmelt increases TSW, however some low risk days occur before snow starts to fall in the early winter. The moderate risk season typically occurs in three portions: 1) partially in late fall when liquid precipitation replenishes TSW lost during the dry summer, 2) primarily during the winter when snowfall accumulates and water is lost gradually to deep percolation, and 3) during a short period in early summer when a lack of rainfall slowly depletes the TSW provided by spring snowmelt. While rainfall timing, distribution, and depths varied by year, most years contained at least the winter and early summer portions of the moderate risk period. Most fires which occurred in the moderate risk period from 1989-2006 occurred during the moderate risk period in early summer.

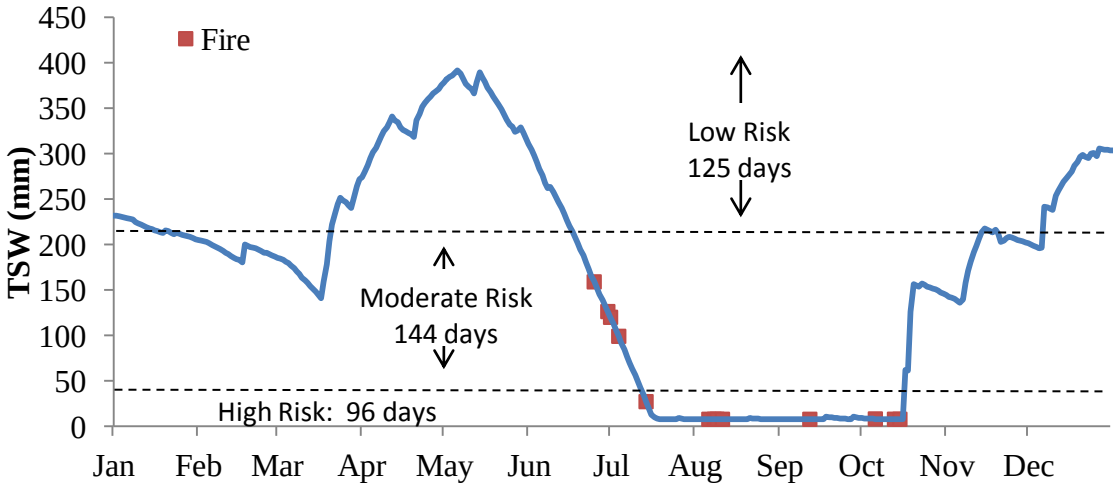

Figure 5.10: A typical year (2004) showing TSW, risk category length, and fire ignitions

KBDI has been used in the past to assess fire risk for future climates (Liu et al., 2010) as well as in the Sierra Nevada range (McKelvey and Busse, 1996). McKelvey and Busse (1996) found that elevations where KBDI did not exceed 500 on a regular basis also had very little or no fire activity. Here, KBDI with values over 500 corresponded exclusively to fire occurrences where TSW at the median hillslope was at a minimum. The fact that TSW approached and remained at a minimum value throughout most of the high risk period indicates that KBDI may be underestimating the true TSW deficit at this site. Better correlation between KBDI and TSW may be obtained by modifying the maximum KBDI value in the drought factor equation to better reflect the water holding capacity of soils in the Blackwood Creek watershed. The modification of the drought factor equation based on local environmental variables was beyond the scope of this study, but should be considered when applying KBDI to regions other than the Southeastern United States where it was developed.

Another drawback to the use of any empirically derived method, including KBDI, is that the equations and relationships between environmental variables and fire risk are based on historical observations which assume climate stationarity, a concept that is now widely accepted to no longer apply (Milly et al., 2008). As climate normals change, so will the relationships between climate variables and fire occurrence which were used to

develop the indices in the past. This may require the implementation of a dynamic component of the index, or the reworking of observational data at intervals depending on the rate of change of climate. The effect of the stationarity assumption has been demonstrated here, in that the risk seasons were found to be markedly different for all three fire risk categories when comparing the MarkSim® baseline climate and the observed climate. The lack in overlap of periods of observation for these two climate datasets may have contributed to poor correlation between the two due to a lack of stationarity. Weather records containing many of the factors required by WEPP which influence TSW, such as wind direction, wind speed, and daily solar radiation could not be found for the Tahoe City weather station. Had such records existed for the period 1960-1990, using them to simulate TSW at the Tahoe City station may have reduced the discrepancies in fire risk seasons.

5.5 Conclusions

Presented here are two methods of assessing forest fire risk, one based on an established fire index which uses observed precipitation and temperature, and the other based on simulated TSW which uses more sophisticated soil, land cover, climate, and topographic inputs. A large dataset of wildfires greater than 400 ha in area which occurred in the Western US states of California and Nevada from 1984-2013 was then used to obtain a shortened list of 150 fires which occurred in the Sierra Nevada mountain range between 1989 and 2006. The Keetch-Byram Drought Index was compared to TSW simulated by the WEPP model to develop fire risk categories based on TSW. Fire risk was assessed using this new metric to determine if fire risk would change under projected future climate change scenarios.

KBDI was found to be a less clear indicator of historic fire timing than periods of minimum TSW. Over 60% of fires in both the Sierra Nevadas and near the Lake Tahoe basin occurred when TSW was simulated to be at a minimum in the Blackwood Creek watershed, whereas KBDI varied from 250-700 over these same fires. KBDI and TSW did, however, show some correlation when KBDI values were below 500, but the KBDI

values over 500 accounted for more than half of all historical fires. Three fire risk categories were, therefore, assigned based on simulated TSW from 1989-2006 to assess the change in the number of days per year corresponding to each fire risk category. The high risk category, when TSW was below 40 mm at the median hillslope, coincided with over 60% of all fires which occurred between 1989 and 2006 in the Sierra Nevadas. Results showed that the number of high risk days increased under three of the four RCP scenarios, while the number of high risk days increased steadily for most scenarios through the 21st century. By 2090, the number of high risk days had increased by nearly two weeks under the least extreme scenario and by three and a half weeks under the most extreme scenario.

Very basic risk categories were defined here for a single hillslope in the Blackwood Creek watershed. If a solution can be found to the water balance problem in the 626 hillslope model, a more thorough TSW study could be conducted based on total TSW in the basin, which may eliminate the long stretch of minimum TSW which clouded the results of KBDI during the high risk season. Additional information could be gathered by using a different climate base station, or by augmenting the current SNOTEL data with information outside of the 1989-2006 window used here. These two improvements could provide important information for forecasting changes in fire risk in the greater Sierra Nevadas as well as basins in the Lake Tahoe region which have a fire deficit.

CHAPTER 6. SUMMARY AND CONCLUSIONS

This study was conducted to develop a simplified method of obtaining future climate data inputs for natural resource models, and then apply that method to three locations within the continental United States to assess the effect of climate change on soil erosion, runoff, and fire risk.

In Chapter 2, The MarkSim® DSSAT weather generator was used to generate downscaled future climate datasets for precipitation, minimum temperature, maximum temperature, and solar radiation values on a daily timescale for multiple locations for localized future climate impact assessments. The downscaled future climate data was then aggregated and formatted into parameter files for use with the CLIGEN weather generator via a user-friendly tool created using a macro-enabled Microsoft Excel Workbook. The macro made obtaining future climate inputs for the WEPP model fast and simple, which allowed for the study of three unique locations in a relatively short time. Additionally, the ability to create SWAT model climate input files was also added as an option with the tool.

Twelve locations throughout the contiguous United States were analyzed using Q-Q plots and R^2 values to determine that the WEPP baseline parameter files and those created by the MarkSim® baseline climate differed enough that only relative change in erosion should be calculated using this downscaling method. WEPP outputs generated for four representative locations were compared for the two baseline climates as well as 3 future time periods and showed that regional variations in precipitation and temperature due to future climate change will have different impacts on water balance, runoff, and soil erosion depending on geographic location.

The updated version of the MarkSim® web application allows users to create downscaled data using the latest IPCC AR5 model family, the baseline MarkSim® climate generated using the AR5 data showed slightly better R^2 values at the four selected sites, but the improvement was not substantial enough to be considered different from the baseline climate comparisons made under the AR4 model family. The AR5 data was used in the impact assessments herein to represent the latest in climate science understanding.

In Chapter 3, predicted changes in precipitation, runoff, and sediment losses were analyzed under a continuous minimally-tilled corn-soybean rotation for a small agricultural field catchment in Northeastern Indiana. Findings indicated that changes due to climate change will be most pronounced in late winter, late spring, and early fall. Precipitation was predicted to increase in the first five months of the year, with minimal changes from June-December. Increasing temperatures were predicted to cause runoff and sediment loss to decrease substantially in late winter due to a reduction in the number of days in which rainfall and snowmelt are incident on frozen soils. Runoff and sediment loss were predicted to increase in late spring due to a 15-25% increase in precipitation coupled with a lack of vegetation in the early growing season. With soybean cultivars unchanged, runoff and sediment loss were also predicted to increase in early fall for years planted to soybeans due to earlier senescence as a result of more rapid crop maturity.

These predicted changes, however, are likely to be mitigated to some degree as a result of farmer adaptations in the form of earlier planting dates and changes in cultivars, especially in the late spring and late fall months. However, the predicted relative increases in sediment losses and runoff in the late spring have greater implications for agrochemical transport to receiving waters. Unmentioned here also is the potential for increased heat stress and crop failure in the late summer months, which could affect soil loss similar to that seen in September.

Results found here were similar to those by other authors using WEPP, specifically Pruski and Nearing (2002), where precipitation and soil loss were predicted to increase

from 1990-2099 while runoff decreased due to dissimilar changes in precipitation and runoff from month to month. They observed a similar increase in precipitation in April and May, resulting in increased runoff and soil loss. However, Pruski and Nearing (2002) modeled a decrease in precipitation in June through September, leading to reductions in runoff and soil loss. The net effect in their study was a decrease in the runoff and sediment loss under soil, slope, and cropping conditions similar to those modeled herein. The increases in temperature resulting in earlier senescence of soybeans have also been noted by other authors using WEPP at a site in Indiana (Savabi and Stockle, 2001). Unlike previous studies, the observation here that a predicted reduction in concrete soil frost reduced runoff in early spring is unique to this study.

Evaluation of various BMPs indicated that buffer strips provided the same or better predicted filtration of sediments as the grassed waterways while maintaining a sediment trap during the fallow period, the combination of both being more effective than using a rye cover crop alone. However, the fallow and spring cover provided by the rye cover crop means that the sediments are retained further up on the hillslope, while the use of only grassed buffers would build up sediment deposits on the toeslope. In practice, buffer strips in this type of terrain will likely be accompanied by grassed waterways, and simulation of grassed waterways and buffer strips without rye cover would likely show less runoff, but may result in higher soil losses due to increased detachment compared to the combination scenario modeled here.

Based on these findings, producers will first need to identify the most critical type of nonpoint source pollution from their fields before selecting a BMP which will be most effective into the future. If off-site soluble nutrient loss requires the most attention, then management practices which reduce total runoff (buffer strips and/or inclusion of a sod/hay crop in rotation) should be considered, while if sediment loss or soil-bound nutrients are of most concern then practices such as grassed waterways or buffer strips should be considered. Conversion to rotations including sod/hay are somewhat unrealistic though, so combinations of practices that maintain corn/soybean row crops but utilize

high levels of crop residues and live vegetation may be more acceptable. Overall, the best management options into the future will likely include in-field (no-till and cover crops) and edge-of-field (grassed waterways and buffer strips) to reduce soil migration to lower slopes as well as filter fine sediments from runoff and increase infiltration prior to discharging agricultural runoff to receiving waters.

In Chapter 4, a small, experimental, agricultural hillslope managed by the USDA-ARS in the Southeastern Coastal Plain of the United States was modeled using WEPP under current and projected future climates to assess the effect of predicted climate change on runoff, soil erosion, and BMP effectiveness. Simulation results showed that runoff and soil loss changed for most months under the existing conventional management, with these changes typically accompanied by similar changes in total rainfall. Predicted climatic shifts caused soil loss and runoff to be reduced in the first three months of the year, while limited change was modeled during the growing season. Late fall and early winter months, when ground cover was low, had predicted increases in runoff and soil loss which corresponded with an increase in total late-year precipitation. Increased air temperatures resulted in the winter cover crop growing faster and unhindered by frost in the early months of the year, reducing predicted soil loss during this traditionally low-cover period. Soil loss was also predicted to increase prior to harvest as a result of the reduction in canopy cover caused by the earlier senescence of cotton due to the projected warmer temperatures. Increased predicted runoff in March and more ET in July from temperature-promoted crop growth also increased irrigation demands during the growing season under the baseline management. Ten management systems were examined under the future projected climate scenarios, and effectiveness of the combination of no-till, rye cover crop, and riparian buffers was the only one that increased into the future. All other management systems had either similar or slightly reduced effectiveness. In general, the effectiveness of the various land management practices did not change much into the future.

This study has several drawbacks which may limit the use of results for management decisions, separate from limitations which have previously been noted regarding the method of future climate data acquisition (Section 2.5). First, an important and largely unpredictable measure of adaptation in agriculture which has not been detailed here is the gradual selection and change-over to crop cultivars better suited for future altered temperature and precipitation patterns. These cultivar changes were not assessed in the current study, and limitations in the predictability of economic drivers for crop viability make speculation and simulation of these changes difficult. As modeling technologies improve, the effect of cultivar changes will need to be assessed alongside BMP implementation to determine the interplay of each to natural resource management. Second, the size of the hillslope examined was small, limiting the extrapolation of results to a larger geographic area. On the other hand, the small controlled area allowed for high resolution records to be obtained for climate, soil, topography, management, and observed runoff and soil loss, resulting in high calibration/validation prediction efficiencies and providing high levels of confidence in the WEPP model results and projections.

Despite these limitations, the results from this study indicate that current conservation practices and BMPs being implemented at this location will likely be sufficient for mitigating soil erosion and runoff into the future.

In Chapter 5, two methods of assessing forest fire risk were used in the Lake Tahoe basin, one based on an established fire index which uses observed precipitation and temperature, and the other based on simulated TSW which uses more sophisticated soil, land cover, climate, and topographic inputs. A large dataset of wildfires greater than 400 ha in area which occurred in the Western US states of California and Nevada from 1984-2013 were used to obtain a shortened list of 150 fires which occurred in the Sierra Nevada mountain range between 1989 and 2006. The Keetch-Byram Drought Index was compared to TSW simulated by the WEPP model to develop fire risk categories based on

TSW. Fire risk was assessed using this new metric to determine if fire risk would change under projected future climate change scenarios.

KBDI was found to be a less clear indicator of historic fire timing than periods of minimum TSW. Over 60% of fires in both the Sierra Nevadas and just near the Lake Tahoe basin occurred when TSW was simulated to be at a minimum in the Blackwood Creek watershed, whereas KBDI varied from 250-700 over these same fires. KBDI and TSW did, however, show some correlation when KBDI values were below 500, but the KBDI values over 500 accounted for more than half of all historical fires. Three fire risk categories were, therefore, assigned based on simulated TSW from 1989-2006 to assess the change in the number of days per year corresponding to each fire risk category. The high risk category, when TSW was below 40 mm at the median hillslope, coincided with over 60% of all fires which occurred between 1989 and 2006 in the Sierra Nevadas. Results showed that the number of high risk days increased under three of the four RCP scenarios, while the number of high risk days increased steadily for most scenarios through the 21st century. By 2090, the number of high risk days had increased by nearly two weeks under the least extreme scenario and by three and a half weeks under the most extreme scenario.

Several trends were observed regarding the three risk categories defined previously. A typical risk year (2004, Figure 5.9) is shown as an example. The highest risk season was identified to be when soil moisture was at a minimum, typically around 10 mm, during the summer months. The majority of the low risk season occurred during the spring, when infiltration of snowmelt increases TSW, however some low risk days occur before snow starts to fall in the early winter. The moderate risk season typically occurs in three portions: 1) partially in late fall when liquid precipitation replenishes TSW lost during the dry summer, 2) primarily during the winter when snowfall accumulates and water is lost gradually to deep percolation, and 3) during a short period in early summer when a lack of rainfall slowly depletes the TSW provided by spring snowmelt. While rainfall timing, distribution, and depths varied by year, most years contained at least the winter and early

summer portions of the moderate risk period. Most fires which occurred in the moderate risk period from 1989-2006 occurred during the short moderate risk period in early summer.

KBDI has been used in the past to assess fire risk for future climates (Liu et al., 2010) as well as in the Sierra Nevada range (McKelvey and Busse, 1996). McKelvey and Busse (1996) found that elevations where KBDI did not exceed 500 on a regular basis also had very little or no fire activity. Here, KBDI with values over 500 corresponded exclusively to fire occurrences where TSW at the median hillslope was at a minimum. The fact that TSW approached and remained at a minimum value throughout most of the high risk period indicates that KBDI may be underestimating the true TSW deficit at this site. Better correlation between KBDI and TSW may be obtained by modifying the maximum KBDI value in the drought factor equation to better reflect the water holding capacity of soils in the Blackwood Creek watershed. The modification of the drought factor equation based on local environmental variables was beyond the scope of this study, but should be considered when applying KBDI to regions other than the Southeastern United States where it was developed.

Another drawback to the use of any empirically derived method, including KBDI, is that the equations and relationships between environmental variables and fire risk are based on historical observations which assume climate stationarity, a concept that is now widely accepted to no longer apply (Milly et al., 2008). As climate normals change, so will the relationships between climate variables and fire occurrence which were used to develop the indices in the past. This may require the implementation of a dynamic component of the index, or the reworking of observational data at intervals depending on the rate of change of climate. The effect of the stationarity assumption has been demonstrated here, in that the risk seasons were found to be markedly different for all three fire risk categories when comparing the MarkSim® baseline climate and the observed climate. The lack in overlap of periods of observation for these two climate datasets may have contributed to poor correlation between the two due to a lack of

stationarity. Weather records containing many of the factors required by WEPP which influence TSW, such as wind direction, wind speed, and daily solar radiation could not be found for the Tahoe City weather station. Had such records existed for the period 1960-1990, using them to simulate TSW at the Tahoe City station may have reduced the discrepancies in fire risk seasons.

Very basic risk categories were defined here for a single hillslope in the Blackwood Creek watershed. If a solution can be found to the water balance problem in the 626 hillslope model output processing, a more thorough TSW study could be conducted based on total TSW in the basin, which may eliminate the long stretch of minimum TSW which clouded the results of KBDI during the high risk season. Additional information could be gathered by using a different climate base station, or by augmenting the current SNOTEL data with information outside of the 1989-2006 window used here. These two improvements could provide important information for forecasting changes in fire risk in the greater Sierra Nevadas as well as basins in the Lake Tahoe region which have a fire deficit.

Climate change was found to vary by region into the future. However, rising temperatures, reduced snowfall, and changes in growing seasons of agricultural crops appear to be common across the three diverse biomes studied. Predicting climate as far as 80 years in the future presents uncertainties in many forms, and it is important to understand that climate change studies are limited by the current state of atmospheric science and projections based on events yet to occur. Studies of this type must be reevaluated with every iteration of the IPCC Assessment Report, as well as every update to the mathematical downscaling and natural resource models used. Weather datasets get larger with time, and the discrepancies between simulated and observed baseline climates are likely to decrease as datasets expand. Despite the limitations presented herein and elsewhere, these studies are critical to understanding, mitigating, and adapting to climate change.

LIST OF REFERENCES

LIST OF REFERENCES

Alexander, R.B., R.A. Smith, G.E. Schwarz, E.W. Boyer, J. V Nolan, and J.W. Brakebill. 2008. Differences in phosphorus and nitrogen delivery to the Gulf of Mexico from the Mississippi River Basin. Environ. Sci. Technol. 42(3): 822–830.

Arnold, J.G., R. Srinivasan, R.S. Muttiah, and J.R. Williams. 1998. Large area hydrologic modeling and assessment part I: model development. J. Am. Water Resour. Assoc. 34(1): 73–89.

Ascough, J.C., O. David, and P. Krause. 2012. Development and application of a modular watershed-scale hydrologic model using the Object Modeling System: runoff response evaluation. Trans. ASABE 55(1): 117–135.

Beaty, R.M., and A.H. Taylor. 2009. A 14 000 year sedimentary charcoal record of fire from the northern Sierra Nevada, Lake Tahoe Basin, California, USA. The Holocene 19(3): 347–358.

Bosch, D.D., R.K. Hubbard, L.T. West, and R.R. Lowrance. 1994. Subsurface flow patterns in a riparian buffer system. Trans. ASAE 37(6): 1783–1790.

Bosch, D.D., T.L. Potter, C.C. Truman, C.W. Bednarz, and T.C. Strickland. 2005. Surface runoff and lateral subsurface flow as a response to conservation tillage and soil-water conditions. Trans. ASAE 48(6): 2137–2144.

Bosch, D.D., J.M. Sheridan, and F.M. Davis. 1999. Rainfall characteristics and spatial correlation for the Georgia Coastal Plain. Trans. ASAE 42(6): 1637–1644.

Bosch, D.D., C.C. Truman, T.L. Potter, L.T. West, T.C. Strickland, and R.K. Hubbard. 2012. Tillage and slope position impact on field-scale hydrologic processes in the South Atlantic Coastal Plain. Agric. Water Manag. 111: 40–52.

Bradshaw, L.S., J.E. Deeming, R.E. Burgan, and J.D. Cohen. 1984. The 1978 National Fire-Danger Rating System: technical documentation. General Technical Report INT-169, USDA, Forest Service, Intermountain Forest and Range Experiment Station, Ogden, UT.

Brooks, E.S., W. Elliot, J. Boll, and J. Wu. 2010. Assessing the sources and transport of fine sediment in response to management practices in the Tahoe Basin using the WEPP model. University of Idaho, Moscow, ID.

Cechova, K., D.C. Flanagan, J.R. Frankenberger, and B.W. Zuercher. 2010. WEPP model application in CEAP watersheds in NE Indiana. ASABE Paper 10-08827, 2010 ASABE Annual International Meeting, Pittsburgh, PA. American Society of Agricultural and Biological Engineers, St. Joseph, Mich. 18 pp.

Chiew, F.H.S., D.G.C. Kirono, D.M. Kent, A.J. Frost, S.P. Charles, B. Timbal, K.C. Nguyen, and G. Fu. 2010. Comparison of runoff modelled using rainfall from different downscaling methods for historical and future climates. J. Hydrol. 387: 10–23.

Chiew, F.H.S., J. Teng, J. Vaze, and D.G.C. Kirono. 2009. Influence of global climate model selection on runoff impact assessment. J. Hydrol. 379(1-2): 172–180.

Cho, J., R.R. Lowrance, D.D. Bosch, T.C. Strickland, Y. Her, and G. Vellidis. 2010a. Effect of watershed subdivision and filter width on SWAT simulation of a Coastal Plain Watershed. J. Am. Water Resour. Assoc. 46(3): 586–602.

Cho, J., G. Vellidis, D.D. Bosch, R. Lowrance, and T. Strickland. 2010b. Water quality effects of simulated conservation practice scenarios in the Little River Experimental watershed. J. Soil Water Conserv. 65(6): 463–473.

Coats, R. 2010. Climate change in the Tahoe basin: regional trends, impacts and drivers. Clim. Change 102: 435–466.

Coats, R., M. Larsen, A. Heyvaert, J. Thomas, M. Luck, and J. Reuter. 2008. Nutrient and sediment production, watershed characteristics, and land use in the Tahoe Basin, California-Nevada. J. Am. Water Resour. Assoc. 44(3): 754–770.

Cooper, J.R., J.W. Gilliam, R.B. Daniels, and W.P. Robarge. 1987. Riparian areas as filters for agricultural sediment. Soil Sci. Soc. Am. J. 51(2): 416–420.

Covert, S.A., P.R. Robichaud, W.J. Elliot, and T.E. Link. 2005. Evaluation of runoff prediction from WEPP-based erosion models for harvested and burned forest watersheds. Trans. ASABE 48(3): 1091–1100.

Daly, C., M. Halbleib, J.I. Smith, W.P. Gibson, M.K. Doggett, G.H. Taylor, J. Curtis, and P.P. Pasteris. 2008. Physiographically sensitive mapping of climatological temperature and precipitation across the conterminous United States. Int. J. Climatol. 28: 2031–2064.

Daniels, R.B., and J.W. Gilliam. 1996. Sediment and chemical load reduction by grass and riparian filters. Soil Sci. Soc. Am. J. 60: 246–251.

Delgado, J.A., M.A. Nearing, and C.W. Rice. 2013. Conservation practices for climate change adaptation. p. 47–115. *In* Advances in Agronomy, Vol . 121. Elsevier.

Dun, S., J.Q. Wu, W.J. Elliot, P.R. Robichaud, D.C. Flanagan, J.R. Frankenberger, R.E. Brown, and A.C. Xu. 2009. Adapting the Water Erosion Prediction Project (WEPP) model for forest applications. J. Hydrol. 366(1-4): 46–54.

Eidenshink, J., B. Schwind, K. Brewer, Z. Zhu, B. Quayle, and S. Howard. 2007. A project for monitoring trends in burn severity. Fire Ecol. 3(1): 3–21.

Elliot, W.J. 2004. WEPP internet interfaces for forest erosion prediction. J. Am. Water Resour. Assoc. 40(2): 299–309.

Elliot, W.J., and D.E. Hall. 1997. Water Erosion Prediction Project (WEPP) forest applications. General Technical Report INT-GTR-365, USDA Forest Service, Forestry Sciences Laboratory, Moscow, ID.

Endale, D.M., D.D. Bosch, T.L. Potter, and T.C. Strickland. 2014. Sediment loss and runoff from cropland in a Southeast Atlantic Coastal Plain landscape. Trans. ASABE 57(6): 1611–1626.

Feyereisen, G.W., T.C. Strickland, D.D. Bosch, C.C. Truman, J.M. Sheridan, and T.L. Potter. 2008. Curve number estimates for conventional and conservation tillages in the southeastern Coastal Plain. J. Soil Water Conserv. 63(3): 120–128.

Flanagan, D.C., J.R. Frankenberger, and J.C Ascough II. 2012. WEPP: Model use, calibration and validation. Trans. ASABE 55(4): 1463–1477.

Flanagan, D.C., J.E. Gilley, and T.G. Franti. 2007. Water Erosion Prediction Project (WEPP): Development history, model capabilities, and future enhancements. Trans. ASABE 50(5): 1603–1612.

Flanagan, D.C., C. Huang, E.A. Pappas, D.R. Smith, and G.C. Heathman. 2008. Assessing conservation effects on water quality in the St. Joseph River Watershed. Proceedings of the Agro-Environment Symposium. Antalya, Turkey. 28 April – 1 May 2008. 36-44.

Flanagan, D.C., S.J. Livingston, C. Huang, and E.A. Warnemuende. 2003. Runoff and pesticide discharge from agricultural watersheds in NE Indiana. ASABE Paper 03-2006, 2003 ASAE Annual International Meeting, Las Vegas, NV. American Society of Agricultural Engineers, St. Joseph, Mich., 15 pp.

Flanagan, D.C., and M.A. Nearing (Eds). 1995. USDA Water Erosion Prediction Project: hillslope profile and watershed model documentation. NSERL Report No. 10, USDA-ARS, National Soil Erosion Research Laboratory, West Lafayette, IN.

Flanagan, D.C., J. Trotochaud, C.W. Wallace, and B.A. Engel. 2014. Tool for obtaining projected future climate inputs for the WEPP and SWAT models. *In* Proceedings ASABE 21st Century Watershed Technology Conference, Hamilton, New Zealand. American Society of Agricultural and Biological Engineers, St. Joseph, Mich., 8 pp.

Fowler, A.M., and K.J. Hennessy. 1995. Potential impacts of global warming on the frequency and magnitude of heavy precipitation. Nat. Hazards 11: 283–303.

Gavigan, T., and C. Curtis. 2007. Total Maximum Daily Load for bedded sediment: Blackwood Creek, Placer County, CA. California Regional Water Quality Control Board, Lahontan Region, South Lake Tahoe, CA.

Gupta, H.V., S. Sorooshian, and P.O. Yapo. 1999. Status of automatic calibration for hydrologic models: comparison with multilevel expert calibration. J. Hydrol. Eng. 4: 135–143.

Hatfield, J.L., K.J. Boote, B.A. Kimball, L.H. Ziska, R.C. Izaurralde, D. Ort, A.M. Thomson, and D. Wolfe. 2011. Climate impacts on agriculture: Implications for crop production. Agron. J. 103(2): 351.

Hatfield, J.L., and J.H. Prueger. 2004. Impacts of changing precipitation patterns on water quality. J. Soil Water Conserv. 59(1): 51–58.

Hatfield, J., G. Takle, R. Grotjahn, P. Holden, R.C. Izaurralde, T. Mader, E. Marshall, and D. Liverman. 2014. Chapter 6: Agriculture. *In* Melillo, J.M., Richmond, T.C. (eds.), Climate Change Impacts in the United States: The Third National Climate Assessment. U.S Global Change Research Program, p. 150–174.

Heathman, G.C., D.C. Flanagan, M. Larose, and B.W. Zuercher. 2008. Application of the Soil and Water Assessment Tool and Annualized Agricultural Non-Point Source models in the St. Joseph River Watershed. J. Soil Water Conserv. 63(6): 552–568.

Hijmans, R.J., S.E. Cameron, J.L. Parra, P.G. Jones, and A. Jarvis. 2005. Very high resolution interpolated climate surfaces for global land areas. Int. J. Climatol. 25(15): 1965–1978.

Howden, S.M., J.-F. Soussana, F.N. Tubiello, N. Chhetri, M. Dunlop, and H. Meinke. 2007. Adapting agriculture to climate change. Proc. Natl. Acad. Sci. U. S. A. 104(50): 19691–6.

IPCC. 2000. Emissions Scenarios - A special report of Working Group III of the Intergovernmental Panel on Climate Change (N Nakicenovic and R Swart, Eds.). Cambridge University Press, Cambridge, England.

IPCC. 2014. Climate Change 2014: Impacts, adaptation, and vulnerability. Part A: Global and sectoral aspects. Contributions of Working Group II to the Fifth Assessment Report of the Intergovernmental Panel on Climate Change (VR Barros, DJ Dokken, KJ Mach, MD Mastrandrea, TE Bilir, M Chatterjee, KL Ebi, YO Estrada, RC Genova, B Girma, ES Kisse, AN Levy, S MacCracken, PR Mastrandrea, and LL White, Eds.). Cambridge University Press, Cambridge, United Kingdom and New York, NY, USA.

Janis, M.J., M.B. Johnson, and G. Forthum. 2002. Near-real time mapping of Keetch-Byram drought index in the south-eastern US. Int. J. Wildl. Fire 11: 281–289.

Joh, H.-K.A.G., J.-W.B. Lee, M.-J.C. Park, H.-J.C. Shin, J.-E.D. Yi, G.-S.D. Kim, R.E. Srinivasan, and S.-J.F. Kim. 2011. Assessing climate change impact on hydrological components of a small forest watershed through SWAT calibration of evapotranspiration and soil moisture. Trans. ASABE 54: 1773–1781.

Jones, P.G., and P.K. Thornton. 1993. A rainfall generator for agricultural applications in the tropics. Agric. For. Meteorol. 63: 1–19.

Jones, P.G., and P.K. Thornton. 1997. Spatial and temporal variability of rainfall related to a third-order Markov model. Agric. For. Meteorol. 86: 127–138.

Jones, P.G., and P.K. Thornton. 1999. Fitting a third-order Markov rainfall model to interpolated climate surfaces. Agric. For. Meteorol. 97: 213–231.

Jones, P.G., and P.K. Thornton. 2000. MarkSim: Software to generate daily weather data for Latin America and Africa. Agron. J. 92: 445–453.

Jones, P.G., and P.K. Thornton. 2013. Generating downscaled weather data from a suite of climate models for agricultural modelling applications. Agric. Syst. 114: 1–5.

Karl, T.R., J.M. Melillo, and T.C. Peterson (Eds). 2009. Global Climate Change Impacts in the United States. Cambridge University Press, New York, NY.

Keetch, J.J., and G.M. Byram. 1968. A drought index for forest fire control. Forest Service Research Paper SE-38, USDA, Forest Service, Southeastern Forest Experiment Station, Asheville, NC.

Kendon, E.J., R.G. Jones, E. Kjellström, and J.M. Murphy. 2010. Using and designing GCM-RCM ensemble regional climate projections. J. Clim. 23: 6485–6503.

Kiniry, J.R., C.E. Simpson, A.M. Schubert, and J.D. Reed. 2005. Peanut leaf area index, light interception, radiation use efficiency, and harvest index at three sites in Texas. F. Crop. Res. 91: 297–306.

Kottwitz, E.R. 1995. USDA-Water Erosion Prediction Project: Hillslope profile and watershed model documentation. Chapter 12: Irrigation Component (DC Flanagan and MA Nearing, Eds.). NSERL Report No. 10, USDA-ARS, National Soil Erosion Research Laboratory, West Lafayette, IN.

Lenderink, G., and E. van Meijgaard. 2008. Increase in hourly precipitation extremes beyond expectations from temperature changes. Nat. Geosci. 1(8): 511–514.

Leonard, R.L., L.A. Kaplan, J.F. Elder, R.N. Coats, and R. Charles. 1979. Nutrient transport in surface runoff from a subalpine watershed, Lake Tahoe Basin, California. Ecol. Monogr. 49(3): 281–310.

Liu, Y., J. Stanturf, and S. Goodrick. 2010. Trends in global wildfire potential in a changing climate. For. Ecol. Manage. 259: 685–697.

Lowrance, R., R.K. Hubbard, and R.G. Williams. 2000. Effects of a managed three zone riparian buffer system on shallow groundwater quality in the Southeastern Coastal Plain. J. Soil Water Conserv. 55(2): 212–220.

Lowrance, R., R. Leonard, and J. Sheridan. 1985. Managing riparian ecosystems to control nonpoint pollution. J. Soil Water Conserv. 40(1): 87–91.

Lowrance, R., J.K. Sharpe, and J.M. Sheridan. 1986. Long-term sediment deposition in the riparian zone of a coastal plain watershed. J. Soil Water Conserv. 41(4): 266–271.

Lowrance, R., R. Todd, J. Fail, O. Hendrickson, L. Asmussen, and R. Leonard. 1984. Riparian forests as nutrient filters in agricultural watersheds. Bioscience 34(6): 374–377.

Marlon, J.R., P.J. Bartlein, D.G. Gavin, C.J. Long, R.S. Anderson, C.E. Briles, K.J. Brown, D. Colombaroli, D.J. Hallett, M.J. Power, E.A. Scharf, and M.K. Walsh. 2012. Long-term perspective on wildfires in the western USA. Proc. Natl. Acad. Sci. 109: E535–E543.

Mausbach, M.J., and A.R. Dedrick. 2004. The length we go: measuring environmental benefits of conservation practices. J. Soil Water Conserv. 59(5): 96–103.

McKelvey, K.S., and K.K. Busse. 1996. Twentieth-century fire atterns on forest service lands. p. 1119–1138. *In* Sierra Nevada Ecosystem Project: Final report to Congress. University of California, Centers for Water and Wildland Resources, Davis, California.

Mearns, L.O., I. Bogardi, F. Giorgi, I. Matyasovszky, and M. Palecki. 1999. Comparison of climate change scenarios generated from regional climate model experiments and statistical downscaling. J. Geophys. Res. 104: 6603–6621.

Mearns, L.O., F. Giorgi, P. Whetton, D. Pabon, M. Hulme, and M. Lal. 2003. Guidelines for use of climate scenarios developed from regional climate model experiments. Data Distribution Centre of the Intergovernmental Panel on Climate Change, Task Group on Data and Scenario Support for Impact and Climate Assessment.

Michalak, A.M., E.J. Anderson, D. Beletsky, S. Boland, N.S. Bosch, T.B. Bridgeman, J.D. Chaffin, K. Cho, R. Confesor, I. Daloglu, J. V Depinto, M.A. Evans, G.L. Fahnenstiel, L. He, J.C. Ho, L. Jenkins, T.H. Johengen, K.C. Kuo, E. Laporte, X. Liu, M.R. McWilliams, M.R. Moore, D.J. Posselt, R.P. Richards, D. Scavia, A.L. Steiner, E. Verhamme, D.M. Wright, and M.A. Zagorski. 2013. Record-setting algal bloom in Lake Erie caused by agricultural and meteorological trends consistent with expected future conditions. Proc. Natl. Acad. Sci. U. S. A. 110(16): 6448–52.

Milly, P.C.D., J. Betancourt, M. Falkenmark, R.M. Hirsch, Z.W. Kundzewicz, L.D. P, and S.R. J. 2008. Climate change. Stationarity is dead: whither water management? Science 319(5863): 573–574.

Moriasi, D.N., J.G. Arnold, M.W. van Liew, R.L. Bingner, R.D. Harmel, and T.L. Veith. 2007. Model evaluation guidelines for systematic quantification of accuracy in watershed simulations. Trans. ASABE 50(3): 885–900.

Moss, R.H., J.A. Edmonds, K.A. Hibbard, M.R. Manning, S.K. Rose, D.P. van Vuuren, T.R. Carter, S. Emori, M. Kainuma, T. Kram, G. a Meehl, J.F.B. Mitchell, N. Nakicenovic, K. Riahi, S.J. Smith, R.J. Stouffer, A.M. Thomson, J.P. Weyant, and T.J. Wilbanks. 2010. The next generation of scenarios for climate change research and assessment. Nature 463(7282): 747–756.

Nash, J.E., and J. V Sutcliffe. 1970. River flow forecasting through conceptual models part I—A discussion of principles. J. Hydrol. 10: 282–290.

NDEP. 2011. Final Lake Tahoe Maximum Daily Load. Nevada Division of Environmental Protection, Carson City, Nevada.

Nearing, M.A. 2001. Potential changes in rainfall erosivity in U.S. with climate change during the 21st century. J. Soil Water Conserv. 56(3): 229–232.

Nearing, M.A., L.D. Ascough, and J.M. Laflen. 1990. Sensitivity analysis of the WEPP hillslope profile erosion model. Trans. ASAE 33(3): 839–849.

Nearing, M.A., F.F. Pruski, and M.R. O'Neal. 2004. Expected climate change impacts on soil erosion rates: A review. J. Soil Water Conserv. 59(1): 43–50.

Nicks, A.D., L.J. Lane, and G.A. Gander. 1995. USDA-Water Erosion Prediction Project: Hillslope profile and watershed model documentation. Chapter 2: Weather Generator (DC Flanagan and MA Nearing, Eds.). NSERL Report No. 10, USDA-ARS National Soil Erosion Research Laboratory, West Lafayette, IN.

NOAA. 2014. Climate Data Online. Available at http://www.ncdc.noaa.gov/cdo-web/.

Nolan, B.K.M., and B.R. Hill. 1991. Suspended-sediment budgets for four drainage basins tributary to Lake Tahoe, California and Nevada, 1984-87. USGS, Water-Resources Investigations Report 91-4054, United State Geological Survey, Sacramento, California.

O'Neal, M.R., M.A. Nearing, R.C. Vining, J. Southworth, and R.A. Pfeifer. 2005. Climate change impacts on soil erosion in Midwest United States with changes in crop management. Catena 61(2-3): 165–184.

Pachauri, R.K., and A. Reisinger (Eds). 2007. Contribution of Working Groups I, II and III to the Fourth Assessment Report of the Intergovernmental Panel on Climate Change. IPCC, Geneva, Switzerland.

Peterson, T.C., and R.S. Vose. 1997. An overview of the Global Historical Climatology Network temperature database. Bull. Am. Meteorol. Soc. 78(12): 2837–2849.

Phillips, J.D. 1989. Nonpoint source pollution control effectiveness of riparian forests along a Coastal Plain river. J. Hydrol. 110(3-4): 221–237.

Potter, T.L., Z. Gerstl, P.W. White, G.S. Cutts, T.M. Webster, C.C. Truman, T.C. Strickland, and D.D. Bosch. 2010. Fate and efficacy of Metolachlor granular and emulsifiable concentrate formulations in a conservation tillage system. J. Agric. Food Chem. 58: 10590–6.

Potter, T.L., C.C. Truman, D.D. Bosch, and C. Bednarz. 2004. Organic compounds in the environment Fluometuron and Pendimethalin runoff from strip and conventionally tilled cotton in the Southern Atlantic Coastal Plain. J. Environ. Qual. 33: 2122–2131.

Pruski, F., and M.A. Nearing. 2002. Climate-induced changes in erosion diring the 21st century for eight U.S. locations. Wat. Resour. Res. 38(12): 1298

Renschler, C.S., and J. Harbor. 2002. Soil erosion assessment tools from point to regional scales - the role of geomorphologists in land management research and implementation. Geomorphology 47: 189–209.

Robichaud, P.R. 2000. Fire effects on infiltration rates after prescribed fire in Northern Rocky Mountain forests, USA. J. Hydrol. 231-232: 220–229.

Robichaud, P.R. 2005. Measurement of post-fire hillslope erosion to evaluate and model rehabilitation treatment effectiveness and recovery. Int. J. Wildl. Fire 14(4): 475–485.

Rosenzweig, C., F.N. Tubiello, R. Goldberg, E. Mills, and J. Bloomfield. 2002. Increased crop damage in the US from excess precipitation under climate change. Glob. Environ. Chang. 12(3): 197–202.

Savabi, M.R., and C.O. Stockle. 2001. Modeling the possible impact of increased CO_2 and temperature on soil water balance, crop yield and soil erosion. Environ. Modell. Software 16(2001): 631-640

Shanley, J.B., and A. Chalmers. 1999. The effect of frozen soil on snowmelt runoff at Sleepers River, Vermont. Hydrol. Process. 13: 1843–1857.

Sheridan, J.M., R. Lowrance, and D.D. Bosch. 1999. Management effects on runoff and sediment transport in riparian forest buffers. Trans. ASAE 42(1): 55–64.

Sheshukov, A. 2011. Seasonal and annual impacts of climate change on watershed response using an ensemble of global climate models. Trans. ASABE 54(6): 2209–2218.

Singh, J., H.V. Knapp, J.G. Arnold, and M. Demissie. 2005. Hydrological modeling of the Iroquois River watershed using HSPF and SWAT. J. Am. Water Resour. Assoc. 41(2): 343–360.

Soto, B., and F. Díaz-Fierros. 1998. Runoff and soil erosion from areas of burnt scrub: Comparison of experimental results with those predicted by the WEPP model. Catena 31(4): 257–270.

Southworth, J., R.A. Pfeifer, M. Habeck, J.C. Randolph, O.C. Doering, and D. Gangadhar Rao. 2002a. Sensitivity of winter wheat yields in the Midwestern United States to future changes in climate, climate variability, and CO_2 fertilization. Clim. Res. 22: 73–86.

Southworth, J., R.A. Pfeifer, M. Habeck, J.C. Randolph, O.C. Doering, J.J. Johnston, and D.G. Rao. 2002b. Changes in soybean yields in the Midwestern United States as a result of future changes in climate, climate variability, and CO_2 fertilization. Clim. Chang. 53: 447–475.

Southworth, J., J.C. Randolph, M. Habeck, O.C. Doering, R.A. Pfeifer, D.G. Rao, and J.J. Johnston. 2000. Consequences of future climate change and changing climate variability on maize yields in the midwestern United States. Agric. Ecosyst. Environ. 82(1-3): 139–158.

Spigel, K.M., and P.R. Robichaud. 2007. First-year post-fire erosion rates in Bitterroot National Forest, Montana. Hydrol. Process. 21(8): 998–1005.

Stubblefield, A.P. 2002. Spatial and temporal dynamics of watershed sediment delivery, Lake Tahoe, California. PhD Dissertation. University of California at Davis, Davis, CA.

Stubblefield, A.P., J.E. Reuter, and C.R. Goldman. 2009. Sediment budget for subalpine watersheds, Lake Tahoe, California, USA. Catena 76: 163–172.

Suttles, J.B., G. Vellidis, D.D. Bosch, R. Lowrance, J.M. Sheridan, and E.L. Usery. 2003. Watershed-scale simulation of sediment and nutrient loads in Georgia Coastal Plain Streams using the annualized AGNPS model. Trans. ASAE 46(5): 1325–1335.

Taylor, A.H., and R.M. Beaty. 2005. Climatic influences on fire regimes in the northern Sierra Nevada Mountains, Lake Tahoe Basin, Nevada, USA. J. Biogeogr. 32: 425–438.

Taylor, K.E., R.J. Stouffer, and G.A. Meehl. 2012. An overview of CMIP5 and the experiment design. Bull. Am. Meteorol. Soc. 93(4): 485–498.

Tetra Tech. 2001. Report for Blackwood Creek TMDL feasibility project Lake Tahoe, California. 2001. Tetra Tech, Lafayette, CA.

Welsch, D.J. 1991. Riparian forest buffers. NA-PR-07-91, USDA, Forest Service, Northeast Area, Radnor, PA.

Westerling, A.L., H.G. Hidalgo, D.R. Cayan, and T.W. Swetnam. 2006. Warming and earlier spring increase Western U.S. forest wildfire activity. Science 313: 940–943.

Wilby, R.L., S.P. Charles, E. Zorita, B. Timbal, P. Whetton, and L.O. Mearns. 2004. Guidelines for use of climate scenarios developed from statistical downscaling methods.

Wilby, R.L., C.W. Dawson, and E.M. Barrow. 2002. SDSM - a decision support tool for the assessment of regional climate change impacts. Environ. Model. Softw. 17: 145–157.

Woznicki, S.A., A.P. Nejadhashemi, and C.M. Smith. 2011. Assessing best management practice implementation strategies under climate change scenarios. Trans. ASABE 54: 171–190.

Zhang, X.-C. 2004. CLIGEN non-precipitation parameters and their impact on WEPP crop simulation. Appl. Eng. Agric. 20(4): 447–454.

Zhang, X.-C. 2005. Spatial downscaling of global climate model output for site-specific assessment of crop production and soil erosion. Agric. For. Meteorol. 135(1-4): 215–229.

Zhang, X.-C. 2007. A comparison of explicit and implicit spatial downscaling of GCM output for soil erosion and crop production assessments. Clim. Change 84(3-4): 337–363.

Zhang, X.-C., Z.-B. Li, and W.-F. Ding. 2005. Validation of WEPP sediment feedback relationships using spatially distributed rill erosion data. Soil Sci. Soc. Am. J. 69(5): 1440.

Zhang, X.-C., W.-Z. Liu, Z. Li, and J. Chen. 2011. Trend and uncertainty analysis of simulated climate change impacts with multiple GCMs and emission scenarios. Agric. For. Meteorol. 151(10): 1297–1304.

Zhang, X.-C., M.A. Nearing, J.D. Garbrecht, and J.L. Steiner. 2004. Downscaling monthly forecasts to simulate impacts of climate change on soil erosion and wheat production. Soil Sci. Soc. Am. J. 68: 1376–1385.

Zuzel, J.F., R.R. Allmaras, and R. Greenwalt. 1982. Runoff and soil erosion on frozen soils in northeastern Oregon. J. Soil Water Conserv. 37(6): 351–354.